Mextram Bipolar Transistor Model Parameter Extraction Using Python

by

Pengyu Li

A thesis submitted to the Graduate Faculty of
Auburn University
in partial fulfillment of the
requirements for the Degree of
Master of Science

Auburn, Alabama
December 12, 2015

Keywords: Mextram, parameter extraction, bipolar transistors

Approved by

Guofu Niu, Professor of Electrical and Computer Engineering
Fa Foster Dai, Professor of Electrical and Computer Engineering
Stuart Wentworth, Associate Professor of Electrical and Computer Engineering

Abstract

This work implements Mextram 504 parameter extraction using python. A 50 GHz SiGe HBT is used to demonstrate effectiveness of this developed extraction program. Comparisons with results extracted using built-in mextram 504 parameter extraction package of IC-CAP , excellent agreements are achieved between our python program and IC-CAP.

Acknowledgments

I would like to express my sincere gratitude to my advisor Dr.Guofu Niu for the continuous support of my study and research, for his patience, motivation, enthusiasm, and immense knowledge. His guidance helped me in all the time of research and writing of this thesis. I would like to thank other members of my committee, Dr. Stuart Wentworth and Dr. Fa Foster Dai for their valuable comments and precious time.

Also, I am grateful for my group members for their kindly accompany through the long, tough but meaningful and unforgettable days in Auburn. Special thanks to Zhen Li, Zhenyu Wang for their encourage and help.

Last but not the least, I would like to express my gratefulness to my parents and my fiancee for their love, encouragement and support.

Table of Contents

Abstract ii

Acknowledgments iii

List of Figures vii

List of Tables xv

1 Introduction 1

  1.1 SiGe HBT fundamentals 1

  1.2 Mextram basics 2

2 Parameter extraction with Python 5

  2.1 Extraction using Python 5

  2.2 Data Input 6

  2.3 Optimization with python 7

  2.4 Parameter extraction strategy 10

3 Measurement and Parameter Initialization 13

  3.1 Measurements 13

    3.1.1 Forward-Gummel measurement 13

    3.1.2 Reverse-Gummel measurement 14

    3.1.3 Output characteristic measurement 16

    3.1.4 Forward-Early measurement 16

    3.1.5 Reverse-Early measurement 20

    3.1.6 R_{CC}-active measurement 21

  3.2 Parameter Initialization 24

    3.2.1 Parameters that can be given an initial value 24

    3.2.2 Parameters from measurements 24

3.2.3 Parameter to be calculated 24
4 Extraction of low current parameters 31
4.1 Base-emitter depletion capacitance 31
4.2 Base-collector depletion capacitance 34
4.3 Collector-substrate depletion capacitance 36
4.4 Avlanche 38
4.5 Reverse Early effect 39
4.6 Forward Early effect 45
4.7 Collector saturation current 48
4.8 Forward base current 49
4.9 Substrate saturation current 51
4.10 Reverse current 52
4.11 Emitter series resistances 54
4.12 Collector series resistances 56
5 Extraction of high current parameters 59
5.1 Self-heating 59
5.2 Knee current 67
5.3 Ohmic resistance 67
5.4 Cut-off frequency 69
5.5 Reverse current at high injection 72
6 Temperature scalling 76
6.1 T-scaling rules 76
6.2 Temperature parameters 79
6.3 Extraction result 85
Bibliography 95
Appendices 98
A Appendix A Full List of Mextram model Parameters 99

A.1 Compact model parameter list 99

List of Figures

1.1 Energy band diagrams of a graded-base SiGe HBT and an Si BJT [3] 1

1.2 The full Mextram equivalent circuit for the vertical NPN transistor[1] 4

3.1 Forward-Gummel measurement setup. 13

3.2 Forward-Gummel measurement I_C, I_B, I_E versus V_{BE}. 14

3.3 Reverse-Gummel measurement setup. 15

3.4 Reverse-Gummel measurement I_C, I_B, I_E andI_{SUB} versus V_{BC}. 15

3.5 Force-I_B output characteristic measurement setup 16

3.6 Force-I_B output measurement I_C-V_{CE}. 17

3.7 Force-I_B output measurement $V_{BE} - V_{CE}$. 18

3.8 Forward-Early measurement setup 18

3.9 Forward-Early measurement $I_B - V_{CB}$ curve. 19

3.10 Forward-Early measurement $I_C - V_{CB}$ curve. 19

3.11 Reverse-Early measurement setup 20

3.12 Reverse-Early $I_E - V_{EB}$. 21

3.13 Reverse-Early $I_B - V_{EB}$. 22

3.14 R_{CC}-active measurement setup 22

3.15 R_{CC}-active measurement I_C, I_B, I_S versus V_{BE}. 23

4.1 Implementation of V_{eff} in Mextram 32

4.2 Implementation of the Mextram depletion capacitances. 32

4.3 Measured(markers) and simulated(line) base emitter depletion capacitance by Python 33

4.4 Measured(markers) and build-in function simulated(line) base emitter depletion capacitance by IC-CAP 33

4.5 Measured(markers) and simulated(line) base collector depletion capacitance by Python 35

4.6 Measured(markers) and build-in function simulated(line) base collector depletion capacitance by IC-CAP 35

4.7 Measured(markers) and simulated(line) collector substrate depletion capacitance by Python 37

4.8 Measured(markers) and build-in function simulated(line) collector substrate depletion capacitance by IC-CAP 37

4.9 Forward-Early measurement simplified circuit 38

4.10 Measured(markers) and simulated(line) G_{EM}t in forward-Early measurement by Python 40

4.11 Measured(markers) and simulated(line) G_{EM} by IC-CAP 40

4.12 Measured(markers) and simulated(line) base current in forward-Early measurement by Python . . . 41

4.13 Measured(markers) and simulated(line) base current in forward-Early measurement by IC-CAP . . . 41

4.14 Reverse-Early measurement simplified circuit . . . 42

4.15 Measured(markers) and simulated(line) emitter current of first time extraction in reverse-Early measurement by Python . . . 43

4.16 First time extraction of actual reverse Early voltage by numerical differentiation of the measured(dash line) and simulated(solid line) collector current of in the reverse-Early measurement by Python . . . 43

4.17 Measured(markers) and simulated(line) emitter current in reverse-Early measurement by Python . . . 44

4.18 Measured(markers) and build-in function simulated(line) emitter current in reverse-Early measurement by IC-CAP . . . 44

4.19 Actual reverse Early voltage by numerical differentiation of the measured(dash line) and simulated(solid line) collector current in the reverse-Early measurement by Python . . . 44

4.20 Actual reverse Early voltage by numerical differentiation of the measured(dash line) and build-in function simulated(solid line) collector current in the reverse-Early measurement by IC-CAP . . . 44

4.21 Measured(markers) and simulated(line) collector current of first time extraction in forward-Early measurement by Python . . . 46

4.22 First time extraction of actual forward Early voltage by numerical differentiation of the measured(dash line) and simulated(solid line) collector current of in the forward-Early measurement by Python 46

4.23 Measured(markers) and simulated(line) collector current in forward-Early measurement by Python 47

4.24 Measured(markers) and build-in function simulated(line) collector current in forward-Early measurement by IC-CAP 47

4.25 Actual forward Early voltage by numerical differentiation of the measured(dash line) and simulated(solid line) collector current in the forward-Early measurement by Python 47

4.26 Actual forward Early voltage by numerical differentiation of the measured(dash line) and simulated(solid line) collector current in the forward-Early measurement by IC-CAP 47

4.27 Forward-Gummel measurement simplified circuit 48

4.28 Measured(markers) and simulated(line) collector current in forward-Gummel measurement by Python 49

4.29 Measured(markers) and simulated(solid line) collector current in forward-Gummel measurement by IC-CAP 49

4.30 Measured forward base current(marker) and simulated forward base current I_B - V_{BE} in Forward-gummel measurement 50

4.31 Reverse-Gummel measurement simplified circuit 51

4.32 Measured (mark) and simulated (line) substrate current in reverse-Gummel measurement 52

4.33 The measured I_B - I_{sub} and simulated I_{ex} + I_{B3} in reverse-Gummel measurement 53

4.34 Measured(markers) and simulated(line) base-emitter bias as function of the base current in the forward-Gummel measurement by Python 55

4.35 Measured(markers) and build-in function simulated(line) base-emitter bias as function of the base current in the forward-Gummel measurement by IC-CAP . 55

4.36 R_{Cc}-active measurement simplified circuit 56

4.37 Measured(markers) and simulated(line) substrate current in the Rcc-active measurement by Python 58

4.38 Measured(markers) and build-in function simulated(line) substrate current in the Rcc-active measurement by IC-CAP 58

5.1 Force-IB output characteristic measurement simplified circuit 59

5.2 Measured(markers) and simulated(line) base-emitter voltage in the output characteristic measurement by Python 66

5.3 Measured(markers) and simulated(line) base-emitter voltage in the output characteristic measurement by IC-CAP 66

5.4 Measured(markers) and simulated(line) collector current in the output-characteristic measurement by Python 68

5.5 Measured(markers) and simulated(line) collector current in the output-characteristic measurement by IC-CAP 68

5.6 Measured(markers) and simulated(line) forward current gain as function of the measurement base current in forward-Gummel measurement by Python 69

5.7 Measured(markers) and simulated(line) forward current gain as function of the measurement base current in forward-Gummel measurement by IC-CAP 69

5.8 Measured(markers) and simulated(line) cut-off frequency in the S-parameter measurement by Python 71

5.9 Measured(markers) and simulated(line) cut-off frequency in the S-parameter measurement by IC-CAP 71

5.10 Measured(markers) and simulated(line) emitter currents in the reverse-Gummel measurement by Python 74

5.11 Measured(red line) and simulated(blue line for build in function purple line for simulator) emitter currents in the reverse-Gummel measurement by IC-CAP . . 74

5.12 Measured(markers) and simulated(line) substrate currents in the reverse-Gummel measurement by Python 74

5.13 Measured(red line) and simulated(blue line for build in function purple line for simulator) substrate currents in the reverse-Gummel measurement by IC-CAP . 74

5.14 Measured(markers) and simulated(line) base currents in the reverse-Gummel measurement by Python 75

5.15 Measured(red line) and simulated(blue line for build in function purple line for simulator) base currents in the reverse-Gummel measurement by IC-CAP 75

6.1 Extracted(markers) and simulated(line) values of the reverse Early voltage . . . 80

6.2 Extracted(markers) and simulated(line) values of the forward Early voltage . . . 81

6.3 Extracted(markers) and simulated(line) values of collector saturation current . . 81

6.4 Extracted(markers) and simulated(line) values of substrate saturation current . 82

6.5 Extracted(markers) and simulated(line) values of forward current gain 82

6.6 Extracted(markers) and simulated(line) values of reverse current gain 83

6.7 Extracted(markers) and simulated(line) values of non-ideal forward base current 83

6.8 Extracted(markers) and simulated(line) values of non-ideal reverse base current 84

6.9 Measured (symbol) and simulated (solid line) I_B-V_{BE} from 223-393 K. (a) 223K. (b) 300K. (c) 393K. 86

6.10 Measured (symbol) and simulated (solid line) I_C-V_{BE} from 223-393 K. (a) 223K. (b) 300K. (c) 393K. 87

6.11 Measured (symbol) and simulated (solid line) I_E-V_{BC} from 2233-393 K. (a) 223K. (b) 300K. (c) 393K. 88

6.12 Measured (symbol) and simulated (solid line) I_{Sub}-V_{BC} from 223-393 K. (a) 223K. (b) 300K. (c) 393K. 89

6.13 Measured (symbol) and simulated (solid line) I_C-V_{CE} from 223-393K at high IB. (a) 223K. (b) 300K. (c) 393K. 90

6.14 Measured (symbol) and simulated (solid line) I_C-V_{CE} from 223-393 K at low IB. (a) 223K. (b) 300K. (c) 393K. 91

6.15 Measured (symbol) and simulated (solid line) V_{BE}-V_{CE} from 223-393 K at high IB. (a) 223K. (b) 300K. (c) 393K. 92

6.16 Measured (symbol) and simulated (solid line) V_{BE}-V_{CE} from 223-393 K at low IB. (a) 223K. (b) 300K. (c) 393K. 93

6.17 Measured (symbol) and simulated (solid line) f_T-I_C from 223-393 K. (a) 223K. (b) 300K. (c) 393K. 94

List of Tables

2.1 A typical grouping of parameters in Mextram that can be used in the extraction procedure.[12] 11

3.1 Forward-Gummel measurement 14

3.2 Reverse-Gummel measurement 14

3.3 Force-I_B output characteristic measurement 16

3.4 Forward-Early measurement 17

3.5 Reverse-Early measurement 20

3.6 R_{CC}-active measurement setup 21

3.7 Parameter initial value [12] 25

3.8 Parameters that can be extracted without optimising[12] 26

3.9 The layout and process quantities[12] 26

6.1 Summery of the occurrence of the temperature parameters in the temperature scaling rules of the electrical parameters. 77

A.1 Mextram 504.12 model parameters overview**??** 99

Chapter 1

Introduction

1.1 SiGe HBT fundamentals

The Silicon-Germanium heterojunction bipolar transistor (SiGe HBT) has gained worldwide attention, since it could get higher current gain, higher cut-off frequency and lower base resistance compared with Si BJT. The heart of SiGe technology is a SiGe hetrojunction bipolar transistor (HBT), which is the first practical bandgap engineering device realized in silicon,is easy to integrated with modern CMOS technology. Adding Ge to Si BJT introduced a number of exciting performance improvements. The base region of SiGe HBTs is typically the region where SiGe alloy is used instead of Si. The basic operational principle of SiGe HBT can be best understood by considering the band diagram shown in Figure 1.1. It illustrates the difference between SiGe HBT and Si BJT by showing the energy-band

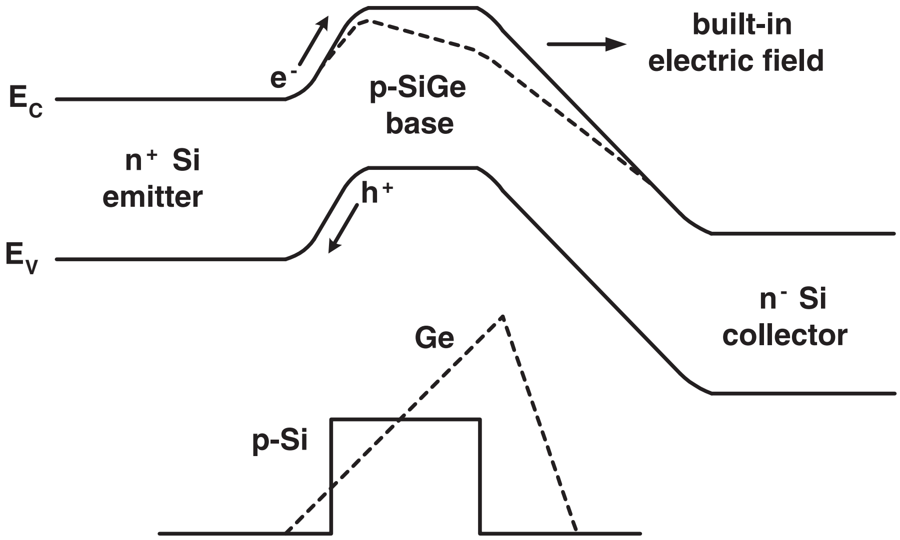

Figure 1.1: Energy band diagrams of a graded-base SiGe HBT and an Si BJT [3]

diagrams for both SiGe HBT and Si BJT biased identically in forward-active mode. The Ge profile linearly increases from zero near emitter-base (EB) junction to some maximum value near collector-base (CB) junction, and then rapidly ramps down to zero [4]. Since the energy bandgap of Ge is smaller than that of Si, adding germanium into the base region of the transistor leads to an additional bandgap shrinkage, which is approximately 75 meV for each 10 percent of Ge introduced[2]. The reduction of bandgap decreases band transit time, which gives a higher f_T. Smaller base bandgap also increases electron injection, which leads to a higher β. At same collector current density, compared with normal BJT, SiGe HBT allows us to have a higher base region doping concentration, which reduces base resistance.

1.2 Mextram basics

Mextram[1][11] model is a widely used vertical bipolar transistor model. It contains many features that the widely-used Ebers-Moll[5] and Gummel-Poon model[6] lacks. Mextram is the acronym of the "most exquisite transistor model". The first Mextram release was introduced as Level 501 in 1985[7] . Later Level 502[8], 503[9] and 504[10] were respectively released in 1986 , 1994 and 2000. And development was never stopped following the requirement of updated technology. The latest accessible version is Level 504.12[1] . Mextram contains descriptions for the following effects:

- Bias-dependent Early effect
- Low-level non-ideal base currents
- High-injection effects
- Ohmic resistance of the epilayer
- Velocity saturation effects on the resistance of the epilayer
- Hard and quasi-saturation (including Kirk effect)
- Weak avalanche in the collector-base junction (optionally including snap-back behaviour)

- Zener-tunneling current in the emitter-base junction
- Charge storage effects
- Split base-collector and base-emitter depletion capacitance
- Substrate effects and parasitic PNP
- Explicit modelling of inactive regions
- Current crowding and conductivity modulation of the base resistance
- First order approximation of distributed high frequency effects in the intrinsic base (high-frequency current crowding and excess phase-shift)
- Recombination in the base (meant for SiGe transistors)
- Early effect in the case of a graded bandgap (meant for SiGe transistors)
- Temperature scaling
- Self-heating
- Thermal noise, shot noise and $1/f$-noise

In Mextram model, there are five internal nodes and 79 parameters, including parameters of model flag, parameters of noise and the reference temperature, parameters of temperature scaling, parameters of individual transistor design and parameters to be determined by the fitting the model to the transistor characteristics of a specific device and at a specific temperature.

Some parts of the model are optional and can be switched on or off by setting flags. These are the extended modeling of reverse behaviour, the distributed high-frequency effects, and the increase of the avalanche current when the current density in the epilayer exceeds the doping level.

Fig.1.2 shows the equivalent circuit of Mextram model as it is specified in its latest release Level 504.12 [1]. The branches representing model currents and charges are schematically associated with different physical regions of a bipolar transistor separated by the base-emitter, base-collector, and substrate-collector junctions.

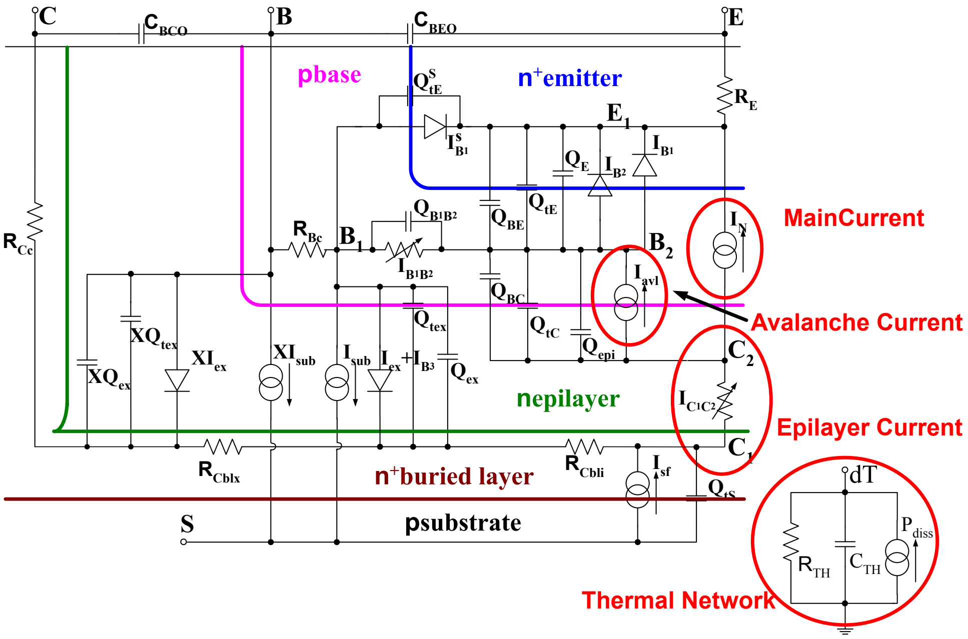

Figure 1.2: The full Mextram equivalent circuit for the vertical NPN transistor[1]

Chapter 2

Parameter extraction with Python

Python is a widely used general-purpose, high-level programming language[13]. Python supports multiple programming paradigms, including object-oriented, imperative and functional programming or procedural styles. It features a dynamic type system and automatic memory management and has a large and comprehensive standard libraries.[14] In our work, we use the lmfit package[17] which is a non-linear optimization interface based on Levenberg-Marquardt algorithm to realize the optimization routine.

2.1 Extraction using Python

Generally, there are two ways to extract Mextram transistor parameters. The first one is using build-in functions of extraction software. These functions has the simplified Mextram formulas implemented in and parameters can be extracted on different conditions of the transistor. However, the disadvantage of this method is that if we change the model of Mextram, these functions will be useless. In our python programming extraction routine , we also have simplified formulas of Mextram model implemented in the program I wrote. Unlike the extraction software, the program is still useful after we make change to the Mextram model as long as we update the formulas.

Another alternative way is using a circuit simulator[15] which has the full Mextram model behaviour. However, using the simulator take a very long time. Also some of the parameters, like the Early voltages and the avalanche parameters can be extracted without correct modelling of the absolute value of the current. For these extractions dummy parameters are optimised together with the Mextram parameters. For instance the extraction of the avalanche parameters needs the correct base current at zero V_{CB}. This is more difficult when using a simulator[12].

2.2 Data Input

Generally, the measurement procedure is done throw device modeling software IC-CAP[16]. The output measurement data is saved in MDM file. In the MDM file, data within a file is organized into multiple groups of tabular data. Each group of tabular data is arranged in columns representing the innermost sweep data and its associated dependent data. In our program we writing a parser program to read the measurement MDM file and capture data. The code is:

```
def mdm_reader(fname):
    f = open(fname, ’r’)
    text = f.read()
    ldata = []
    for begin_match, end_match in  zip(re.finditer(’BEGIN_DB’, text), re.finditer
    (’END_DB’, text)):
        s = begin_match.end()
        e = end_match.start()
        body = text[s:e]
        data = read_block(body)
        ldata.append(data)
    # convert to numpy array
    adata = np.array(ldata)
    f.close()
    return adata


def read_block(body):
```

```
    lines = body.strip().split('\n')
    output = cStringIO.StringIO()
    for line in lines:
        tline= line.strip()
        if tline.startswith('ICCAP_VAR') or tline.startswith('#'):
            new_line = '%' + tline
        else:
            new_line = tline
        # only write non blank lines
        if (new_line):
            output.write(new_line + '\n')
    output.seek(0)
    data = np.loadtxt(output, comments='%')
    return data
```

2.3 Optimization with python

In parameter extraction routine, as the simulation data is calculated from the parameters we want to extract, changing the parameters and match the simulation data with measurement data will give us the value of the parameters. In our work we use lmfit package to realize the optimization function. Take the base-collector depletion capacitance extraction as an example, we first calculate C_{bc} as function of x_P and p_C then use the minimize function which will change x_P and p_C to make calculated C_{bc} match the measurement C_{bc}. And this is realized by code :

```
import mdmreader
from lmfit import minimize, Parameters, Parameter, report_fit,fit_report
from myplot import *
```

```
import os


def cbc_reader(fname):


    data = mdmreader.mdm_reader(fname)

    vcb_m = data[:,:,0][0]

    cbc_m = data[:,:,1][0]

    x,y = vcb_m,cbc_m

    return x, y

#calculate cbc as function of xp and pc

def cbc_caculation(pars,x,y):

    x = -x

    vals = pars.valuesdict()

    CJC = vals['cjc']

    XP = vals['xp']

    VDC = vals['vdc']

    PC = vals['pc']

    CBCO = vals['cbco']

    AJC = vals['ajc']

    TEMP = vals['temp']

    KBdivQQ = vals['kq']


    Tk = TEMP +273.15

    vt  = KBdivQQ * Tk

    bjc = (AJC-XP)/(1-XP);

    vfc = VDC * (1-pow(bjc,-1.0/PC))

    e         = np.exp((x-vfc)/(0.1*VDC))
```

```
    vjc       = x  - 0.1*VDC*np.log(1+e)
    dvjc_dvbc = 1.0/(1.0+e)
    dvtc_dvbc = ( pow(1-vjc/VDC,-PC)-bjc ) * dvjc_dvbc + bjc
    model = CJC*( (1-XP)*dvtc_dvbc + XP) + CBCO
    return model - y

#find the value of cjc
def findcj(voltage, cap):
    for i in range(len(voltage)):
        if voltage[i] == 0:
            return cap[i]
    z = np.polyfit(voltage, cap,3)
    p = np.poly1d(z)
    return p(0)


def cbc_optimization(data, mdmpath):
    ofname = 'cap\\POR_Vbc_Cbc_300K.mdm'
    fname = os.path.join(mdmpath, ofname)
    x,y = cbc_reader(fname)
    cbc_params = Parameters()
    cbc_params.add('cjc', value=findcj(x, y), min = 0, max = 1e-9)
    cbc_params.add('xp', value=data.xp, min = 0, max = 1)
    cbc_params.add('vdc', value = data.vdc, vary = False)
    cbc_params.add('pc', value = data.pc, min = 0.01, max = 1)
    cbc_params.add('cbco', value = data.cbco,vary = False)
    cbc_params.add('ajc', value = data.ajc,vary = False)
```

```
cbc_params.add('temp', value = data.temp,vary = False)
cbc_params.add('kq', value = data.kq,vary = False)



result = minimize(cbc_caculation, cbc_params,args=(x,y) )


final = y + result.residual
report_fit(cbc_params)
```

2.4 Parameter extraction strategy

A reliable, robust and unambiguous parameter extraction method is very important. The use of a very accurate compact model with poorly extracted parameters will produce bad prediction of device and circuit performance.[18]The general strategy of parameter extraction is to put parameters in small groups and extract these parameters simultaneously out of measured data sensitive to these parameters.[12]

In Mextram, most of the parameters can be extracted directly from measured data, including depletion capacitance C-V, *dc* Gummel plots, *dc* output characteristics, *dc* Early voltage measurement, and *ac* S-parameter measurement. Some special measurements are taken to extract terminal resistance, such as R_E-flyback and R_{Cc}-active methods.

The electrical parameter extraction includes low-current parameters extraction and high-current parameters extraction. Low-current parameters extraction is straightforward. However, high-current parameters extraction is much more difficult because in that regime many physics effects play a role. In general, we first extract low-current parameters then high-current parameters, a typical sequence of the Mextram parameters extraction is given in Table 2.1. The frame of the extraction program is :

```
q = BJT()
```

Base-emitter depl. cap.	C_{j_E}, p_E, (V_{d_E})
Base-collector depl. cap.	C_{j_C}, p_C, X_p
Substrate-emitter depl. cap.	C_{j_S}, p_S, (V_{d_S})
Forward-Early	W_{avl}, V_{avl}
Reverse-Early	V_{er}
Forward-Early	V_{ef}
Forward-Gummel	I_s
Forward-Gummel	β_f, I_{Bf}, m_{Lf}
Reverse-Gummel	R_E
R_{Cc}-active	R_{Cc}
Reverse-Gummel	I_{Ss}, (I_{ks})
Reverse-Gummel	β_{ri}, I_{Br}, V_{Lr}
Output-characteristic	R_{th}, I_k
Forward-Gummel	R_{Cv}, (V_{d_C})
Cut-off frequency	SCR_{Cv}, I_{hc}, τ_E, τ_{epi}, (τ_B, α_{X_i})

Table 2.1: A typical grouping of parameters in Mextram that can be used in the extraction procedure.[12]

```
cbe_optimization(q, mdmpath)

cbc_optimization(q, mdmpath)

csc_optimization(q, mdmpath)

avl_optimization(q, mdmpath)

i = 0

fro index in range(2):

    vear_optimization(q, mdmpath)

    veaf_optimization(q, mdmpath)

is_optimization(q, mdmpath)

hfe_optimization(q, mdmpath)

re_optimization(q, mdmpath)

rcc_optimization(q, mdmpath)

iss_optimization(q, mdmpath)

hfc_optimization(q, mdmpath)
```

```
iks_optimization(q, mdmpath)
rth_optimization(q, mdmpath)
j = 0
fro index in range(2):
    ik_optimization(q, mdmpath)
    icib_optimization(q, mdmpath)
    ik_optimization(q, mdmpath)
    ft_optimization(q, mdmpath)
reverse_optimization(q, mdmpath)
taue_optimization(q, mdmpath)
f = open('par.txt', 'w')
f.write(str(q.Param_Defs))
f.close()
```

Chapter 3

Measurement and Parameter Initialization

The first step for extraction of parameters of a single transistor is get the measurement data. In order to extract reliable parameters it is important that the measurements are done over a large range of collector, base and emitter biasing conditions.

3.1 Measurements

3.1.1 Forward-Gummel measurement

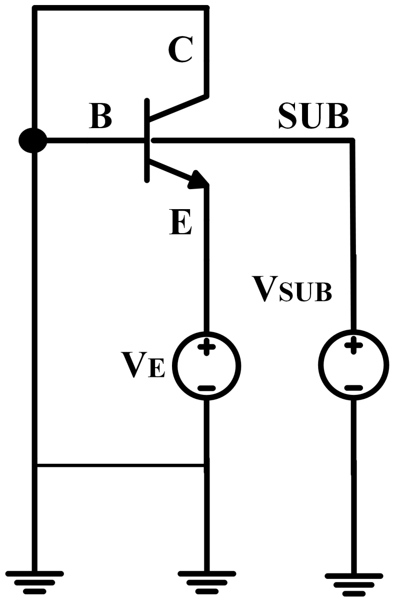

Figure 3.1: Forward-Gummel measurement setup.

In the forward-Gummel measurement setup, as shown in Figure 3.1 base and collector are grounded. Emitter voltage is swept. The reverse junction bias is 0 V to avoid the generation of avalanche current and self-heating effects. The measured I_C, I_B, I_E versus V_{BE} is shown is Figure 3.2

T (K)	V_E			V_B (V)	V_C	V_{SUB} (V)
	Start (V)	Stop (V)	Step (mV)			
393	0	-1.2	2	0	0	-1
300	-0.3	-1.2	2	0	0	-1
223	-0.5	-1.3	2	0	0	-1

Table 3.1: Forward-Gummel measurement

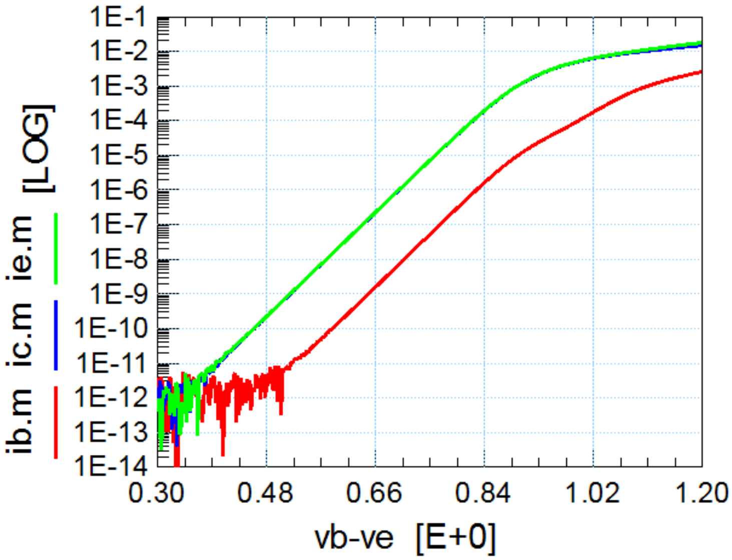

Figure 3.2: Forward-Gummel measurement I_C, I_B, I_E versus V_{BE}.

3.1.2 Reverse-Gummel measurement

In the reverse-Gummel measurement, as shown in Figure 3.3, base and emitter are grounded. Collector voltage is swept. Figure 3.4 shows the measured I_C, I_B, I_E andI_{SUB} versus V_{BC}.

T (K)	V_C(V)			V_B (V)	V_E(V)	V_{SUB} (V)
	Start (V)	Stop (V)	Step (mV)			
393	0	-1.2	2	0	0	-1.2
300	-0.3	-1.2	2	0	0	-1.2
223	-0.5	-1.3	2	0	0	-1.2

Table 3.2: Reverse-Gummel measurement

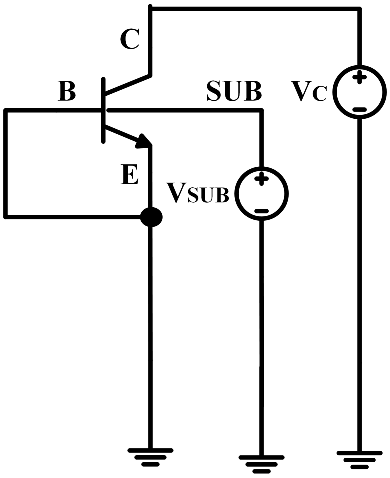

Figure 3.3: Reverse-Gummel measurement setup.

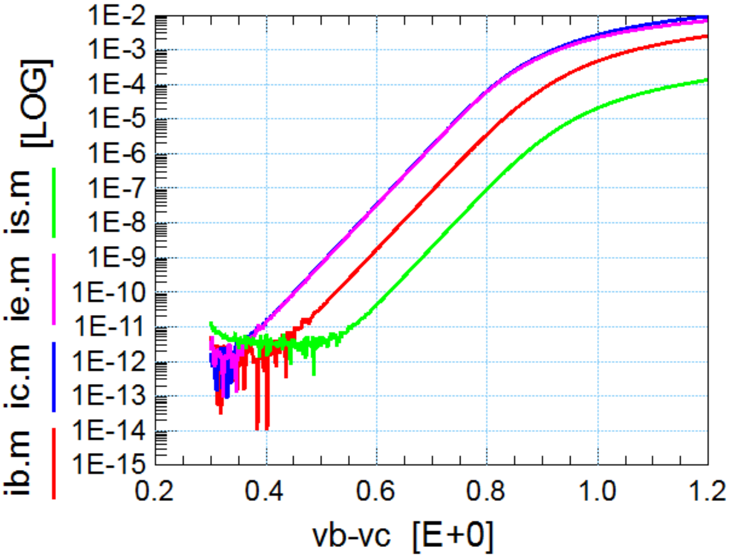

Figure 3.4: Reverse-Gummel measurement I_C, I_B, I_E andI_{SUB} versus V_{BC}.

T (K)	I_B	V_C			V_E (V)	V_{SUB} (V)
		Start (V)	Stop (V)	Step (mV)		
393	65.4n, 211.46n, 671.45n 2.05u, 15.18u,33.46u, 91.24u, 174.04u, 275.97u	0	4.4	50	0	-1
300	39.54n, 85.74n, 185.22n 480.67n, 2.44u,13.84u, 23.82u, 37.69u, 57.72u	0	4.4	50	0	-1
223	50.38n, 140.17n, 383.65n 1.01u, 5.38u,17.60u, 30.36u, 47.75u, 74.86u	0	4.4	50	0	-1

Table 3.3: Force-I_B output characteristic measurement

3.1.3 Output characteristic measurement

In the output characteristic measurement shown in Figure 3.5, Force-I_B method is used. Nine I_B currents are used in Force-I_B method. Figure 3.6 and 3.7 shows measured I_C-V_{CE} and $V_{BE} - V_{CE}$ respectively.

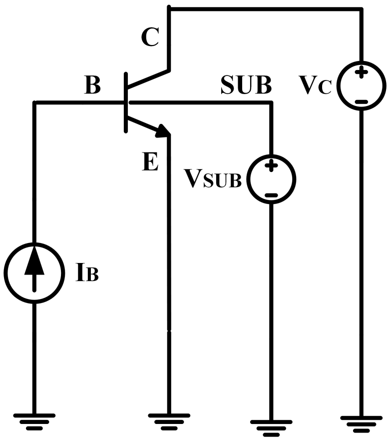

Figure 3.5: Force-I_B output characteristic measurement setup

3.1.4 Forward-Early measurement

In the forward-early measurement shown if Figure 3.8, the collector voltage V_C is increased while keeping the base-emitter voltage constant. The maximum collector voltage

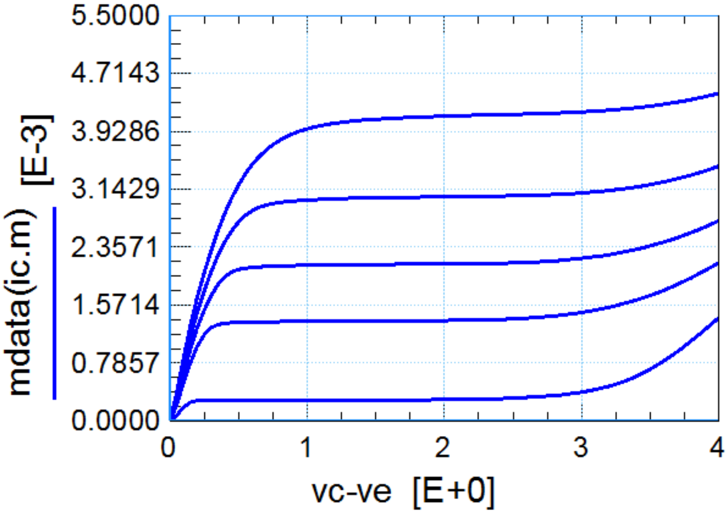

Figure 3.6: Force-I_B output measurement I_C-V_{CE}.

T (K)	V_C (V)			V_E (V)	V_B (V)	V_{SUB} (V)
	Start (V)	Stop (V)	Step (mV)			
393	0	$V_{CB,max1}$	50	-0.60 V	0	-1
300	0	$V_{CB,max2}$	50	-0.68 V	0	-1
223	0	$V_{CB,max3}$	50	-0.8 V	0	-1

Table 3.4: Forward-Early measurement

$V_{CB,max}$ is obtained from this measurement as the voltage where the base current becomes negative. The measured $I_B - V_{CB}$ and $I_C - V_{CB}$ are shown in Figure 3.9 and 3.10 respectively.

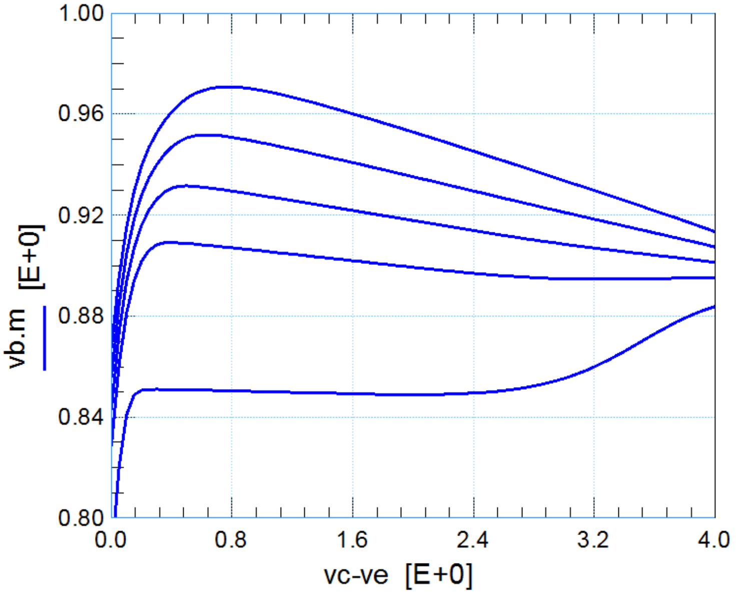

Figure 3.7: Force-I_B output measurement $V_{BE} - V_{CE}$.

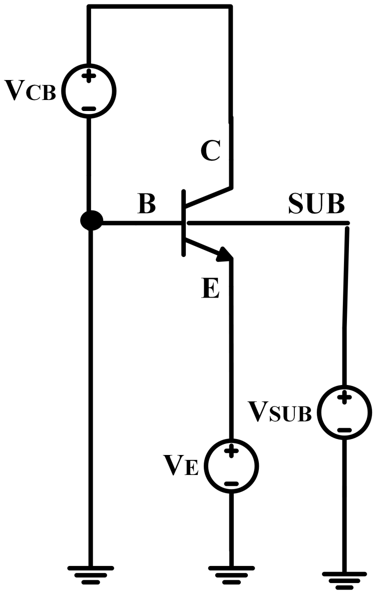

Figure 3.8: Forward-Early measurement setup

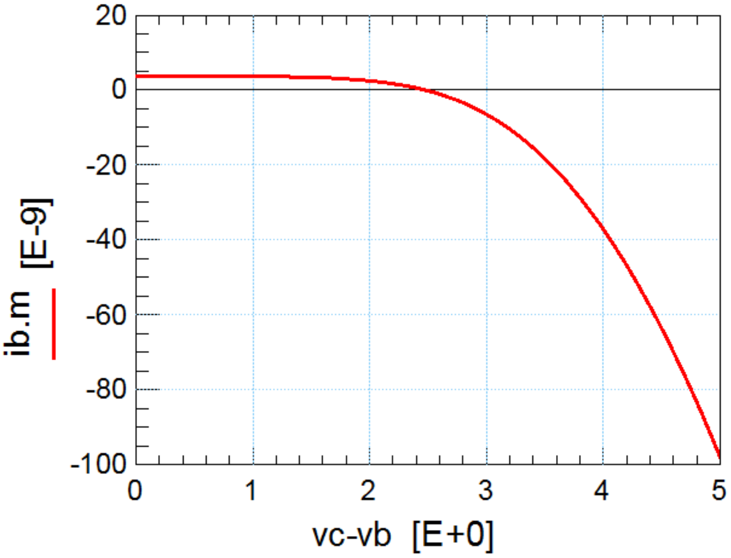

Figure 3.9: Forward-Early measurement $I_B - V_{CB}$ curve.

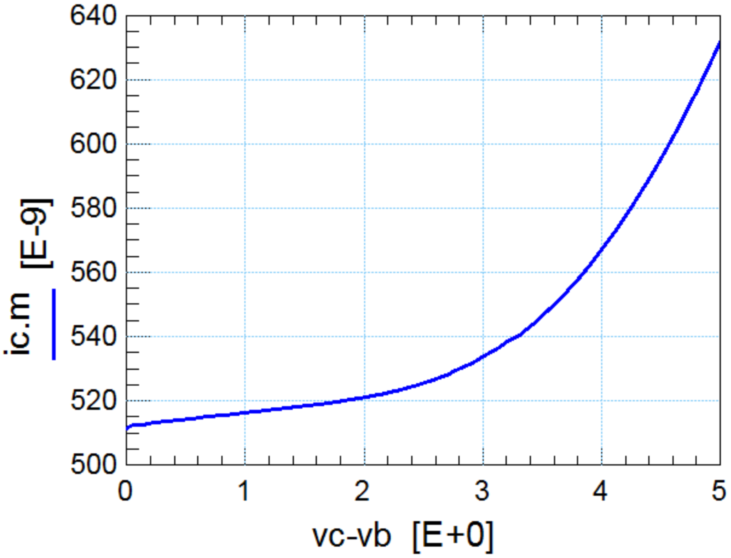

Figure 3.10: Forward-Early measurement $I_C - V_{CB}$ curve.

T (K)	V_E (V)			V_C (V)	V_B (V)	V_{SUB} (V)
	Start (V)	Stop (V)	Step (mV)			
393	0	$V_{EB,max1}$	50	-0.50 V	0	-1
300	0	$V_{EB,max2}$	50	-0.65 V	0	-1
223	0	$V_{EB,max3}$	50	-0.76 V	0	-1

Table 3.5: Reverse-Early measurement

3.1.5 Reverse-Early measurement

In the reverse-early measurement shown in Figure 3.11, the emitter voltage V_E is increased while keeping the base-collector voltage constant. In the reverse-early measurement, the measured base current should be constant at first, then it will eventually decrease due to the generation of avalanche current in the reversed biased base-emitter junction. The maximum reverse emitter voltage $V_{EB,max}$ is obtained from the measurement by looking to the point where this effect occur. The measured I_E and I_B versus V_{EB} are shown in Figure 3.12 and 3.13.

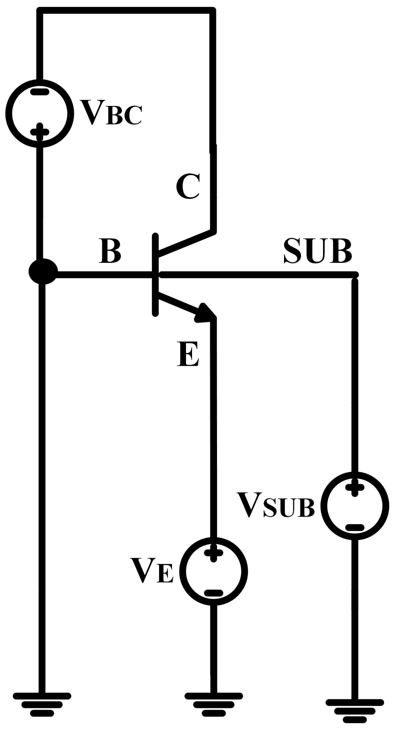

Figure 3.11: Reverse-Early measurement setup

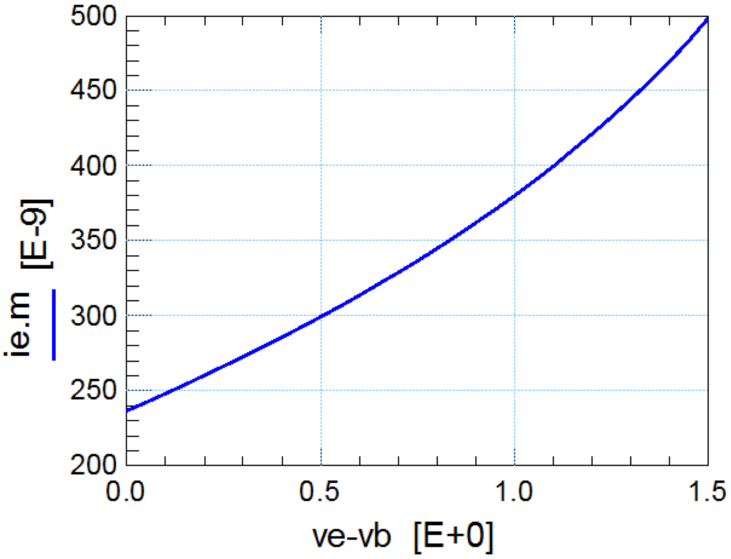

Figure 3.12: Reverse-Early $I_E - V_{EB}$.

T (K)	V_{SUB} (V)	V_E			V_B (V)	V_C (V)
		Start (V)	Stop (V)	Step (mV)		
393	-1	-0.6	-1.4	5	0	-0.6
300	-1	-0.6	-1.4	5	0	-0.6
223	-1	-0.6	-1.4	5	0	-0.6

Table 3.6: R_{CC}-active measurement setup

3.1.6 R_{CC}-active measurement

In the R_{CC} measurement shown in Figure 3.14, the base-collector is forward biased and the base-collector is 0.6V. The base-emitter voltage is swept from 0.6V to 1.4V. In this case the collector current remains positive and reasonably large. The voltage drop over the collector resistance makes that internally the base-collector bias that drives the substrate current is increased even further than the externally applied 0.6V. The substrate current can be measured and we can use a simple model for this current to extract R_{CC}. Figure 3.15 shows the measured I_C, I_B, I_S versus V_{BE}.

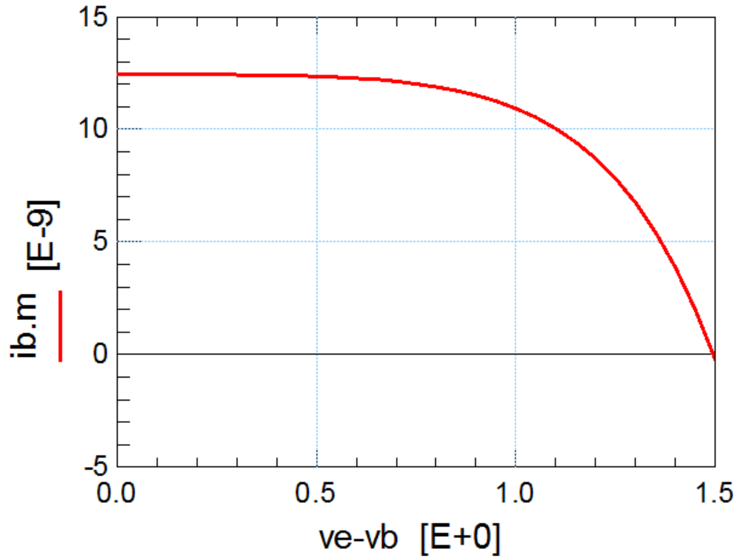

Figure 3.13: Reverse-Early $I_B - V_{EB}$.

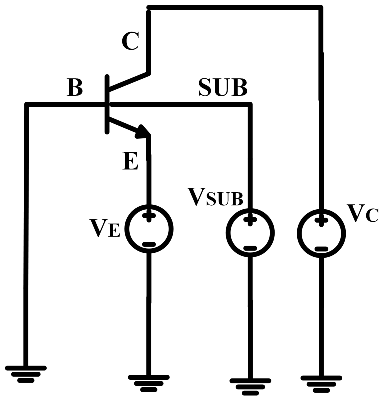

Figure 3.14: R_{CC}-active measurement setup

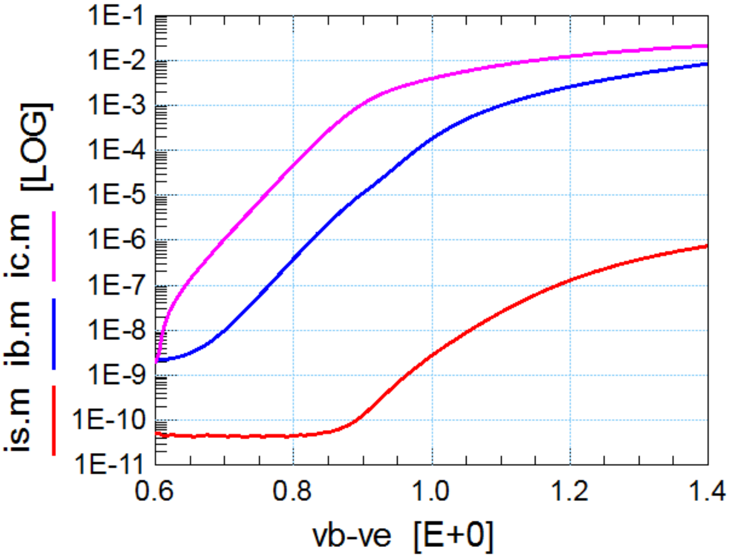

Figure 3.15: R_{CC}-active measurement I_C, I_B, I_S versus V_{BE}.

3.2 Parameter Initialization

The first step in the determination of parameter is to generate an initial parameter set. In general, the parameter extraction means to minimize the difference between the measurement data and simulation data. This is done by using some algorithm that optimises the value of the parameter. For the optimization, the initial value of the parameter is very important. If the initial value is good, the optimising process will be precise and fast. Furthermore, the chance of getting stuck in a local minimum with very unphysical values for the parameters is much smaller than stared with a random initial value.

3.2.1 Parameters that can be given an initial value

Table 3.7 shows the parameters and their initial values. Some of them are process dependent.

3.2.2 Parameters from measurements

Table 3.8 shows a list of parameters whose initial value can be obtained from measurement data and it also shows the way to get the values. Note that the last three quantities are help variables and not parameters of Mextram.

3.2.3 Parameter to be calculated

At last, we have same parameters whose initial value need to be calculated from laylout and process data (shows in Table). We also need following constant to get the initial values.

Boltzmann constant is :

$$k = 1.3806226 \cdot 10^{-23}\,\mathrm{JK}^{-1}, \tag{3.1}$$

Parameter	value	remark
LEVEL	504	
T_{ref}	TEMP	The actual measurement temperature
DTA	0	T_{ref} already describes the actual temperature
EXMOD	1	
EXPHI	1	
EXAVL	0	
m_{LF}	2	
X_{lb1}	0	
V_{Lr}	0.3	
X_{ext}	0.5	
a_{xi}	0.3	
V_{de}	0.9	Somewhat depending on process
p_E	0.4	
C_{BEO}	0.0	
C_{BCO}	0.0	
m_τ	1.0	
τ_B	-1.0	
τ_R	-1.0	
d_{Eg}	0.0	
X_{rec}	0.0	
A_{QB0}	0.3	Somewhat depending on process
A_E	0.0	Somewhat depending on process
A_B	1.0	Somewhat depending on process
A_{ex}	0.5	Somewhat depending on process
A_{epi}	2.0	Somewhat depending on process
A_C	0.5	Somewhat depending on process
$dV_{g\beta f}$	0.05	
$dV_{g\beta r}$	0.05	
V_{gB}	1.18	
V_{gC}	1.18	
V_{gj}	1.18	
$dV_{g\tau e}$	0.0	
V_{ds}	0.6	Somewhat depending on process
p_S	0.3	
V_{gs}	1.18	
A_S	2.0	Somewhat depending on process
R_{th}	0.0	

Table 3.7: Parameter initial value [12]

Param	Way of extraction
C_{jE}	Zero bias values of base-emitter capacitance
C_{jC}	Zero bias values of base-collector capacitance
C_{jS}	Zero bias values of substrate-collector capacitance
R_E	Numerical derivative in R_E-flyback measurement
V_{er}	Numerical derivative in reverse-Early measurement
V_{ef}	Numerical derivative in forward-Early measurement
β_f	Maximum of forward current gain
β_{ri}	Maximum of internal reverse current gain
I_S	From forward-gummel collector current without Early effect
I_{Ss}	From reverse-gummel substrate current without Early effect
τ_E, τ_B	$1/[10\ \pi\ \max(f_T)]$
I_{B0}	Zero bias value of the base current in forward-Early measurement
I_{C0}	Zero bias value of the collector current in forward-Early measurement
I_{E0}	Zero bias value of the emitter current in reverse-Early measurement

Table 3.8: Parameters that can be extracted without optimising[12]

MULT	Numbers of transistors in parallel
H_{em}	Emitter width(Dimension on silicon)
L_{em}	Emitter strip length(dimension on silicon)
ρ_p	Pinched sheet resistance of the base
N_{base}	Number of base stripes
N_{epi}	Collector epilayer doping level
W_{epi}	Collector epilayer thickness

Table 3.9: The layout and process quantities[12]

The elementary charge can be described as :

$$q = 1.6021918 \cdot 10^{-19}\,\mathrm{C}, \tag{3.2}$$

Dielectric constant is shown as:

$$\varepsilon = 1.036\dot{1}0^{-10}\,\mathrm{C/Vm}, \tag{3.3}$$

The saturated drift velocity is:

$$v_{sat} = 8.0\dot{1}0^{4}\,\mathrm{m/s}. \tag{3.4}$$

From layout data we can calculate the emitter surface and periphery

$$A_{em} = H_{em} \cdot Lem, \tag{3.5}$$

$$P_{em} = 2(H_{em} + L_{em}). \tag{3.6}$$

From the layout data and direct extraction estimates we can calculate the fraction of the BE depletion capacitance $XC_{jE}$and the fraction of the BC depletion capacitance XC_{jC}

$$XC_{jE} = \frac{P_{em}}{P_{em} + 6A_{em}/\mu m}, \tag{3.7}$$

$$XC_{jC} = XC_{jE}\frac{V_{er} \cdot C_{jE}}{V_{ef} \cdot C_{jC}}. \tag{3.8}$$

The zero bias value of the variable base resistance $R_{Bv}$and the constant part of the base resistance R_{Bc} can be estimated as

$$R_{Bv} = \frac{H_{em}\rho_p}{3N_{base}^2 L_{em}} \tag{3.9}$$

$$R_{Bc} = R_{Cc} = \frac{300\Omega\mu m}{L_{em}} \tag{3.10}$$

The initial values of the collector-emitter high injection knee current I_K and base-substrate high injection knee current I_{kS} are

$$I_K = \frac{V_{er}(1 - XC_{je})C_{je}}{\tau_B}, \tag{3.11}$$

$$I_{kS} = (500\mu A/\mu m^2) * A_{em}. \tag{3.12}$$

$$\tag{3.13}$$

The initial values of saturation current of the non-ideal reverse base current I_{Br} and saturation current of the non-ideal forward base current I_{Bf}

$$I_{Br} = 100I_S, \tag{3.14}$$

$$I_{Bf} = 100I_S. \tag{3.15}$$

The epilayer thickness used in weak-avalanche model W_{avl} and voltage determining curvature of avalanche current V_{avl} can be estimated as

$$W_{avl} = W_{epi}, \tag{3.16}$$

$$V_{avl} = \frac{qN_{epi}W_{epi}^2}{2\varepsilon}. \tag{3.17}$$

We also need some spreading parameters for the epilayer: α_l is the spreading angle at low current levels($I_C < I_{hc}$) while α_h is the spreading angle at high current levels. These quantities are process and geometry dependent. We can use the following values if we are only interested in generating an initial parameters set:

$$\tan\alpha_{\mathrm{l}} = 0.5, \tag{3.18}$$

$$\tan\alpha_{\mathrm{h}} = 1.0, \tag{3.19}$$

$$S_{Fl} = \tan\alpha_{\mathrm{l}}\mathrm{W}_{\mathrm{epi}}(\frac{1}{\mathrm{H}_{\mathrm{em}}} + \frac{1}{\mathrm{L}_{\mathrm{em}}}), \tag{3.20}$$

$$S_{Fh} = \frac{2}{3}\tan\alpha_{\mathrm{h}}\mathrm{W}_{\mathrm{epi}}(\frac{1}{\mathrm{H}_{\mathrm{em}}} + \frac{1}{\mathrm{L}_{\mathrm{em}}}). \tag{3.21}$$

The latter quantity is the current spreading factor for high injection, and is a parameter used in the high-current avalanche model. We can now calculate the epilayer parameters. The collector-base diffusion voltage:

$$V_{dc} = V_T ln(N_{epi}^2/n_i^2), \tag{3.22}$$

Resistance of the un-modulated epilayer is :

$$R_{Cv} = \frac{W_{epi}}{q\mu_0 N_{epi} A_{em}} \frac{1}{(1+S_{Fl})^2}, \tag{3.23}$$

Critical current for velocity saturation in the epilayer can be estimated as :

$$I_{hc} = q\mu_0 N_{epi} A_{em} v_{sat} (1+S_{Fl})^2, \tag{3.24}$$

The initial value of space charge resistance of the epilayer is :

$$SCR_{Cv} = \frac{W_{epi}^2}{2\varepsilon v_{saat} A_{em}} \frac{1}{(1+S_{Fl})^2}, \tag{3.25}$$

The constant part of C_{jC}, collector-base grading coefficient, coefficient for the current modulation of the collector-base depletion capacitance are:

$$X_p = xd_0/W_{epi}, \tag{3.26}$$

$$p_C = 0.3/(1 - X_p), \tag{3.27}$$

$$m_C = (1 - X_p)/2, \tag{3.28}$$

The transit time of stored epilayer charge and transit time of reverse extrinsic stored base charge are:

$$\tau_{epi} = \frac{W_{epi}^2}{4\mu_0 V_T} \tag{3.29}$$

$$\tau_R = (\tau_B + \tau_{epi}\frac{1 - XC_{jc}}{XC_{jc}}). \tag{3.30}$$

Chapter 4

Extraction of low current parameters

4.1 Base-emitter depletion capacitance

The bias dependence of the depletion capacitances is in Mextram generally considered as :

$$C_j = \frac{C_0}{(1 - \frac{V}{V_{bi}})^p}, \tag{4.1}$$

Here C_0 is the zero bias depletion capacitance, V_j is the internal P-N junction bias, V_{bi} is the junction built-in voltage and p is the grading coefficient. This method will cause singularity when applied voltage is equal to the built-in voltage. An effective junction bias V_{eff} is employed in Mextram model and the capacitance can be expressed as:

$$C_j = \frac{C_0}{(1 - \frac{V_{eff}}{V_{bi}})^p}, \tag{4.2}$$

The V_{eff} is given by:

$$V_{eff} = V - V_{ch} ln(1 + e^{\frac{V - V_F}{V_{ch}}}), \tag{4.3}$$

The advantage of using V_{eff} is that when the applied voltage is larger than built-in voltage the V_{eff} is equal to applied voltage and when the applied voltage is larger than built-in voltage the V_{eff} is equal to a constant V_F and the value of the constant V_F is given:

$$V_F = V_{bi}(1 - a_j^{-\frac{1}{p}}). \tag{4.4}$$

Figure 4.1 and 4.2 shows the behavior of V_{eff} and V_j:

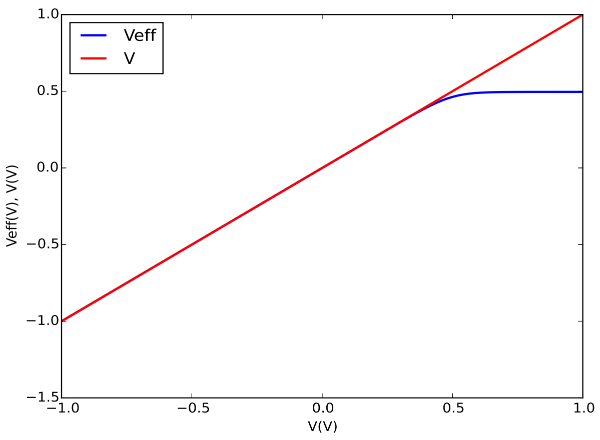

Figure 4.1: Implementation of V_{eff} in Mextram

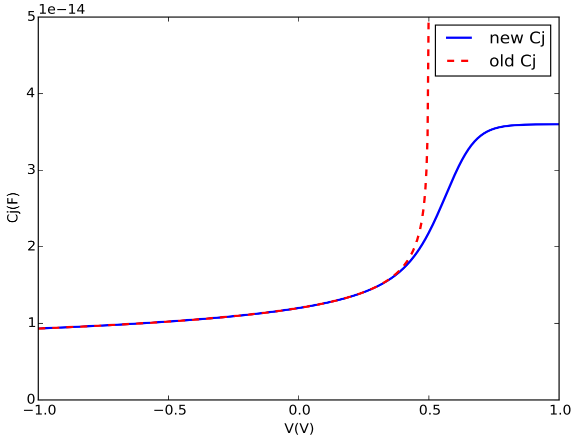

Figure 4.2: Implementation of the Mextram depletion capacitances.

The measurement C_{BE} is consisted by three parts: depletion capacitance, overlap capacitance and diffusion capacitance.The depletion capacitance and overlap capacitance dominate as long as V_{BE} bias is not too high. The base-emitter depletion capacitance can be expressed by the formula:

$$C_{BE,dep} = \frac{C_{jE}}{(1-\frac{V_{jE}}{V_{DE}})^{p_E}} + C_{BEO}, \tag{4.5}$$

The constant capacitance C_{BEO} describes any overlap capacitance between base and emitter. C_{j_E} is the zero-bias emitter base depletion capacitance, V_{d_E} is diffusion voltage and p_E describes emitter-base grading coefficient. V_{FE} is defined using the model constant a_{jE}.

$$V_{FE} = V_{d_E}\left(1 - a_{jE}^{-1/p_E}\right), \tag{4.6}$$

The effective junction bias is :

$$V_{jE} = V_{BE} - 0.1V_{d_E} ln(1 + e^{\frac{V_{BE}-V_{FE}}{0.1V_{dE}}}). \tag{4.7}$$

Actually, the sum of C_{jE} and C_{BEO} give the overall zero bias capacitance and cannot be separated clearly.

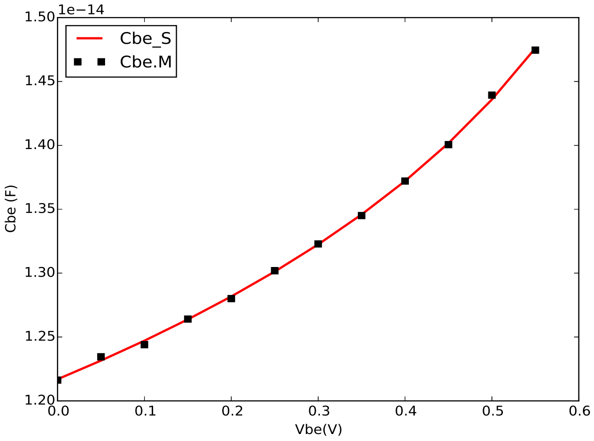

Figure 4.3: Measured(markers) and simulated(line) base emitter depletion capacitance by Python

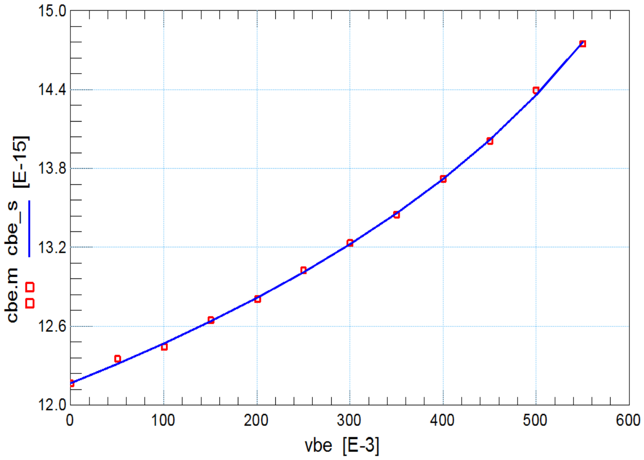

Figure 4.4: Measured(markers) and build-in function simulated(line) base emitter depletion capacitance by IC-CAP

C_{j_E} , p_E and V_{d_E} can be extracted directly by applying Equation 4.5 to fit $C_{BE} - V_{BE}$. The extraction result is shown in Figure 4.3 – figure 4.4.

4.2 Base-collector depletion capacitance

The extraction of the base-collector depletion capacitance is almost the same with the base- emitter depletion capacitance. Parameter X_p is introduced to describe the finite thickness of collector epilayer. The base-collector depletion capacitance can be written as:

$$C_{BC,dep} = \frac{(1 - X_p)C_{jc}}{(1 - V_{jc}/V_{d_c})^{p_C}} + X_p C_{jc} + C_{BCO}, \tag{4.8}$$

The constant capacitance C_{BCO} describes base-collector overlap capacitance. C_{j_C} describes zero bias collector-base depletion capacitance, p_C is collector-base grading coefficient, V_{d_C} is collector-base built-in voltage.

V_{FC} is defined using the model constant a_{j_C}.

$$V_{FC} = V_{d_C}\left(1 - \frac{a_{jC} - X_p{}^{-1/p_C}}{1 - X_p}\right), \tag{4.9}$$

The effective junction bias is :

$$V_{j_C} = V_{BC} + 0.1V_{d_C}\ln(1 + e^{(V_{BC} - V_{FC})/0.1V_{d_C}}). \tag{4.10}$$

The parameter can be extracted here is C_{j_C}, p_C and X_P by fitting the $C_{BC} - V_{BC}$ curve as shown in Figure4.5 - 4.6. Help parameter V_{d_C} will be re-extracted with other high current parameter later, because it has strong impact on the current gain roll-off, cut-off frequency roll-off and output characteristics quasi-saturation region.

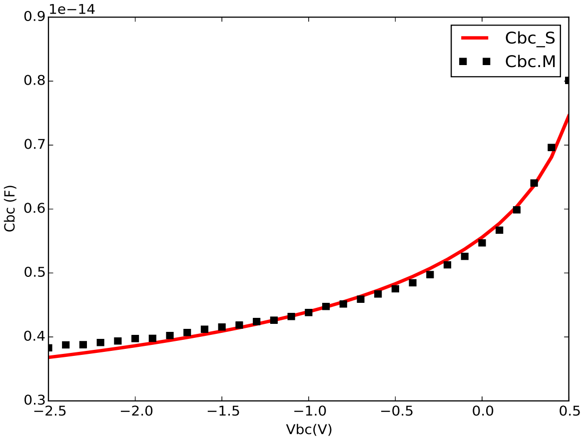

Figure 4.5: Measured(markers) and simulated(line) base collector depletion capacitance by Python

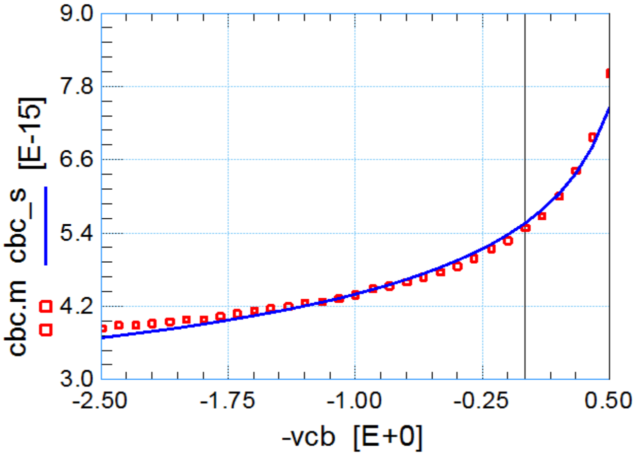

Figure 4.6: Measured(markers) and build-in function simulated(line) base collector depletion capacitance by IC-CAP

4.3 Collector-substrate depletion capacitance

The extraction of collector-substrate capacitance is also similar to the base-emitter capacitance. The collector-substrate depletion capacitance can be written as :

$$C_{SC} = \frac{C_{js}}{(1 - V_{js}/V_{ds})^{p_S}} + C_{p.CS}, \tag{4.11}$$

C_{j_S} describes zero bias collector-substrate depletion capacitance and P_S is collector-substrate grading coefficient , V_{d_S} is collector-substrate built-in voltage. $C_{p.CS}$ is not a part of Mextram model, it is included here for convenience in the case of de-embedding problems.

V_{FS} is defined using the model constant a_{j_C}.

$$V_{FS} = V_{d_S}\left(1 - a_{j_C}^{-1/p_S}\right), \tag{4.12}$$

The effective junction bias is :

$$V_{j_S} = V_{SC} + 0.1V_{d_S}\ln(1 + e^{(V_{SC}-V_{FS})/0.1V_{dS}}). \tag{4.13}$$

C_{j_S} and p_S can be extracted directly through Equation 4.11. Figure 4.7 - 4.8 show the extracted $C_{SC} - V_{SC}$ result.

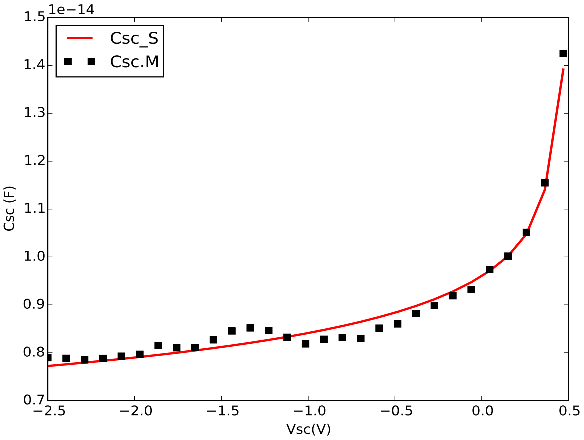

Figure 4.7: Measured(markers) and simulated(line) collector substrate depletion capacitance by Python

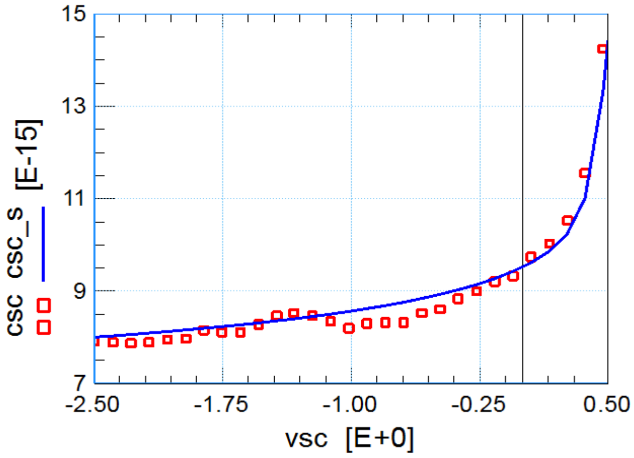

Figure 4.8: Measured(markers) and build-in function simulated(line) collector substrate depletion capacitance by IC-CAP

4.4 Avlanche

In modern transistor because we have low breakdown voltage we can not neglect avalanche effect. The avalanche current is a result of impact ionisation in the epilayer due to the high electric fields. This generation of avalanche currents strongly depends on the maximum electric field. The low current avalanche parameters are extracted from base current under forward-early measurement shown in Figure 4.9. Because of avalanche current the base voltage will drop down as the increase of V_{CB}. So that the avalanche current can be written as:

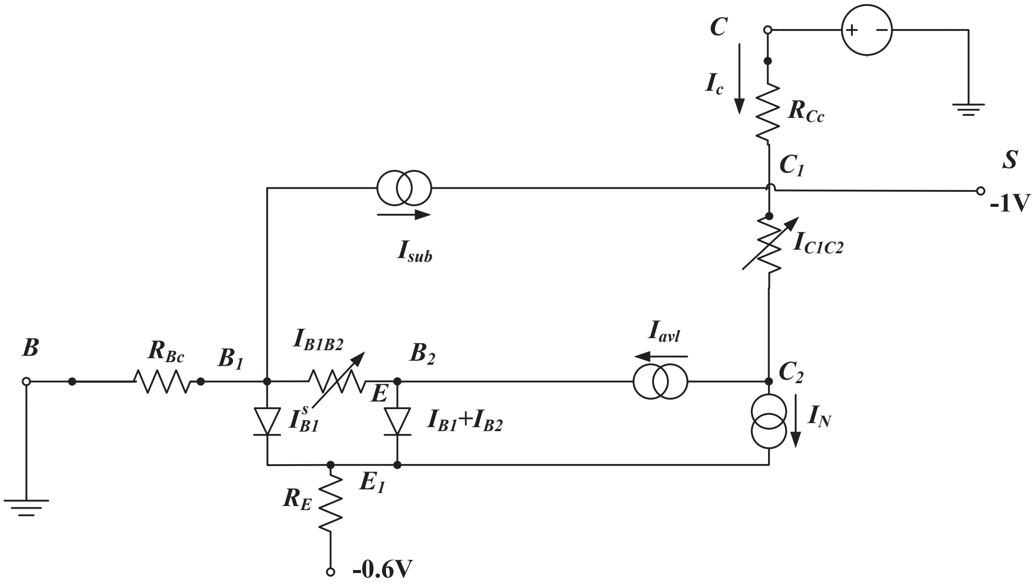

Figure 4.9: Forward-Early measurement simplified circuit

$$I_{avl} = I_{B0} - I_B. \tag{4.14}$$

Here I_{B0} is a help variable that shows the base current at $V_{CB} = 0$ .The avalanche current can also be describe as:

$$I_{avl} = I_C \, G_{EM}, \tag{4.15}$$

G_{EM} is the generation coefficient. From the measurement data we can calculate the measurement G_{EM} as:

$$G_{EM}.m = \frac{I_{B0} - I_B}{I_C} \tag{4.16}$$

The simulation G_{EM} is :

$$G_{EM} = \frac{A_n}{B_n} E_M \lambda_D \{exp[\frac{-B_n}{E_M}] - exp[-\frac{B_n}{E_M}(1 + \frac{W_{avl}}{\lambda_D})]\}, \tag{4.17}$$

A_n and B_n are material constants, which are avalanche coefficient and critical electric field respectively.λ_D is the extrapolated depletion thickness where the electric field is zero, effective width of the epilayer for avalanche current W_{AVL} and voltage describing the curvature of the avalanche current V_{AVL} are parameters we need to extract here.

$$\lambda_D = \frac{W_{avl}^2}{2V_{avl}} E_M, \tag{4.18}$$

E_M is the maximum electric field in the depletion region and it can be obtained from:

$$E_M = \frac{V_{d_C} + V_{CB} + 2\,V_{avl}}{W_{avl}} \sqrt{\frac{V_{d_C} + V_{CB}}{V_{d_C} + V_{CB} + V_{avl}}}. \tag{4.19}$$

W_{AVL} and V_{AVL} can be extracted from the comparison of the simulated and measured G_{EM}. The extraction result is shown in Figure 4.12- 4.13. As the collector-base bias gets larger, the base current drops below zero because of the avalanche effect.

4.5 Reverse Early effect

In Mextram model the forward and reverse Early effects are bias-dependent. The parameters V_{er} and V_{ef} are the values of these bias-dependent Early voltage when both the base-emitter and base-collector bias are zero. The reverse-early voltage V_{er} is extracted from the reverse-Early measurement as shown in Figure 4.14. The emitter current is :

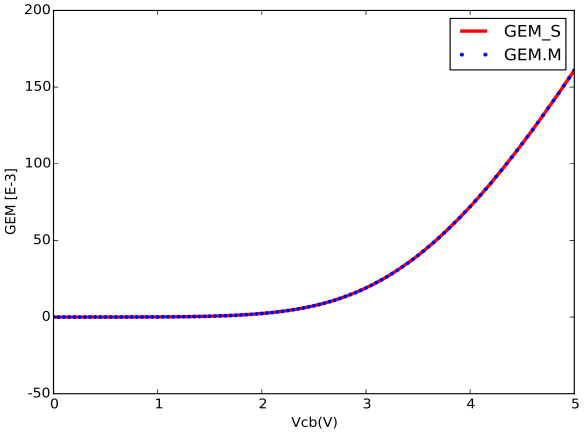

Figure 4.10: Measured(markers) and simulated(line) G_{EM}t in forward-Early measurement by Python

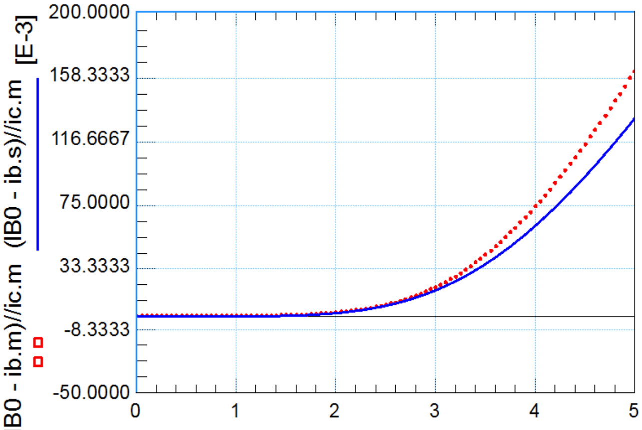

Figure 4.11: Measured(markers) and simulated(line) G_{EM} by IC-CAP

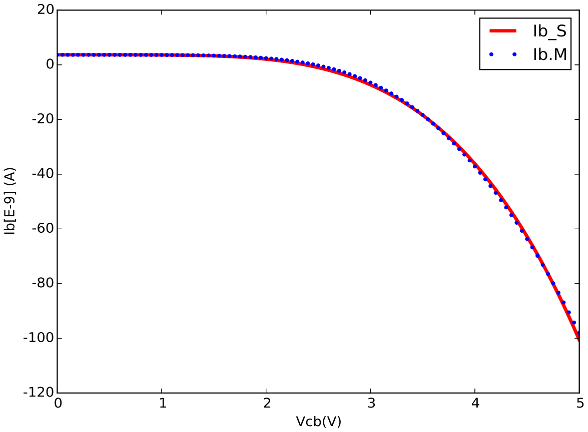

Figure 4.12: Measured(markers) and simulated(line) base current in forward-Early measurement by Python

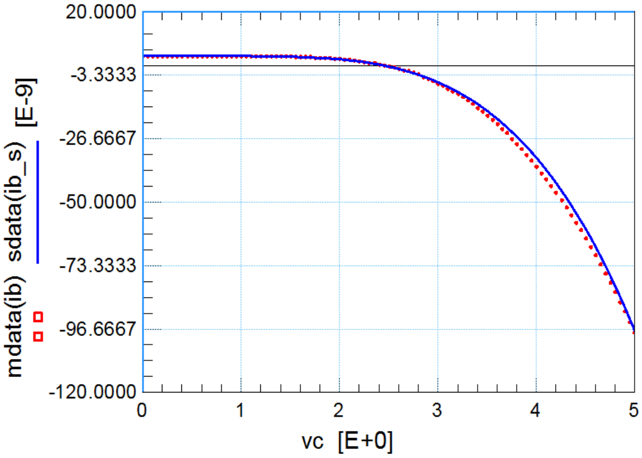

Figure 4.13: Measured(markers) and simulated(line) base current in forward-Early measurement by IC-CAP

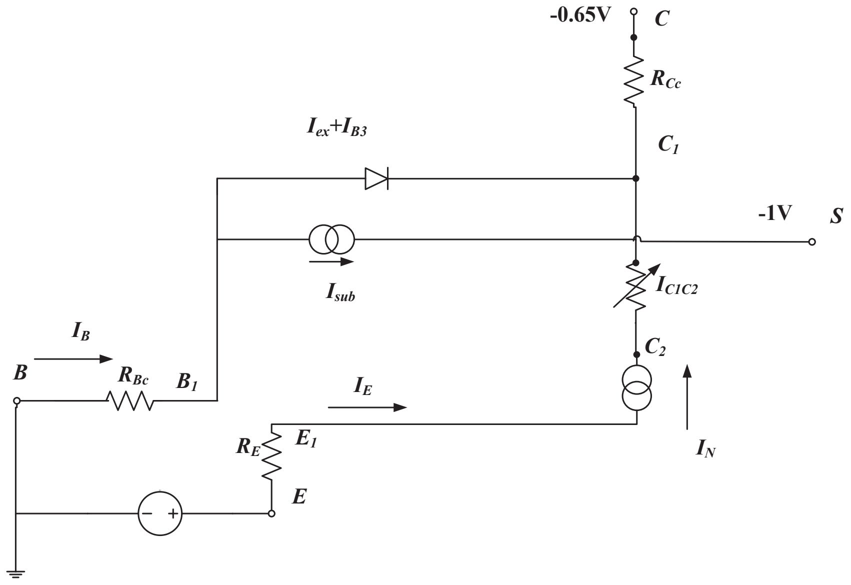

Figure 4.14: Reverse-Early measurement simplified circuit

$$I_E = I_{E0}\frac{1+\frac{V_{t_C}}{V_{ef}}}{1+\frac{V_{t_E}}{V_{er}}+\frac{V_{t_C}}{V_{ef}}}. \tag{4.20}$$

Here I_{E0} is a help variable which is the emitter current at $V_{BE}=0$, V_{t_E} and V_{t_C} are variables related to base-emitter depletion charges and base-collector depletions charges. The forward early voltage parameter V_{ef} also has a key effect on emitter current which means if we want to extract V_{er}, we must have a good estimate value of V_{ef}. Therefore, we will do the extraction twice, first we extract V_{er} and the first time extraction result is shown in Figure 4.15 and 4.16, then V_{ef}, then redo this procedure again. For the calculation of the normalised charges V_{t_E} and V_{t_C} we neglect the voltage drop over the resistance.

$$V_{t_E} = \frac{V_{d_E}}{1-p_E}\left[1-(1-V_{jE}/V_{d_E})^{1-p_E}\right] + a_{jE}(V_{BE}-V_{jE}), \tag{4.21a}$$

$$V_{t_C} = (1-X_p)\left(\frac{V_{d_C}}{1-P_C}\left[1-(1-V_{jC}/V_{d_C})^{1-p_C}\right]+b_{jC}(V_{BC}-V_{jC})\right)+X_pV_{BC}. \tag{4.21b}$$

The early voltage is given by:

$$V_{reverse-early} = I_E\left(\frac{\partial I_E}{\partial V_{EB}}\right)^{-1} \tag{4.22a}$$

$$= I_{E0}\frac{1+\frac{V_{t_C}}{V_{ef}}}{1+\frac{V_{t_E}}{V_{er}}+\frac{V_{t_C}}{V_{ef}}}\frac{V_{er}\left(1+\frac{V_{t_E}}{V_{er}}+\frac{V_{t_C}}{V_{ef}}\right)^2}{I_{E0}\left(1+\frac{V_{t_C}}{V_{ef}}\right)\frac{dV_{t_E}}{dV_{BE}}} \tag{4.22b}$$

$$= \frac{C_{j_E}V_{er}}{C_{BE}}\left(1+\frac{V_{t_E}}{V_{er}}+\frac{V_{t_C}}{V_{ef}}\right). \tag{4.22c}$$

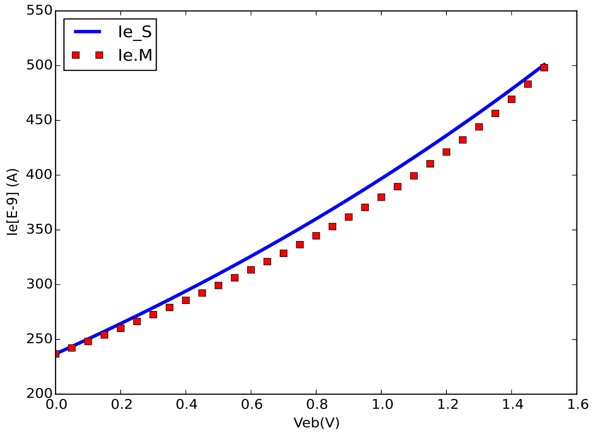

Figure 4.15: Measured(markers) and simulated(line) emitter current of first time extraction in reverse-Early measurement by Python

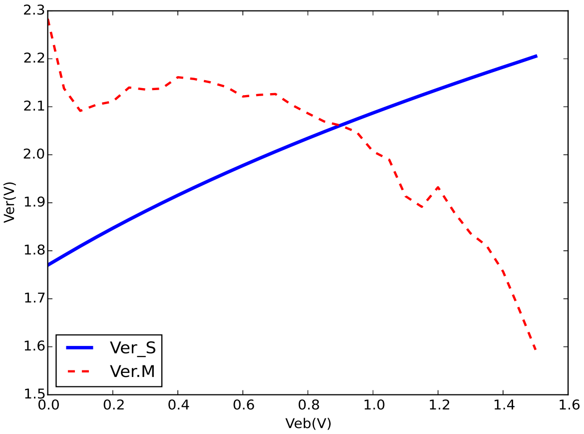

Figure 4.16: First time extraction of actual reverse Early voltage by numerical differentiation of the measured(dash line) and simulated(solid line) collector current of in the reverse-Early measurement by Python

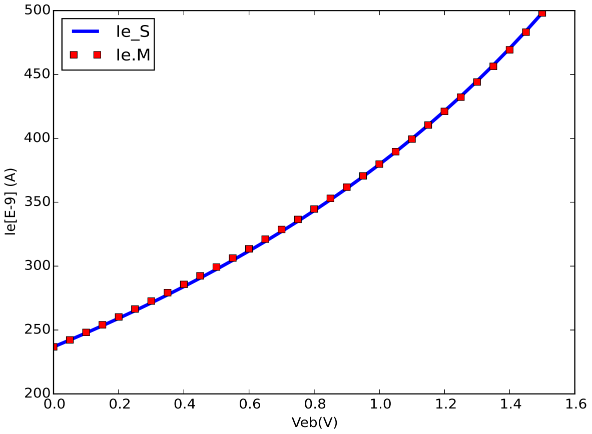

Figure 4.17: Measured(markers) and simulated(line) emitter current in reverse-Early measurement by Python

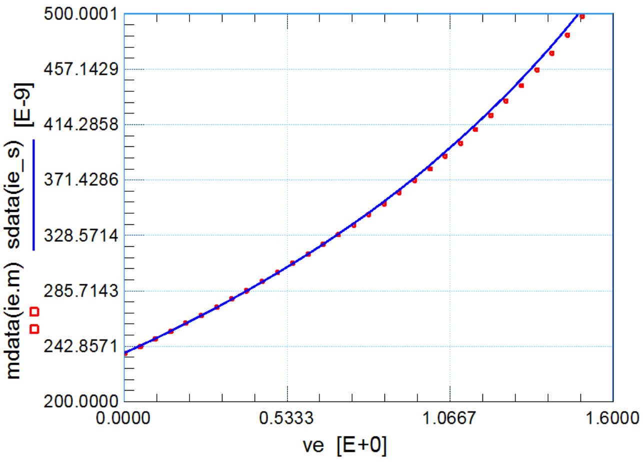

Figure 4.18: Measured(markers) and build-in function simulated(line) emitter current in reverse-Early measurement by IC-CAP

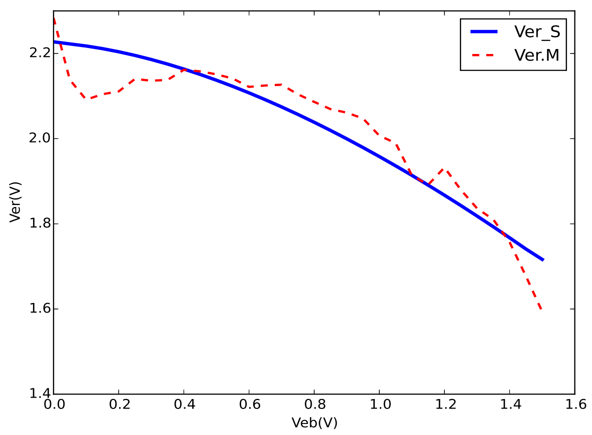

Figure 4.19: Actual reverse Early voltage by numerical differentiation of the measured(dash line) and simulated(solid line) collector current in the reverse-Early measurement by Python

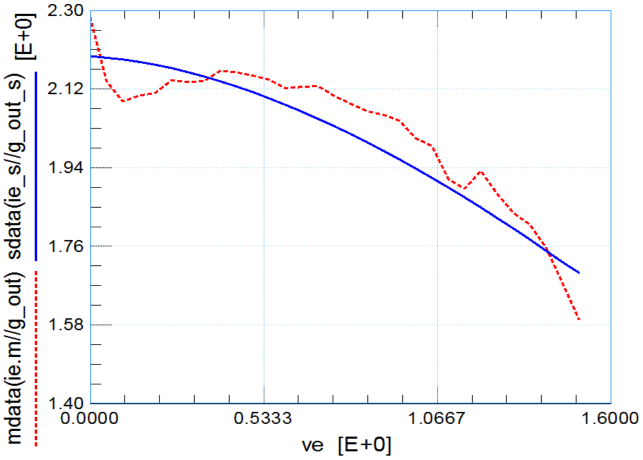

Figure 4.20: Actual reverse Early voltage by numerical differentiation of the measured(dash line) and build-in function simulated(solid line) collector current in the reverse-Early measurement by IC-CAP

C_{j_E} is the zero-bias emitter base depletion capacitance, C_{BE} is emitter base depletion capacitance. Note that the measurement point of reverse-early voltage is not actual measurement data, it is calculated from measurement emitter current and measurement emitter voltage. As the result shown in Figure 4.17 to 4.20, we match the measurement and simulated emitter current and reverse early voltage together to extract V_{er}.

4.6 Forward Early effect

The forward-early voltage parameter v_{ef} is extracted in forward-early measurement shown in Figure 4.9. The approximation for the collector current in forward-early measurement can be written as:

$$I_C = I_{C0} \frac{1 + \frac{V_{t_E}}{V_{er}}}{1 + \frac{V_{t_E}}{V_{er}} + \frac{V_{t_C}}{V_{ef}}}. \tag{4.23}$$

I_{C0} is a help variable which stand for collector current at zero base collector bias.

Then we can calculate the Early voltage:

$$\begin{aligned} V_{forward-early} &= I_C \left(\frac{\partial I_C}{\partial V_{CB}} \right)^{-1} \qquad (4.24)\\ &= I_{C0} \frac{1 + \frac{V_{t_E}}{V_{er}}}{1 + \frac{V_{t_E}}{V_{er}} + \frac{V_{t_C}}{V_{ef}}} \frac{V_{ef} \left(1 + \frac{V_{t_E}}{V_{er}} + \frac{V_{t_C}}{V_{ef}}\right)^2}{I_{C0} \left(1 + \frac{V_{t_E}}{V_{er}}\right) \frac{dV_{t_C}}{dV_{CB}}} \qquad (4.25)\\ &= \frac{C_{jC} V_{ef}}{C_{BC}} \left(1 + \frac{V_{t_E}}{V_{er}} + \frac{V_{t_C}}{V_{ef}}\right). \qquad (4.26) \end{aligned}$$

C_{j_C} describes zero bias collector-base depletion capacitance and C_{BC} is collector-base depletion capacitance. Changing V_{ef} can match the simulation collector current and forward early voltage to measurement data, so that V_{ef} can be extracted here. Result is shown in Figure 4.23 - 4.26.

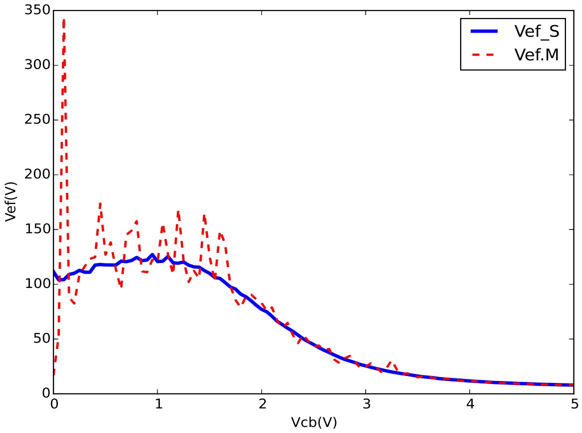

Figure 4.21: Measured(markers) and simulated(line) collector current of first time extraction in forward-Early measurement by Python

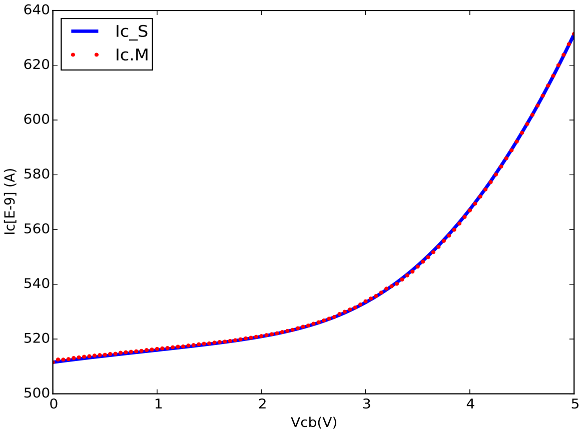

Figure 4.22: First time extraction of actual forward Early voltage by numerical differentiation of the measured(dash line) and simulated(solid line) collector current of in the forward-Early measurement by Python

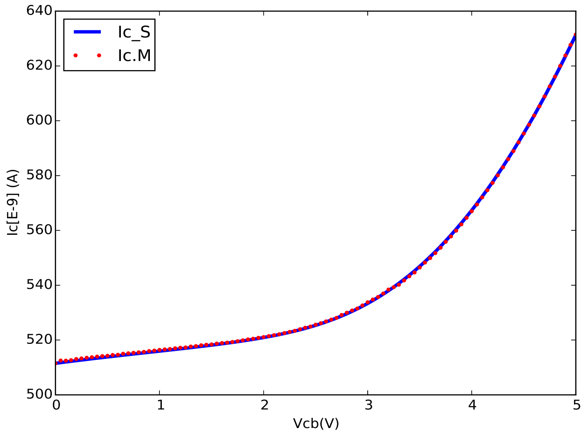

Figure 4.23: Measured(markers) and simulated(line) collector current in forward-Early measurement by Python

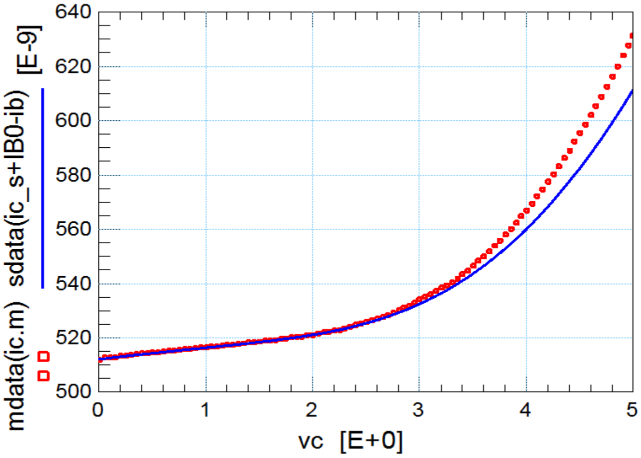

Figure 4.24: Measured(markers) and build-in function simulated(line) collector current in forward-Early measurement by IC-CAP

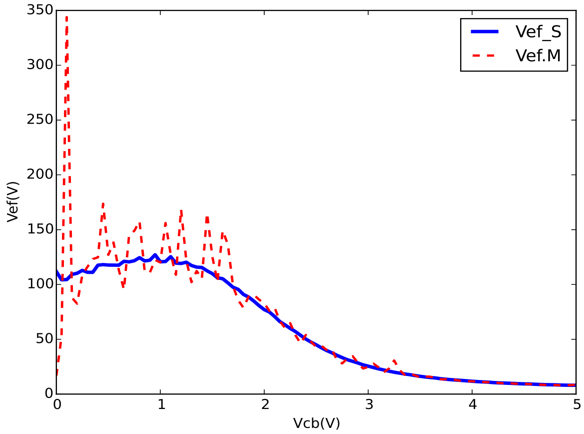

Figure 4.25: Actual forward Early voltage by numerical differentiation of the measured(dash line) and simulated(solid line) collector current in the forward-Early measurement by Python

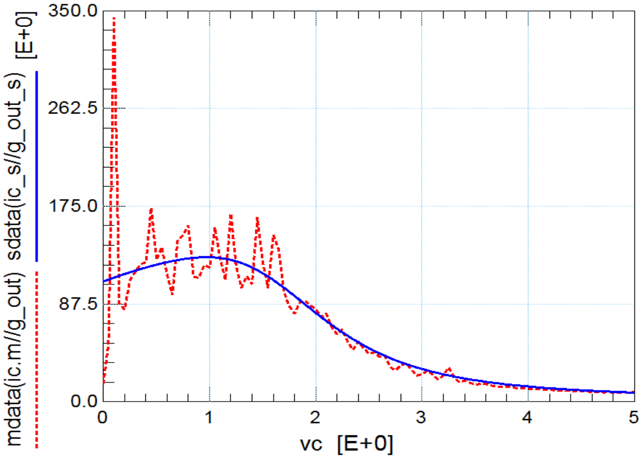

Figure 4.26: Actual forward Early voltage by numerical differentiation of the measured(dash line) and simulated(solid line) collector current in the forward-Early measurement by IC-CAP

4.7 Collector saturation current

Since we have a good description of Early effect, we can extract the collector saturation current using forward-Gummel measurement(shown in Figure 4.27) at low base-emitter bias.

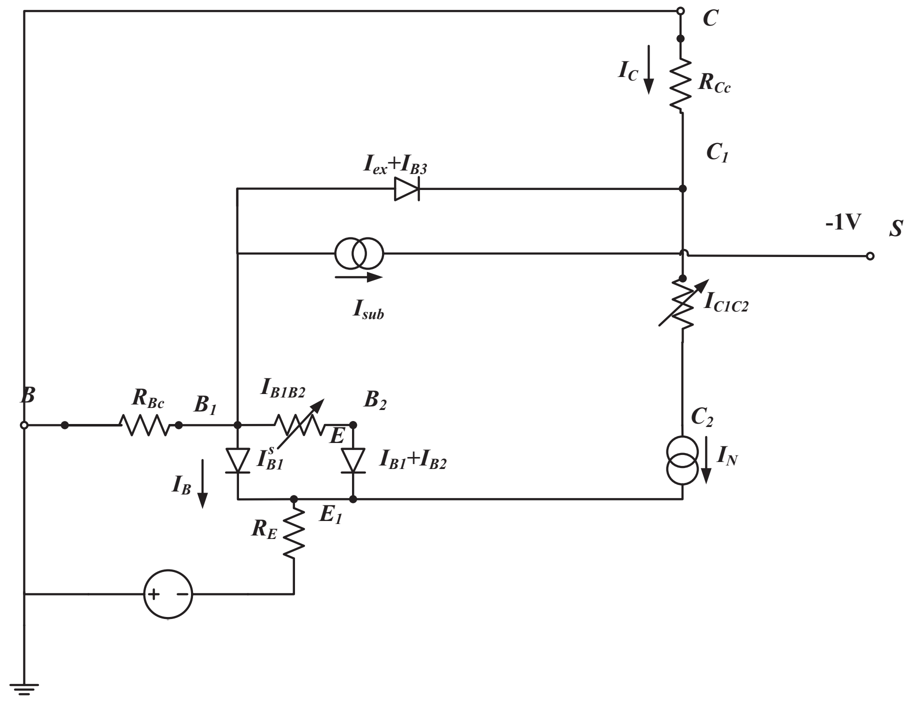

Figure 4.27: Forward-Gummel measurement simplified circuit

The collector current I_S is proportional to the increase of base-emitter bias at low bias. At high bias the resistance effect can not be neglected and the actual V_{B_2E1} will be much less than V_{BE} we used , which is the reason that measurement data and simulation data is split in high bias. So we will only focus on the low bias behavior and optimize data at low bias area. The collector current can be describe as:

$$I_C = \frac{I_S\, e^{V_{BE}/V_T}}{1 + \frac{V_{t_E}}{V_{er}} + \frac{V_{t_C}}{V_{ef}}}. \tag{4.27}$$

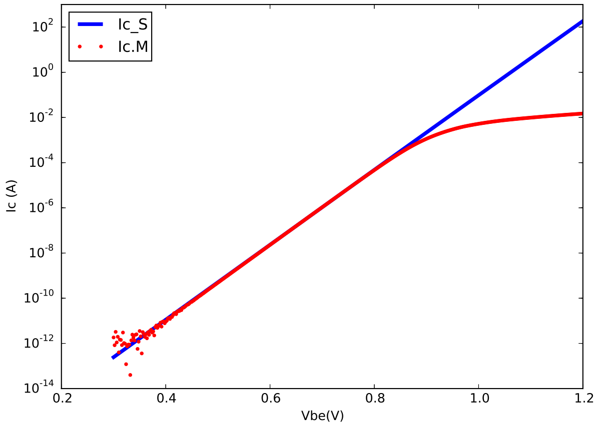

Figure 4.28: Measured(markers) and simulated(line) collector current in forward-Gummel measurement by Python

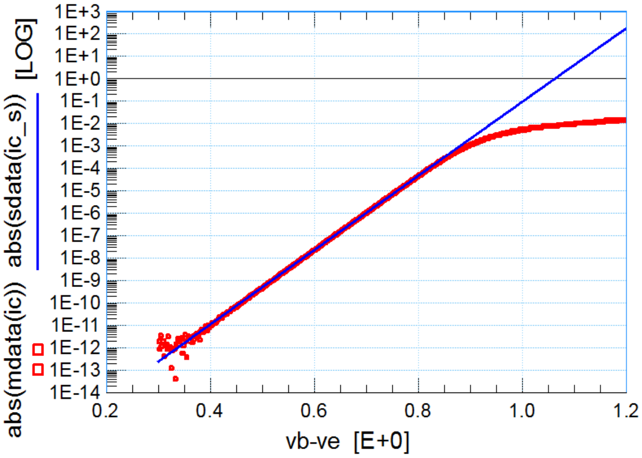

Figure 4.29: Measured(markers) and simulated(solid line) collector current in forward-Gummel measurement by IC-CAP

V_{t_E} and V_{t_C} have been defined in (4.21). Here V_T is the thermal voltage, which needs to be determined accurately from the actual absolute temperature. Changing collector saturation current I_S can make the simulation collector current match the measurement collector current thus I_S can be extracted and the result is shown in Figure 4.28 - 4.29.

4.8 Forward base current

The parameters of forward base current are extracted from base current in forward-Gummel measurements (shown in Figure 4.27) by comparing the measurement forward base current and simulated forward base current. The forward current only depends on the internal base-emitter voltage $V_{B_2E_1}$ and neglect the voltage drops on base resistance.

We use the Equation (4.27) to calculate internal base-emitter bias from measured I_C:

$$V_{B_2E_1} = V_T \ln\left[\frac{I_C}{I_S}\left(1 + \frac{V_{t_E}}{V_{er}} + \frac{V_{t_C}}{V_{ef}}\right)\right], \tag{4.28}$$

As we take the internal bias equal to the external bias V_{BE}, we must make sure that resistance effects are not important so we need to fit the curve at low base-emitter bias.

V_{t_E} and V_{t_C} are given in (4.21).The ideal and non-ideal base current can be calculated:

$$I_{B1} = \frac{I_S}{\beta_f} e^{V_{B_2E_1}/V_T}, \tag{4.29a}$$

$$I_{B2} = I_{Bf}\left(e^{V_{B_2E_1}/m_{Lf}V_T} - 1\right), \tag{4.29b}$$

Here ideal forward current gain β_f, saturation current of the non ideal forward base current

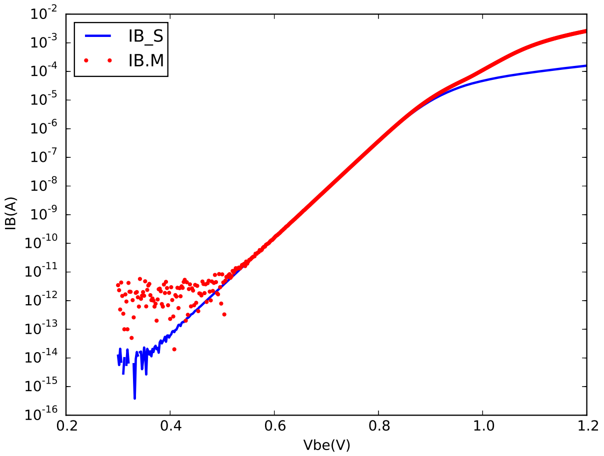

Figure 4.30: Measured forward base current(marker) and simulated forward base current I_B - V_{BE} in Forward-gummel measurement

I_{Bf} and none-ideality factor of the non-ideal forward base current m_{Lf} are used.

β_f, I_{Bf} and m_{Lf} are extracted here from the comparison of simulated forward base current and the measurement forward base current shown in Figure 4.30. Again we only extract data from the low bias area at high bias the voltage drop at R_{Cc} can not be ignored which is the reasons that measured and simulated base current can not match together at high bias.

4.9 Substrate saturation current

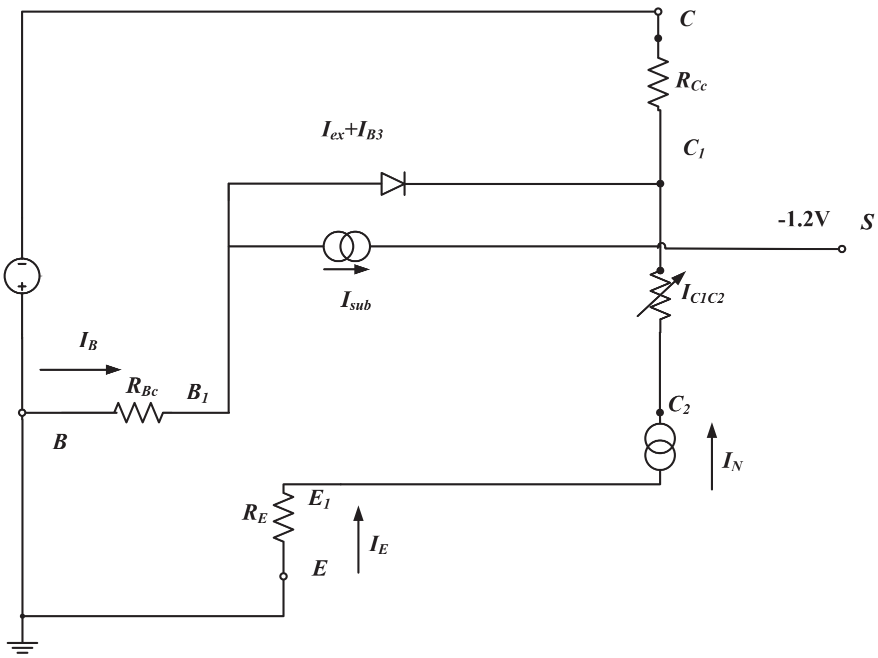

Figure 4.31: Reverse-Gummel measurement simplified circuit

The substrate saturation current is extracted in reverse-Gummel measurement as shown in Figure 4.31 by fitting the substrate current . We will neglect the voltage drop and the substrate current can be calculate by:

$$I_{sub} = I_{Ss} \exp(\frac{V_{BC}}{V_T}), \tag{4.30}$$

I_{Ss} can be extracted directly from the substrate current. The extraction result is given in Figure 4.32. At high bias, because of the voltage drop over R_{Cc} measured and simulated substrate current can not be fit at high base-collector bias.

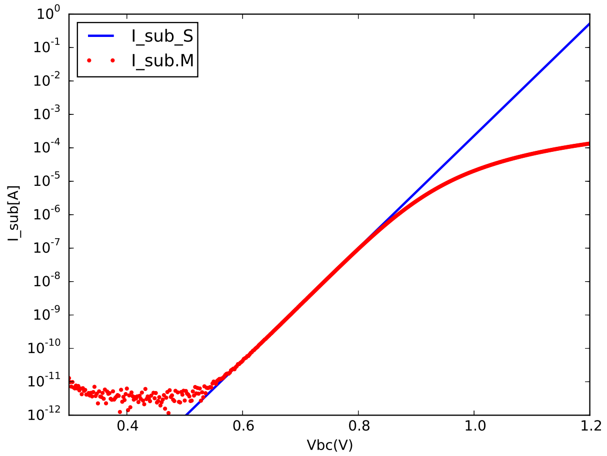

Figure 4.32: Measured (mark) and simulated (line) substrate current in reverse-Gummel measurement

4.10 Reverse current

The reverse current parameters are extracted from reverse-Gummel measurement. In the reverse-Gummel measurement (shown in Figure 4.27) the base-collector is forward biased which means the external base current contains internal base current and substrate current.

The internal base-collector bias $V_{B_1C_1}$ is calculated :

$$V_{B_1C_1} = V_T \ln\left[\frac{I_E}{I_S}\left(1 + \frac{V_{t_E}}{V_{er}} + \frac{V_{t_C}}{V_{ef}}\right)\right], \tag{4.31}$$

Note here we use measurement emitter current.From $V_{B_1C_1}$ we can calculate extrinsic reverse base current I_{ex} and non-ideal reverse base current I_{B3}. They can be described as:

$$I_{ex} = \frac{I_S}{\beta_{ri}} e^{V_{B_1C_1}/V_T}, \tag{4.32}$$

$$I_{B3} = I_{Br} \frac{e^{V_{B_1C_1}/V_T}}{e^{V_{B_1C_1}/2V_T} + e^{V_{Lr}/2V_T}}. \tag{4.33}$$

The reverse current gain β_{ri}, Saturation current of the non-ideal reverse base current I_{Br} and Cross-over voltage of the non-ideal reverse base current V_{Lr} are variable of I_{ex} and I_{B3}, so that they can be extracted by fitting the curve. The measured reverse base current and simulated reverse base current plot is given in Figure 4.33. Again we need only concentrate on the low base-collector bias. At high base-collector bias the votage drop at R_E can not be neglect and the internal base-emitter will be forward biased, and current will flow from base to emitter. This is the reason measured reverse base current is bigger than simulated reverse base current.

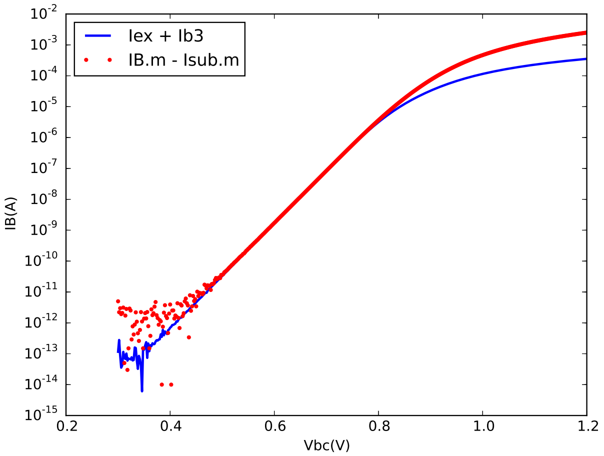

Figure 4.33: The measured I_B - I_{sub} and simulated $I_{ex} + I_{B3}$ in reverse-Gummel measurement

4.11 Emitter series resistances

One of the simplest way to extract the emitter resistance is from the Giacoletto method [19] [20]. The collector current is kept zero and the V_{BE} is increased . The collector-emitter saturation voltage can be estimated as $V_{CES} \approx I_E R_E$. Then the emitter resistance can be obtained by taking the derivative of V_{CES} with regard to I_E:

$$R_E = \frac{\partial V_{CES}}{\partial I_E}. \tag{4.34}$$

However, here we use another method[21] , here the emitter series resistances is extracted in forward-Gummel measurement(shown in Figure 4.27). The external base-emitter bias can be described as a sum of then internal junction bias and voltage drop over series resistance:

$$V_{BE} = V_{B_2E_1} + V_{B_1B_2} + I_B\, R_{Bc} + (I_B + I_C)\, R_E + V_{off,Rb}, \tag{4.35}$$

The internal junction bias $V_{B_2E_1}$ can be solved iteratively using the measurement base current and Equation4.29.

The voltage drop over the pinched resistance gives only small contribution but we do want to include the variation of the resistance due to charge modulation and current crowding. The charge modulation can is:

$$R_{mod} = \frac{R_{Bv}}{q_B}, \tag{4.36}$$

$$I_C = \frac{I_f - I_r}{q_B} \simeq \frac{I_s\, exp(V_{B_2E_1}/V_T)}{q_B}, \tag{4.37}$$

This is only true under the assumption that quasi-saturation is not important which means that I_r can be neglect. We also assume that non-ideal base current is negligible, the voltage drop is:

$$I_B\, R_{mod} \simeq I_C R_{Bv}/\beta_f, \tag{4.38}$$

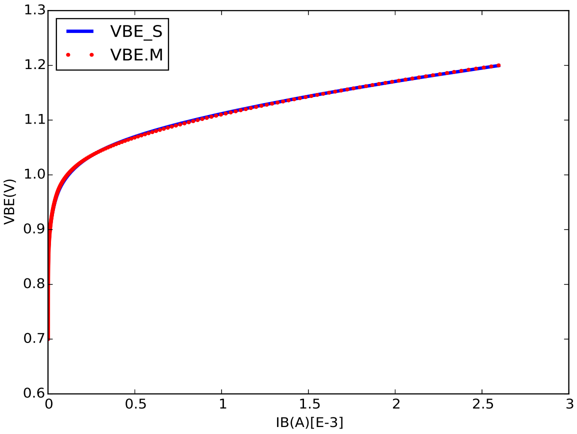

Figure 4.34: Measured(markers) and simulated(line) base-emitter bias as function of the base current in the forward-Gummel measurement by Python

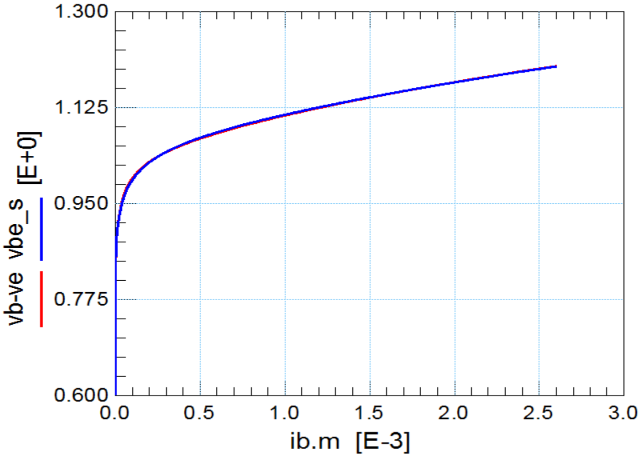

Figure 4.35: Measured(markers) and build-in function simulated(line) base-emitter bias as function of the base current in the forward-Gummel measurement by IC-CAP

To include some current crowding effect and the fact that a part of the base current might go through the side-wall we can get:

$$V_{B_1B_2} = V_T \ln\left(1 + \frac{R_{Bv}\, I_C\,(1 - Xl_{B_1})}{\beta_f\, V_T}\right). \tag{4.39}$$

The emitter series resistance R_E is the only variable in Equation 4.35 thus it can be extracted by fitting the curve. There are also some other methods to extract emitter series mentioned in [22] [23].

4.12 Collector series resistances

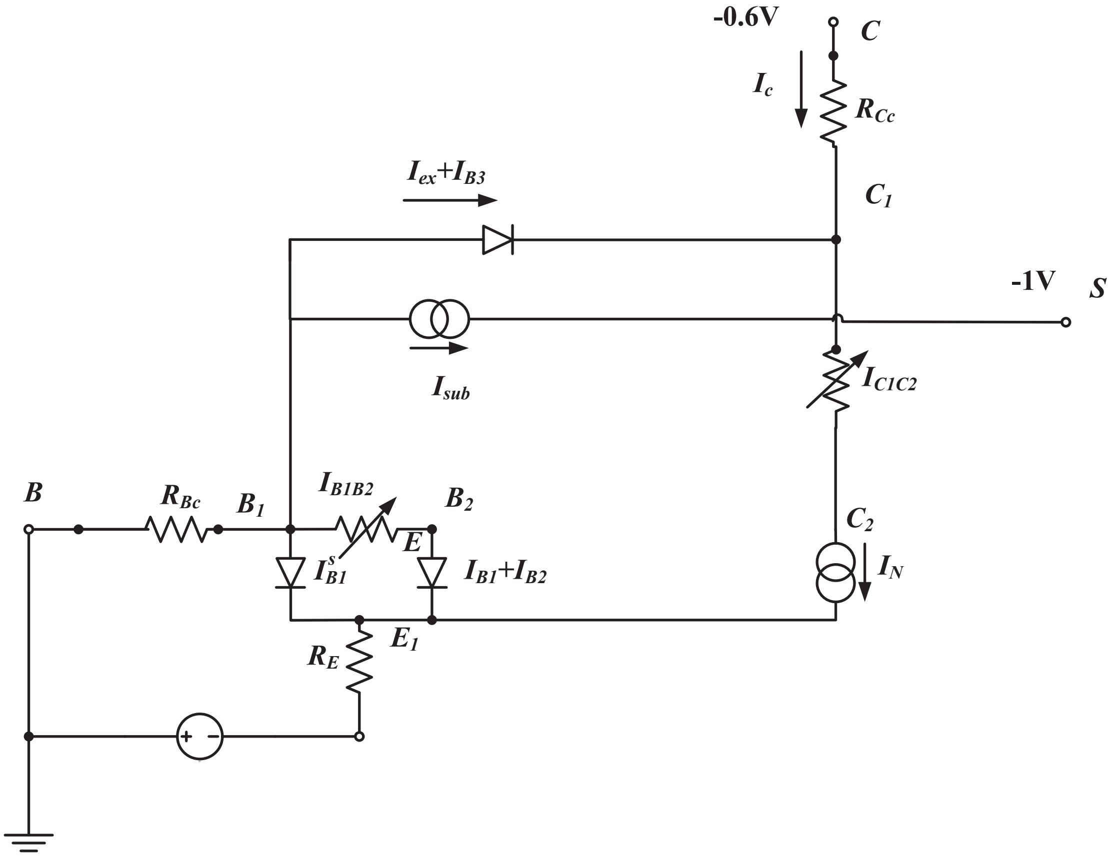

Figure 4.36: R_{Cc}-active measurement simplified circuit

The collector series resistance R_{Cc} can be extracted from the substrate current in the dedicated $R_{Cc} - active$ measurement. The intrinsic base-collector bias can be shown as:

$$V_{B_1C_1} = V_{BC} + R_{Cc}I_C - R_{Bc}I_B, \tag{4.40}$$

We will neglect the voltage drop so the substrate current can be described as:

$$I_{sub} = \frac{2 I_{Ss} e^{V_{B_1 C_1}/V_T}}{1 + \sqrt{1 + \frac{I_S}{I_{ks}} e^{V_{B1C1}/V_T}}}. \tag{4.41}$$

Again we will only extract parameters using the low bias data. At high bias, because of the voltage drop over R_{bcli},$V_{B_1 C_4}$ will be smaller than $V_{B_1 C_1}$, so the measurement substrate current is smaller than simulated one at high bias. The collector series resistance and constant part of the base resistance R_{Bc} can be extracted from the comparison of the simulated and measured substrate current.

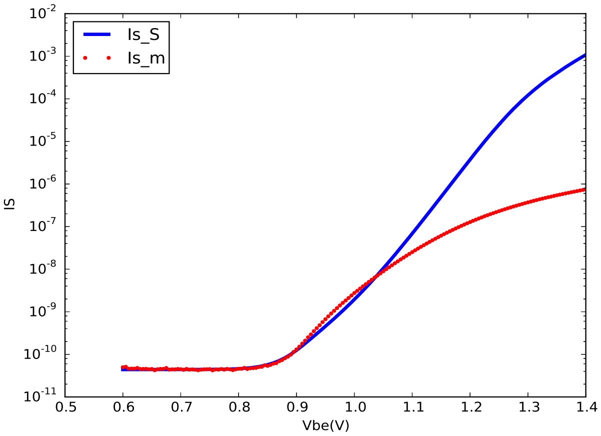

Figure 4.37: Measured(markers) and simulated(line) substrate current in the Rcc-active measurement by Python

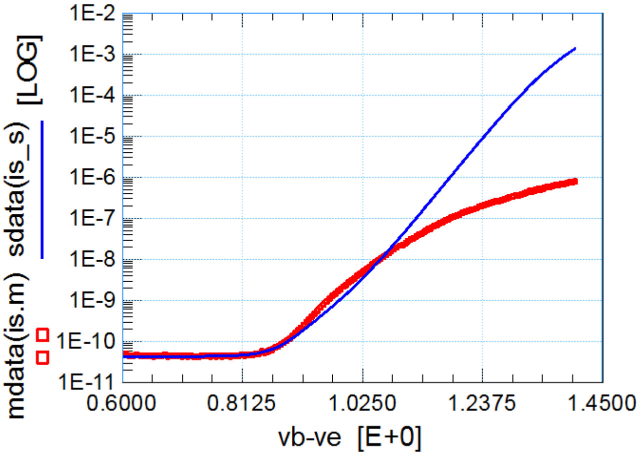

Figure 4.38: Measured(markers) and build-in function simulated(line) substrate current in the Rcc-active measurement by IC-CAP

Chapter 5

Extraction of high current parameters

5.1 Self-heating

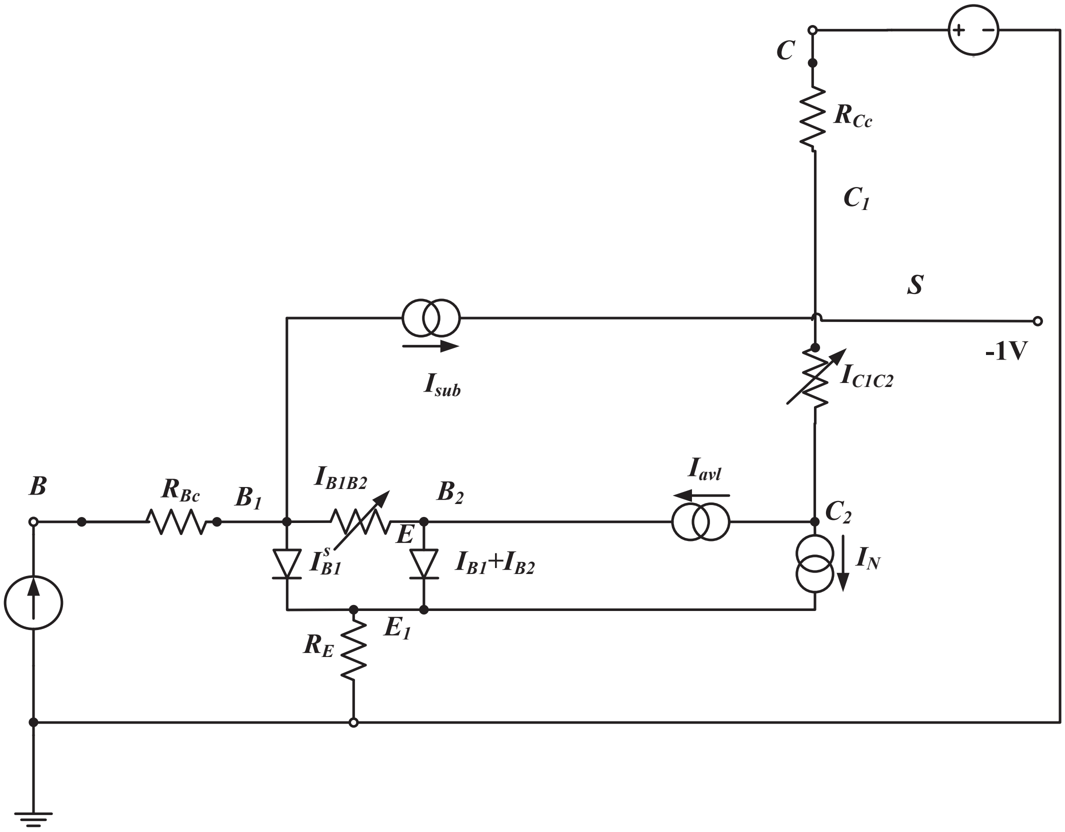

Figure 5.1: Force-IB output characteristic measurement simplified circuit

For the high current parameters we will need include temperature scaling rules, see in next chapter. Thermal resistance R_{th} is extracted from the base emitter voltage at high V_{CE} using the output-characteristic measurements shown in Figure 5.1. Since the junction temperature is determined by the thermal resistance for a given power dissipation, accurate modeling of the thermal resistance R_{th} is critical for the modeling of junction temperature, and therefore the temperature characteristics of device Due to the self-heating the temperature of the transistor will rise with an amount of:

$$\Delta T = R_{th}\left(I_B V_{BE} + I_C V_{CE}\right). \tag{5.1}$$

The collector part is the most important to self-heating and the values of R_{th} are about 100-500 °C/W. The temperature will increase with the increase of V_{CE}, and V_{BE} can be express by:

$$V_{BE} \simeq V_T ln\left(\frac{I_B \beta_{fT}}{I_{sT}}\right) \tag{5.2}$$

Note that from here on we will using parameters that after temperature scaling rule. As the base current is constant and β_f will decrease with the temperature growing and the I_s increases with the increases of temperature. The base-emitter voltage will decrease. The thermal resistance can be extracted from drop of the base-emitter voltage in the output-characteristic measurement for which the base current is constant.

The base-emitter is:

$$V_{BE} = V_{B_2E_1} + V_{B_1B_2} + I_B R_{B_CT} + (I_C + I_B)R_{ET}, \tag{5.3}$$

The voltage drop $V_{B_1B_2}$ can be estimated as:

$$V_{B_1B_2} = V_T \log\left(1 + \frac{R_{BvT} I_B (1 - X i_{B_i})}{V_T q_B}\right). \tag{5.4}$$

The only unknown part of this equation is the normalized base charge q_B, and it can be calculated:

$$q_1 = 1 + \frac{V_{t_E}}{\mathrm{V_{erT}}} + \frac{V_{t_C}}{\mathrm{V_{efT}}}, \tag{5.5}$$

$$q_B = q_1\,(1 + 0.5\,n_0 + 0.5\,n_B). \tag{5.6}$$

where n_0 and n_B are the electron densities in the base at the emitter edge and at the collector edge, the voltages V_{tE} and V_{tC} describe the curvature of the depletion charges as function of junction biases. In order to get q_B we need to know n_0 , n_B, V_{tE} and V_{tC}.

The electron densities in the base at the emitter edge n_0 can be calculated from $V_{B_2E_1}$ as :

$$f_1 = \frac{4\,\mathrm{I_{sT}}}{\mathrm{I_{kT}}}\; e^{V_{B_2E_1}/V_T}, \tag{5.7a}$$

$$n_0 = \frac{f_1}{1+\sqrt{1+f_1}}. \tag{5.7b}$$

The voltage V_{t_E} also can be calculated from the voltage:

$$V_{FE} = \mathrm{V_{d_ET}}\left(1 - \mathrm{a_{jE}^{-1/p_E}}\right), \tag{5.8}$$

$$V_{jE} = V_{B_2E_1} - 0.1\mathrm{V_{d_ET}}\ln\{1+\exp[(\mathrm{V_{B_2E_1}} - \mathrm{V_{FE}})/0.1\mathrm{V_{d_ET}}]\}, \tag{5.9}$$

$$V_{t_E} = \frac{\mathrm{V_{d_ET}}}{1-\mathrm{p_E}}\left[1 - (1 - V_{jE}/\mathrm{V_{d_ET}})^{1-\mathrm{p_E}}\right] + a_{jE}(V_{B_2E_1} - V_{jE}). \tag{5.10}$$

The electron densities in the base at the collector edge n_B and the voltage V_{tC} is much more complicated, for the n_B:

$$f_2 = \frac{4\,\mathrm{I_{sT}}}{\mathrm{I_{kT}}}\; e^{V^*_{B_2C_2}/V_T}, \tag{5.11a}$$

$$n_B = \frac{f_2}{1+\sqrt{1+f_2}}. \tag{5.11b}$$

We need to calculate $V^*_{B_2C_2}$ for calculation of n_B, The voltage and current at which quasi-saturation or Kirk effect start are given by:

$$V_{qs}^{th} = \mathrm{V_{dCT}} + 2\,\mathrm{V_T}\ln\left(\frac{\mathrm{I_{C_1C_2}}\,\mathrm{R_{CvT}}}{2\mathrm{V_T}} + 1\right) - \mathrm{V_{B_2C_1}}, \tag{5.12}$$

$$V_{qs} = \frac{1}{2}\left(V_{qs}^{th} + \sqrt{(V_{qs}^{th})^2 + 4\,(0.1\,\mathrm{V_{d_CT}})^2}\right), \tag{5.13}$$

$$I_{qs} = \frac{V_{qs}}{\mathrm{SCR_{Cv}}}\ \frac{V_{qs} + \mathrm{I_{hc}\ SCR_{Cv}}}{V_{qs} + \mathrm{I_{hc}\ R_{CvT}}}, \tag{5.14}$$

Here R_{Cv} is ohmic resistance of the total epilayer, SCR_{Cv} is space-charge resistance of the epilayer, I_{hc} is critical current for hot carrier behaviour. $V_{B_2C_1}$ can be obtained by:

$$V_{B_2C_1} = V_{B_2E_1} + I_C R_{CcT} + (I_B + I_C)R_{ET} - V_{CE}, \tag{5.15}$$

From this we calculate:

$$\alpha = \frac{1 + \mathrm{a_{x_i}}\ \ln\{1 + \exp[(\mathrm{I_{C_1C_2}}/\mathrm{I_{qs}} - 1)/\mathrm{a_{x_i}}]\}}{1 + \mathrm{a_{x_i}}\ \ln\{1 + \exp[-1/\mathrm{a_{x_i}}]\}}, \tag{5.16}$$

Here a_{xi} is smoothing parameter for the onset of quasi-saturation. We need to solve:

$$\alpha\ I_{qs} = \frac{V_{qs}}{\mathrm{SCR_{Cv}\ y_i^2}}\ \frac{V_{qs} + \mathrm{SCR_{Cv}\ I_{hc}\ y_i}}{V_{qs} + \mathrm{R_{CvT}\ I_{hc}}}, \tag{5.17}$$

which leads to:

$$v = \frac{V_{qs}}{\mathrm{I_{hc}\ SCR_{Cv}}}, \tag{5.18}$$

$$y_i = \frac{1 + \sqrt{1 + 4\,\alpha\, v\,(1 + v)}}{2\,\alpha\,(1 + v)} \tag{5.19}$$

The injection thickness is given by:

$$\frac{x_i}{W_{epi}} = 1 - \frac{y_i}{1 + p_W y_i}, \tag{5.20}$$

Here p_W is normalized hole density in the collector epilayer at the buried layer edge.

$$g = \frac{I_{C_1C_2} R_{CvT}}{2V_T}\ \frac{x_i,}{W_{epi}}, \tag{5.21}$$

The hole density p_0^* at the base-collector junction is given by

$$p_0^* = \frac{g-1}{2} + \sqrt{\left(\frac{g-1}{2}\right)^2 + 2g + p_W(p_W + g + 1)}, \tag{5.22}$$

$$e^{V^*_{B_2C_2}/V_T} = p_0^*(p_0^* + 1)\, e^{\mathrm{V_{d_CT}}/\mathrm{V_T}}. \tag{5.23}$$

$V^*_{B_2C_2}$ is proportional to $V_{B_2E_1}$ and $I_{C_1C_2}$, so that n_B can be calculated from $V_{B_2E_1}$ and $I_{C_1C_2}$.

Now we need to calculate the voltage V_{t_C} is shown as :

$$B_1 = \frac{1}{2}\mathrm{SCR_{Cv}}(\mathrm{I_{C_1C_2}} - \mathrm{I_{hc}}), \tag{5.24}$$

$$B_2 = \mathrm{SCR_{Cv}}\ \mathrm{R_{CvT}}\ \mathrm{I_{hc}}\ \mathrm{I_{C_1C_2}}, \tag{5.25}$$

$$V_{x_i=0} = B_1 + \sqrt{B_1^2 + B_2}, \tag{5.26}$$

The junction voltage is now the external voltage plus the voltage drop over the epilayer:

$$V_{\mathrm{junc}} = V_{B_2C_1} + V_{x_i=0}, \tag{5.27}$$

$$V_{ch} = \mathrm{V_{d_cT}}\ \left(0.1 + 2\,\frac{\mathrm{I_{C_1C_2}}}{\mathrm{I_{C_1C_2}} + \mathrm{I_{qs}}}\right), \tag{5.28}$$

$$b_{jC} = \frac{a_{jC} - \mathrm{X_{pT}}}{1 - \mathrm{X_{pT}}}, \tag{5.29}$$

$$V_{FC} = \mathrm{V_{d_CT}}\left(1 - \mathrm{b_{jC}^{-1/p_C}}\right), \tag{5.30}$$

$$V_{jC} = V_{\mathrm{junc}} - V_{ch}\ln\{1 + \exp[(V_{\mathrm{junc}} - V_{FC})/V_{ch}]\}, \tag{5.31}$$

$$I_{\mathrm{cap}} = \frac{\mathrm{I_{hc}}\ \mathrm{I_{C_1C_2}}}{\mathrm{I_{hc}} + \mathrm{I_{C_1C_2}}}, \tag{5.32}$$

$$f_I = \left(1 - \frac{I_{\mathrm{cap}}}{\mathrm{I_{hc}}}\right)^{\mathrm{m_C}}, \tag{5.33}$$

Here f_I is collector current modulation coefficient. m_C is collector current modulation coefficient.

$$V_{C_V} = \frac{\mathrm{V_{dCT}}}{1-\mathrm{p_C}} \left[1 - f_I \left(1 - V_{jC}/\mathrm{V_{dCT}}\right)^{1-\mathrm{p_C}}\right] + f_I \, b_{jC}(V_{\mathrm{junc}} - V_{jC}), \tag{5.34}$$

$$V_{t_C} = (1 - \mathrm{X_{pT}}) \, \mathrm{V_{C_V}} + \mathrm{X_{pT}} \mathrm{V_{B_2C_1}}. \tag{5.35}$$

V_{t_C} is also proportional to $V_{B_2E_1}$ and $I_{C_1C_2}$. This means that in principle all quantities can be written as function of $V_{B_2E_1}$ and $I_{C_1C_2}$. The following two equation can be solved iteratively:

$$I_{B.m} = I_{B.s}(V_{B_2E_1}, I_{C_1C_2}), \tag{5.36a}$$

$$I_N((V_{B_2E_1}, I_{C_1C_2}) = I_{C_1C_2}. \tag{5.36b}$$

Here $I_{B.m}$ is the measured base current, $I_{B.s}$ is the sum of all forward base currents. The ideal base current then is:

$$I_{B_1} = (1 - Xi_{Bi}) \frac{I_S}{\beta_f} \left(e^{V_{B_2E_1}/V_T} - 1\right), \tag{5.37}$$

The Ideal side-wall base current is :

$$I^S_{B_1} = Xi_{Bi} \frac{I_S}{\beta_f} \left(e^{V_{B_2E_1}/V_T} - 1\right), \tag{5.38}$$

The Non-ideal forward base current is :

$$I_{B_2} = I_{BfT} \left(e^{V_{B_2E_2}/m_{LF}V_T}\right) + G_{min}(V_{B_2E_1} + V_{B_2C_1}), \tag{5.39}$$

The main current can be shown as :

$$I_N = I_{sT} * \frac{e^{VB_2E_1/V_T} - e^{V^*_{B_2C_2}/V_T}}{qB}, \tag{5.40}$$

The sum of all forward base current is :

$$I_B = I_{B_1} + I_{B_1}^S + I_{B_2}. \tag{5.41}$$

$V_{B_2E_1}$ and $I_{C_1C_2}$ can be solved iteratively together. Then simulated V_{BE} can be solved through Equation 5.3. As temperature scaling is included, changing thermal resistance R_{th} will change Δ_T and thus all temperature scaling parameters will be influenced. Thus, R_{th} can be extracted from the comparison of the simulated and measured V_{BE} as shown in Figure 5.2 - 5.3. The base-emitter voltage increase sharply at beginning and drop down to keep the base-current constant. At high base-emitter bias the avalanche effect will happen which lead to the increase of base-emitter bias.

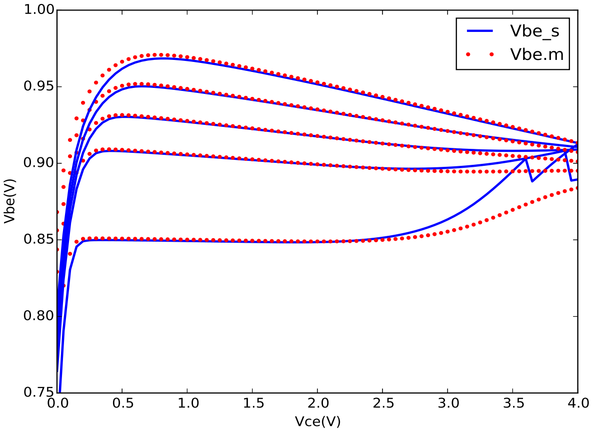

Figure 5.2: Measured(markers) and simulated(line) base-emitter voltage in the output characteristic measurement by Python

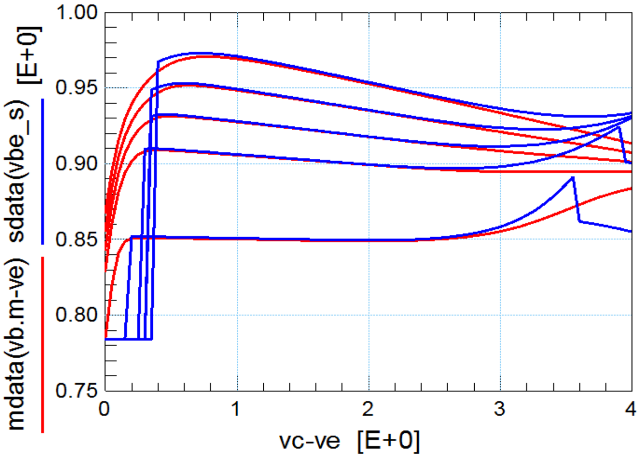

Figure 5.3: Measured(markers) and simulated(line) base-emitter voltage in the output characteristic measurement by IC-CAP

5.2 Knee current

The knee current is extracted from the collector current at high V_{CE} using the output-characteristic measurements shown in Figure 5.1. The extraction of knee current use the same way that extract R_{th} that we solve $I_{C_1C_2}$ and $V_{B_2E_1}$ iteratively together. The collector current is:

$$I_{C_1C_2} = I_{sT} * \frac{e^{V_{B_2E_1}/V_T} - e^{V^*_{B_2C_2}/V_T}}{qB}. \tag{5.42}$$

The knee current I_K can change $I_{C_1C_2}$ by changing electron density in the base at emitter edge n_0 in Equation 5.7. The internal base-collector bias $V^*_{B_2C_2}$ can be calculate from current $I_{C_1C_2}$ and the internal base collector bias $V_{B_2C_1}$ as shown in Equation 5.15 – Equation 5.23. The base charge q_B can also be calculated from $I_{C_1C_2}$, and $V_{B_2E_1}$. The knee current can be extracted by matching the simulation collector current to the measurement collector current as shown in Figure 5.4 - 5.5.

The collector current increase sharply as the collector-emitter bias increase from 0V. Then collector current curve become flat but increase slowly as the saturation current increase with increasing power dissipation. At high collector-emitter bias, the collector current increase because the avalanche effect.

5.3 Ohmic resistance

The ohmic resistance R_{C_V} is extracted from the decrease of the current gain in the forward-Gummel measurement shown in Figure 4.27 . Here we also use the same way as before to solve $I_{C_1C_2}$ and $V_{B_2E_1}$ iteratively together. The current gain is:

$$h_{fe} = \frac{I_{C_1C_2}}{I_{B.m}}. \tag{5.43}$$

Note here we use measurement base current. The ohmic resistance R_{C_V} can change $I_{C_1C_2}$ by changing V_{qs} in Equation 5.12. Then R_{C_V} can be extracted from comparison of measurement current gain and simulation current gain and the result is shown in Figure 5.6 - 5.7. The

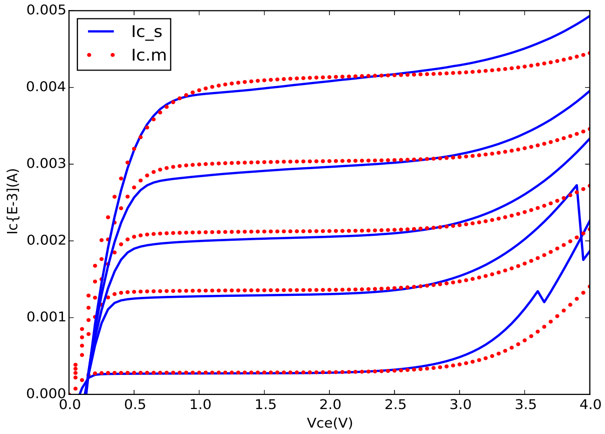

Figure 5.4: Measured(markers) and simulated(line) collector current in the output-characteristic measurement by Python

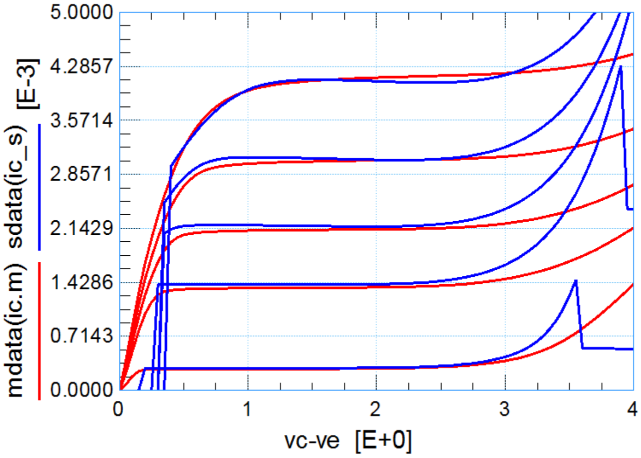

Figure 5.5: Measured(markers) and simulated(line) collector current in the output-characteristic measurement by IC-CAP

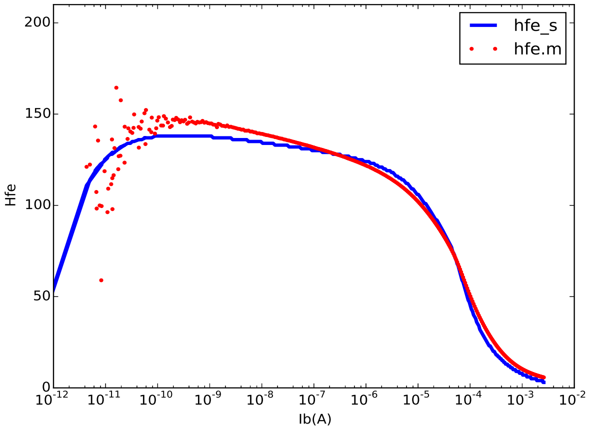

Figure 5.6: Measured(markers) and simulated(line) forward current gain as function of the measurement base current in forward-Gummel measurement by Python

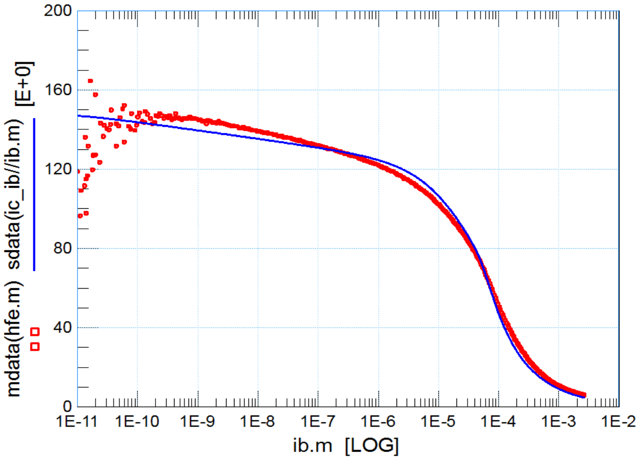

Figure 5.7: Measured(markers) and simulated(line) forward current gain as function of the measurement base current in forward-Gummel measurement by IC-CAP

decrease of current gain is due to the quasi-saturation. The voltage drop over R_{Cc} will result in the internal base-collector bias $V_{B_2C_2}$ forward biased and cause collector current decrease. However, the diffusion voltage V_{dc} of the collector also cause current gain to decrease. In practice we fix the diffusion voltageV_{dc} based on the doping level of the epilayer.

5.4 Cut-off frequency

The cur-off frequency f_T is defined as the frequency where the current gain $h_f e$ becomes unity. The cut-off frequency is determined by:

$$\frac{1}{2\pi f_T} = \tau_T = \frac{dQ}{dI_C} \mid_{vce}, \tag{5.44}$$

The τ_T is the total emitter-collector transit time. It is related to the differential charge dQ and current dI_C under a constant collector-emitter bias.

The first step is to solve $V_{B_2E_1}$ iteratively using Equation 5.3 - 5.41 as we do before. And here we use the measurement collector current as $I_{C_1C_2}$.

Then we will determine the small signal variations

$$dV_{CE} = \frac{\partial V_{CE}}{\partial V_{B_2E_1}} dV_{B_2E_1} + \frac{\partial V_{CE}}{\partial V_{B_2C_1}} dV_{B_2C_1} + \frac{\partial V_{CE}}{\partial I_{C_1C_2}} dI_{C_1C_2} = 0, \tag{5.45a}$$

$$dI_N = \frac{\partial I_N}{\partial V_{B_2E_1}} dV_{B_2E_1} + \frac{\partial I_N}{\partial V_{B_2C_1}} dV_{B_2C_1} + \frac{\partial I_N}{\partial I_{C_1C_2}} dI_{C_1C_2} = dI_{C_1C_2}, \tag{5.45b}$$

We can calculate $dV_{B_2E_1}/dIC_1C_2$ and $dV_{B_2C_1}/dIC_1C_2$ under a constant V_{CE} by solving these equations. The differential charge can be calculated similar to differential voltage and current above:

$$dQ = \frac{\partial Q}{\partial V_{B_2E_1}} dV_{B_2E_1} + \frac{\partial Q}{\partial V_{B_2C_1}} dV_{B_2C_1} + \frac{\partial Q}{\partial I_{C_1C_2}} dI_{C_1C_2}, \tag{5.46}$$

Then the transit time can be calculated as:

$$\tau_T = \frac{\partial Q}{\partial V_{B_2E_1}} \frac{dV_{B_2E_1}}{dI_{C_1C_2}} + \frac{\partial Q}{\partial V_{B_2C_1}} \frac{dV_{B_2C_1}}{dI_{C_1C_2}} + \frac{\partial Q}{\partial I_{C_1C_2}}. \tag{5.47}$$

In this way the cut-off frequency can be calculated as function of collector current and collector-emitter bias.

The parameters that can be extracted here are critical current for velocity saturation in the epilayer I_{hc}, space charge resistance of the epilayer SCR_{cv} , transit time of stored epilayer charge τ_{epi} and minimum transit time of stored emitter charge τ_E. The extraction result is given in Figure 5.8 and 5.9.

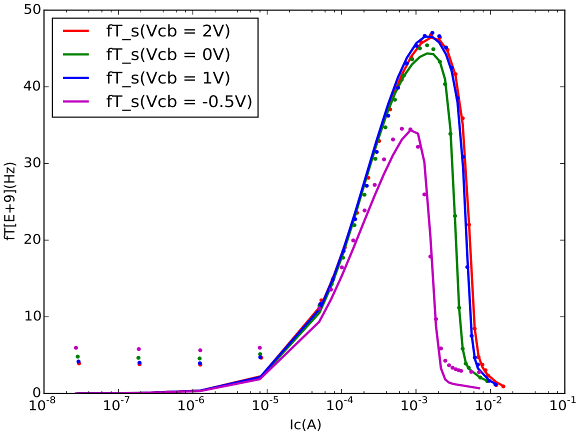

Figure 5.8: Measured(markers) and simulated(line) cut-off frequency in the S-parameter measurement by Python

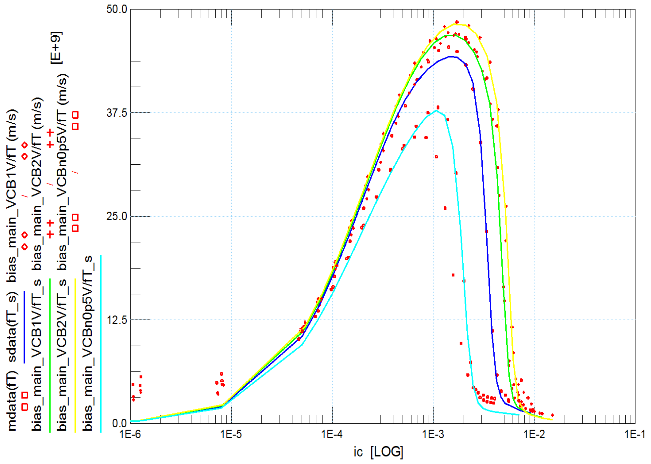

Figure 5.9: Measured(markers) and simulated(line) cut-off frequency in the S-parameter measurement by IC-CAP

5.5 Reverse current at high injection

The partitioning factor of the extrinsic regions X_{ext} is extracted at reverse-Gummel measurement from the absolute values of the reverse currents I_B, I_E and I_{sub}. The main current is :

$$I_N = I_{sT} \frac{e^{V_{B_2C_2}/V_T}}{q_B} \tag{5.48}$$

Mextram uses the Kull model in reverse and following the Kull model[24] we introduce::

$$k_0 = \sqrt{1 + 4\ \exp[(V_{B_2C_2} - \mathrm{V_{dC}})/\mathrm{V_T}]} \tag{5.49a}$$

$$k_W = \sqrt{1 + 4\ \exp[(V_{B_2C_1} - \mathrm{V_{dC}})/\mathrm{V_T}]} \tag{5.49b}$$

$$E_c = V_T\ \left[2\,k_0 - 2\,k_W - \ln\left(\frac{k_0 + 1}{k_W + 1}\right)\right] \tag{5.49c}$$

$$I_{epi} = \frac{-\,(E_c + V_{B_2C_2} - V_{B_2C_1})}{\mathrm{R_{Cv}}} \tag{5.49d}$$

The junction voltage $V_{B_2C_1} = V_{B_1C_1}$ can be solve iteratively using $I_N = I_{epi}$. The non-ideal reverse base current is :

$$I_{B_3} = \mathrm{I_{BrT}}\ \frac{\mathrm{e}^{\mathrm{V_{B_1C_1}/V_T}} - 1}{\mathrm{e}^{\mathrm{V_{B_1C_1}/2V_T}} + \mathrm{e}^{\mathrm{V_{Lr}/2V_T}}} \tag{5.50}$$

The substrate current includes high injection:

$$I_{\mathrm{sub}} = \frac{2\mathrm{I_{SsT}}\ \left(\mathrm{e}^{\mathrm{V_{B_1C_1}/V_T}} - 1\right)}{1 + \sqrt{1 + 4\ \frac{\mathrm{I_1sT}}{\mathrm{I_{ksT}}}\ e^{V_{B_1C_1}/V_T}}} \tag{5.51}$$

The extrinsic base current is given by:

$$g_1 = \frac{4\,\mathrm{I_{sT}}}{\mathrm{I_{kT}}}\ e^{V_{B_1C_1}/V_T} \tag{5.52a}$$

$$n_{B\mathrm{ex}} = \frac{4\,\mathrm{I_{sT}}}{\mathrm{I_{kT}}}\ \frac{e^{V_{B_1C_1}/V_T} - 1}{1 + \sqrt{1 + g_1}} \tag{5.52b}$$

$$I_{\mathrm{ex}} = (1 - X_{ext})\frac{\mathrm{I_{kT}}}{2\,\beta_{\mathrm{riT}}}\,n_{B\mathrm{ex}} \tag{5.52c}$$

The ideal base current then is:

$$I_{B_1} = (1 - \mathrm{XI_{B_1}})\;\frac{\mathrm{I_{sT}}}{\beta_{\mathrm{f_T}}}\;\left(\mathrm{e}^{\mathrm{V_{B_2C_2}/V_T}}\right) \tag{5.53}$$

The junction voltage which we need for the calculation of XI_{ex} and XI_{sub} is :

$$V_{BC_1} = V_{B_1C_1} + (I_{ex} + I_{sub} + I_{B_3})\,R_{BcT} \tag{5.54}$$

Extrinsic reverse base current is given:

$$Xg_1 = \frac{4\,\mathrm{I_{sT}}}{\mathrm{I_{kT}}}\,e^{V_{BC_1}/V_T} \tag{5.55a}$$

$$Xn_{B\mathrm{ex}} = \frac{4\,\mathrm{I_{sT}}}{\mathrm{I_{kT}}}\,\frac{e^{V_{BC_1}/V_T} - 1}{1 + \sqrt{1 + Xg_1}} \tag{5.55b}$$

$$XI_{ex} = \mathrm{X_{ext}}\,\frac{\mathrm{I_{kT}}}{2\,\beta_{\mathrm{riT}}}\,\mathrm{Xn_{Bex}} \tag{5.55c}$$

Substrate current is described as :

$$XI_{sub} = X_{ext}\,\frac{2\mathrm{I_{SsT}}\;\left(\mathrm{e}^{\mathrm{V_{B_1C_1}/V_T}} - 1\right)}{1 + \sqrt{1 + 4\;\frac{\mathrm{I_1sT}}{\mathrm{I_{ksT}}}\;e^{V_{BC_1}/V_T}}} \tag{5.56}$$

Then we can calculate the external base-collector bias:

$$V_{BC} = V_{BC_1} + (I_{ex} + XI_{ex} + I_N)\,R_{BcT} \tag{5.57}$$

Note that $V_{B_2C_2}$ need to be solve iteratively using equations above. Then we can get the following current:

$$I_E = I_N \tag{5.58a}$$

$$I_B = I_{ex} + XI_{ex} + I_{sub} + XI_{sub} + I_{B_3} \tag{5.58b}$$

$$I_{sub,ext} = -I_{sub} - XI_{sub} \tag{5.58c}$$

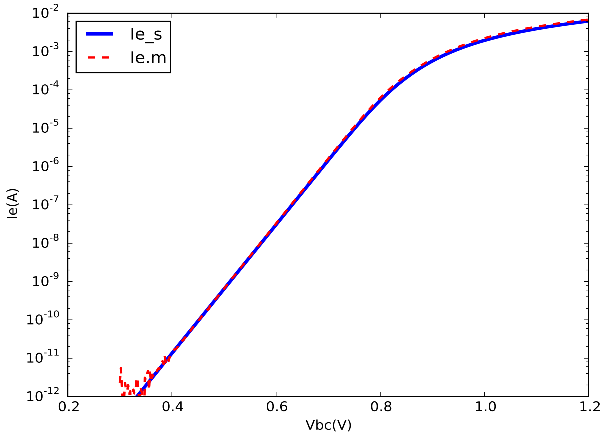

Figure 5.10: Measured(markers) and simulated(line) emitter currents in the reverse-Gummel measurement by Python

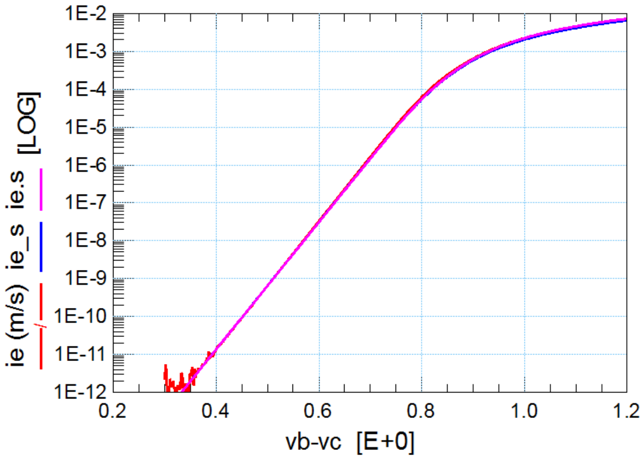

Figure 5.11: Measured(red line) and simulated(blue line for build in function purple line for simulator) emitter currents in the reverse-Gummel measurement by IC-CAP

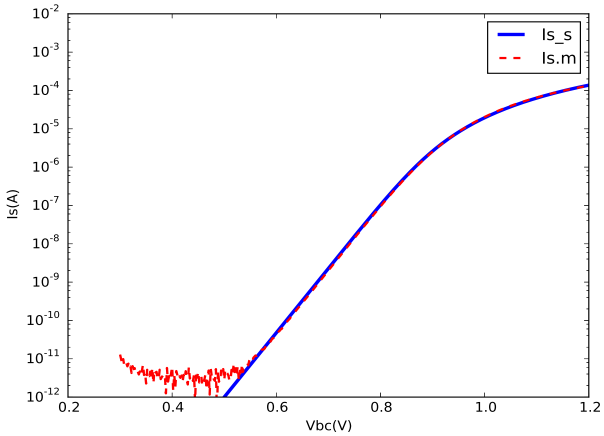

Figure 5.12: Measured(markers) and simulated(line) substrate currents in the reverse-Gummel measurement by Python

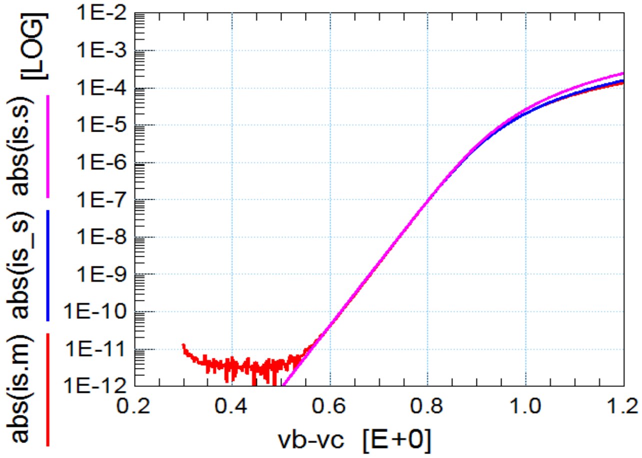

Figure 5.13: Measured(red line) and simulated(blue line for build in function purple line for simulator) substrate currents in the reverse-Gummel measurement by IC-CAP

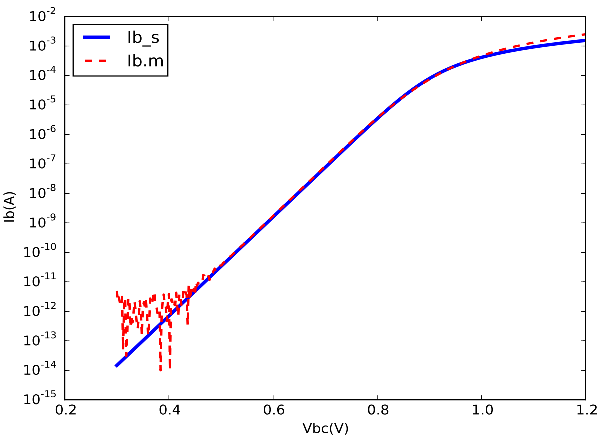

Figure 5.14: Measured(markers) and simulated(line) base currents in the reverse-Gummel measurement by Python

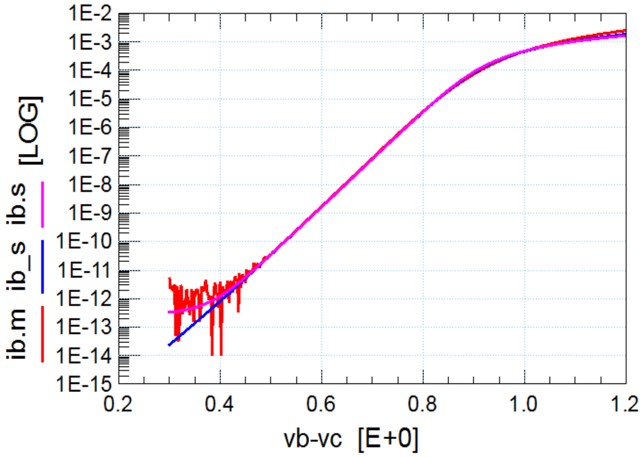

Figure 5.15: Measured(red line) and simulated(blue line for build in function purple line for simulator) base currents in the reverse-Gummel measurement by IC-CAP

Chapter 6

Temperature scalling

6.1 T-scaling rules

To be able to extract the high-current parameters correctly, it is important to take temperature scaling into account. In Table 6.1 the cross reference between the temperature parameters and the electrical parameters is listed.

The actual simulation temperature is denoted by TEMP (in °C). The temperature at which the parameters are determined is $\mathrm{T_{ref}}$ (also in °C).

Conversion to Kelvin

$$T_K = \mathrm{TEMP} + \mathrm{DTA} + 273.15 + \mathrm{V_{dT}}, \tag{6.1a}$$

$$T_{\mathrm{amb}} = \mathrm{TEMP} + \mathrm{DTA} + 273.15, \tag{6.1b}$$

$$T_{RK} = \mathrm{T_{ref}} + 273.15, \tag{6.2}$$

$$t_N = \frac{T_K}{T_{RK}}, \tag{6.3}$$

Depletion capacitances The junction diffusion voltages $\mathrm{V_{d_E}}$, $\mathrm{V_{d_C}}$, and $\mathrm{V_{d_S}}$ with respect to temperature are

$$U_{d_E T} = -3\,V_T\,\ln t_N + \mathrm{V_{d_E}}\,\mathrm{t_N} + (1 - \mathrm{t_N})\,\mathrm{V_{g_B}}, \tag{6.4}$$

$$\mathrm{V_{d_E T}} = \mathrm{U}_{d_E T} + \mathrm{V_T}\ln\{1 + \exp[(\mathrm{V_{d,low}} - \mathrm{U}_{d_E T})/\mathrm{V_T}]\}, \tag{6.5}$$

1	A_{QB0}	V_{er}, V_{ef}, I_s, β_f, R_{Bv}, τ_B, τ_R, I_{ks}, dE_g
2	A_E	R_E, β_f
3	A_B	R_{Bv},β_f,I_s,I_k τ_B, τ_R, τ_E, I_{ks}
4	A_{epi}	R_{c_v}, τ_{epi}, τ_R
5	A_{ex}	R_{B_C}
6	A_c	R_{C_C}
7	A_S	I_{S_S}, I_{ks}
8	$dV_{g\beta r}$	β_{ri}
9	V_{g_B}	I_s, C_{j_E}, V_{d_E}, V_{er}, I_{ks}
10	V_{g_C}	C_{j_C}, V_{d_C}, X_p, I_{Br}, V_{ef}
11	V_{g_j}	I_{Br}
12	$dV_{g\tau_E}$	τ_E
13	V_{g_S}	I_{S_S}, I_{ks}, C_{j_S}, V_{d_S}
14	$dV_{g\beta f}$	β_f

Table 6.1: Summery of the occurrence of the temperature parameters in the temperature scaling rules of the electrical parameters.

$$U_{d_C T} = -3\, V_T\, \ln t_N + \mathrm{V_{d_C}}\ \mathrm{t_N} + (1 - \mathrm{t_N})\ \mathrm{V_{g_C}}, \tag{6.6}$$

$$\mathrm{V_{d_C T}} = \mathrm{U}_{d_C T} + \mathrm{V_T} \ln\{1 + \exp[(\mathrm{V_{d,low}} - \mathrm{U}_{d_C T})/\mathrm{V_T}]\}, \tag{6.7}$$

$$U_{d_S T} = -3\, V_T\, \ln t_N + \mathrm{V_{d_S}}\ \mathrm{t_N} + (1 - \mathrm{t_N})\ \mathrm{V_{g_S}}, \tag{6.8}$$

$$\mathrm{V_{d_S T}} = \mathrm{U}_{d_S T} + \mathrm{V_T} \ln\{1 + \exp[(\mathrm{V_{d,low}} - \mathrm{U}_{d_S T})/\mathrm{V_T}]\}. \tag{6.9}$$

The zero-bias capacitances scale with temperature as

$$\mathrm{C_{j_E T}} = \mathrm{C_{j_E}}\ \left(\frac{\mathrm{V_{d_E}}}{\mathrm{V_{d_E T}}}\right)^{\mathrm{p_E}}, \tag{6.10}$$

$$\mathrm{C_{j_S T}} = \mathrm{C_{j_S}}\ \left(\frac{\mathrm{V_{d_S}}}{\mathrm{V_{d_S T}}}\right)^{\mathrm{p_S}}, \tag{6.11}$$

The collector depletion capacitance is divided in a variable and a constant part. The constant part is temperature independent.

$$\mathrm{C_{j_C T} = C_{j_C}\ \left[(1 - X_p)\ \left(\frac{V_{d_C}}{V_{d_C T}}\right)^{p_C} + X_p\right]},\tag{6.12}$$

$$\mathrm{X_{pT} = X_p\ \left[(1 - X_p)\ \left(\frac{V_{d_C}}{V_{d_C T}}\right)^{p_C} + X_p\right]^{-1}}.\tag{6.13}$$

Resistances The various parameters A describe the mobility of the corresponding regions: $\mu \propto t_N^{-\mathrm{A}}$. The temperature dependence of the zero-bias base charge goes as $Q_{B0T}/Q_{B0} = t_N^{\mathrm{A_{Q_{B0}}}}$.

$$\mathrm{R_{ET} = R_E\ t_N^{A_E}},\tag{6.14}$$

$$\mathrm{R_{BvT} = R_{Bv}\ t_N^{A_B - A_{Q_{B0}}}},\tag{6.15}$$

$$\mathrm{R_{BcT} = R_{Bc}\ t_N^{A_{ex}}},\tag{6.16}$$

$$\mathrm{R_{CvT} = R_{Cv}\ t_N^{A_{epi}}},\tag{6.17}$$

$$\mathrm{R_{CcT} = R_{Cc}\ t_N^{A_C}}.\tag{6.18}$$

Current gains

$$\mathrm{\beta_{fT} = \beta_f\ t_N^{A_E - A_B - A_{Q_{B0}}}\ \exp[-dV_{g\beta f}/V_{\Delta T}]},\tag{6.19}$$

$$\mathrm{\beta_{riT} = \beta_{ri}\ \exp[-dV_{g\beta r}/V_{\Delta T}]},\tag{6.20}$$

Currents and voltages

$$\mathrm{I_{sT} = I_s\ t_N^{4 - A_B - A_{Q_{B0}} + dA_{I_s}}\ \exp[-V_{g_B}/V_{\Delta T}]},\tag{6.21}$$

$$\mathrm{I_{kT} = I_k\ t_N^{1 - A_B}},\tag{6.22}$$

$$\mathrm{I_{BfT} = I_{Bf}\ t_N^{(6-2m_{Lf})}\ \exp[-V_{g_j}/m_{Lf}\ V_{\Delta T}]}, \tag{6.23}$$

$$\mathrm{I_{BrT} = I_{Br}\ t_N^{2}\ \exp[-V_{g_C}/2V_{\Delta T}]}, \tag{6.24}$$

$$\mathrm{V_{efT} = V_{ef}\ t_N^{A_{Q_{B0}}}\ \left[(1-X_p)\ \left(\frac{V_{d_C}}{V_{d_CT}}\right)^{p_C} + X_p\right]^{-1}}, \tag{6.25}$$

$$\mathrm{V_{erT} = V_{er}\ t_N^{A_{Q_{B0}}}\ \left(\frac{V_{d_E}}{V_{d_ET}}\right)^{-p_E}}, \tag{6.26}$$

The temperature dependence of $\mathrm{I_{Ss}}$ and$\mathrm{I_{ks}}$ is given by $\mathrm{A_S}$ and $\mathrm{V_{g_S}}$. $\mathrm{A_S}$ equals $\mathrm{A_C}$ for a closed buried layer (BN) and $\mathrm{A_S}$ equals $\mathrm{A_{epi}}$ for an open buried layer.

$$\mathrm{I_{SsT} = I_{Ss}\ t_N^{4-A_S}\ \exp[-V_{g_S}/V_{\Delta T}]}, \tag{6.27}$$

$$\mathrm{I_{ksT} = I_{ks}\ t_N^{1-A_S}\ \frac{I_{sT}}{I_s}\ \frac{I_{Ss}}{I_{SsT}}}, \tag{6.28}$$

When either $\mathrm{I_s = 0}$ or $\mathrm{I_{SsT} = 0}$ we take $\mathrm{I_{ksT} = I_{ks}\ t_N^{1-A_S}}$.

Transit times

$$\mathrm{\tau_{ET} = \tau_E\ t_N^{(A_B-2)}\ \exp[-dV_{g\tau_E}/V_{\Delta T}]}, \tag{6.29}$$

$$\mathrm{\tau_{BT} = \tau_B\ t_N^{A_{Q_{B0}}+A_B-1}} \tag{6.30}$$

$$\mathrm{\tau_{epiT} = \tau_{epi}\ t_N^{A_{epi}-1}}, \tag{6.31}$$

$$\mathrm{\tau_{RT} = \tau_R\ \frac{\tau_{BT}+\tau_{epiT}}{\tau_B+\tau_{epi}}}. \tag{6.32}$$

6.2 Temperature parameters

There are many different methods to extract temperature parameters. One method is optimizing the temperature parameters of all data over temperatures. The disadvantage of this method is that we do not extract the individual parameters at each parameter. If there are unexpected differences between the model simulation and hardware data, it is difficult to know whether it is the weakness of the electrical model or temperature scaling model. The second method is to extract the electrical parameters at all temperatures isothermally. The main advantage is that one can check the correctness of existing temperature scaling equations by comparing extracted and simulated electrical parameters.[18]

For each temperature parameter, we choose one electrical parameter from which we will extract the temperature parameter. This is easier than doing a fit over all the electrical parameters and it gives more control.

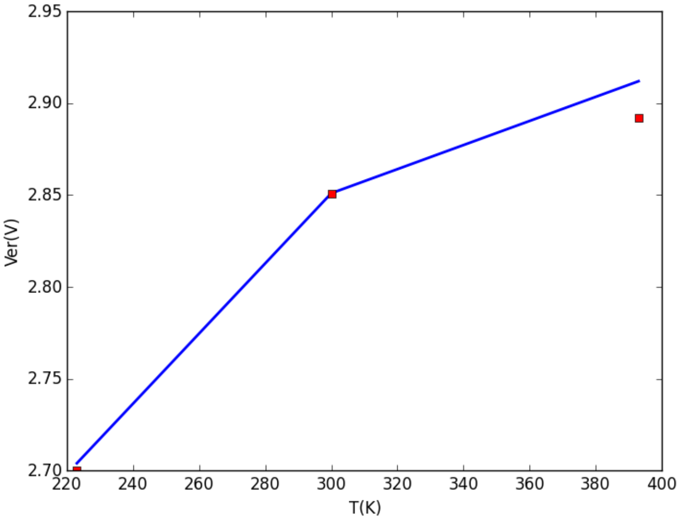

Figure 6.1: Extracted(markers) and simulated(line) values of the reverse Early voltage

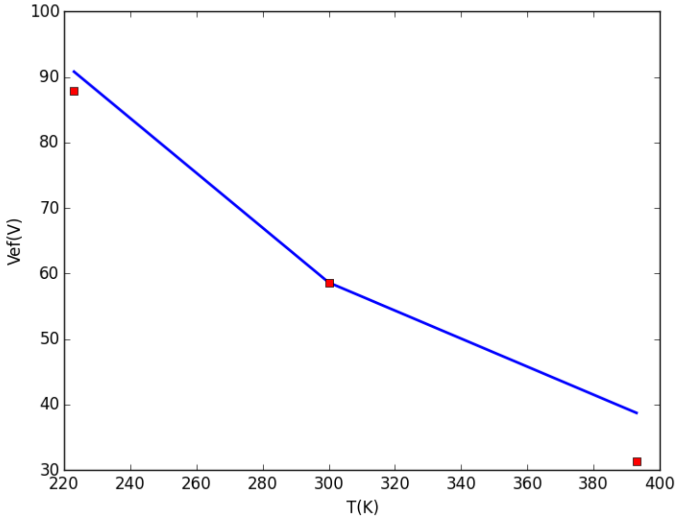

Figure 6.2: Extracted(markers) and simulated(line) values of the forward Early voltage

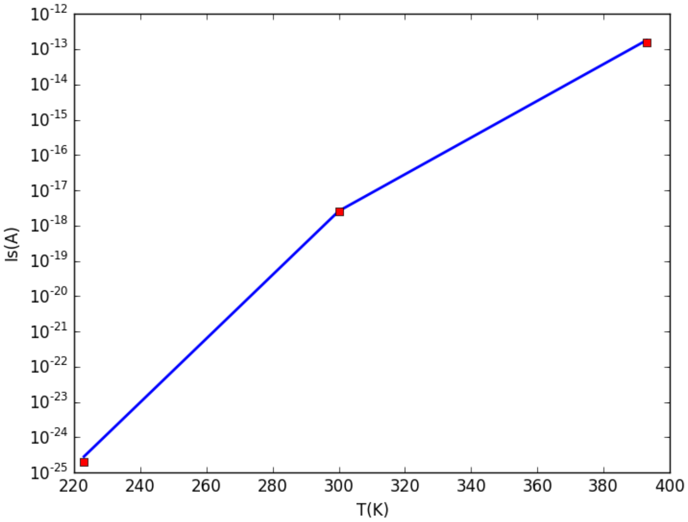

Figure 6.3: Extracted(markers) and simulated(line) values of collector saturation current

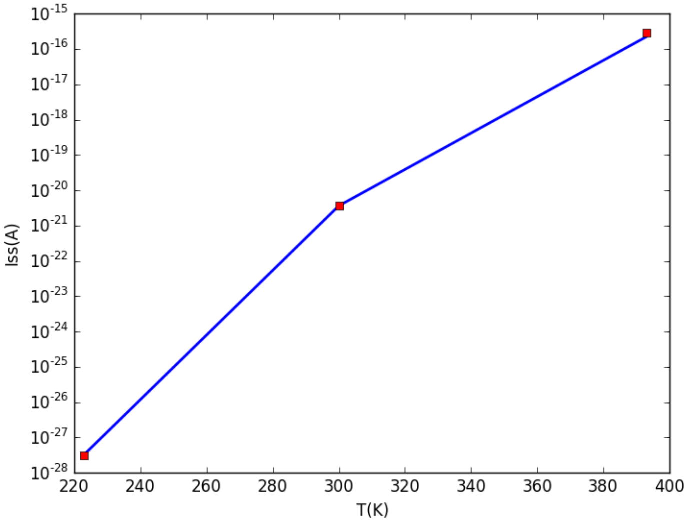

Figure 6.4: Extracted(markers) and simulated(line) values of substrate saturation current

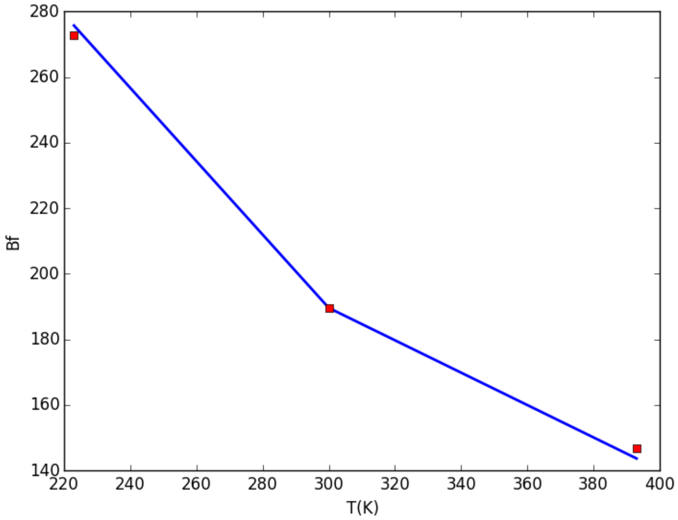

Figure 6.5: Extracted(markers) and simulated(line) values of forward current gain

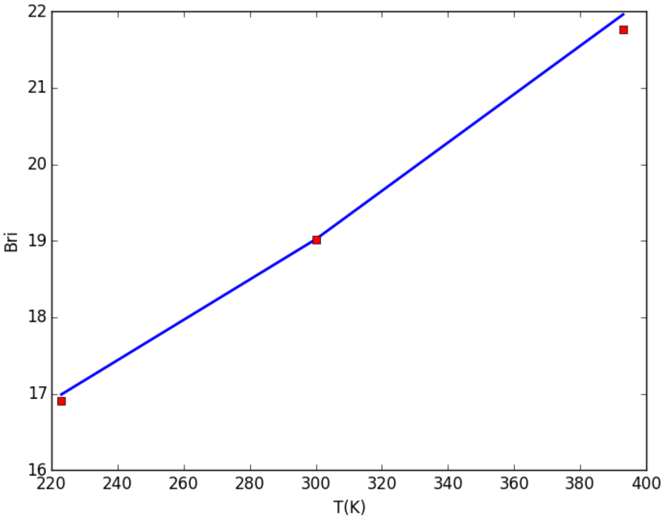

Figure 6.6: Extracted(markers) and simulated(line) values of reverse current gain

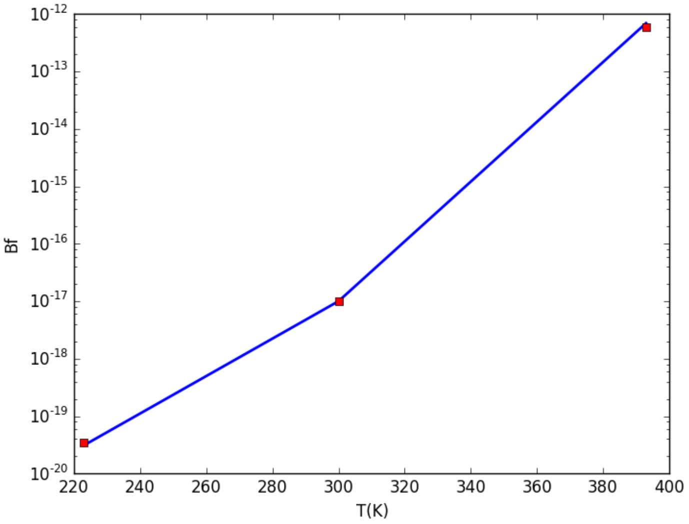

Figure 6.7: Extracted(markers) and simulated(line) values of non-ideal forward base current

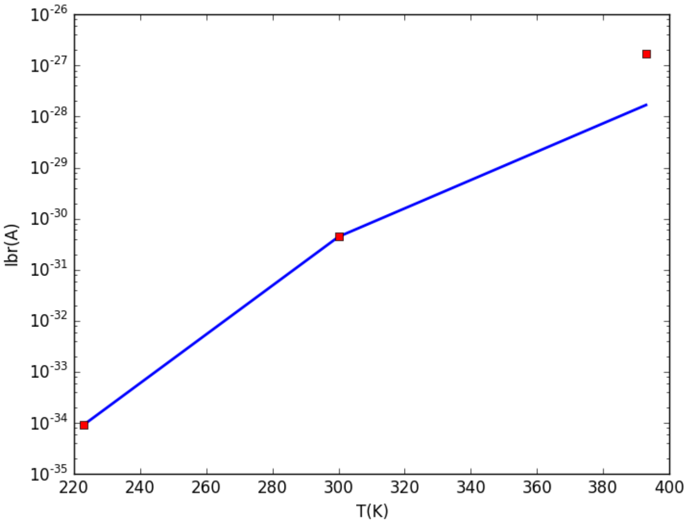

Figure 6.8: Extracted(markers) and simulated(line) values of non-ideal reverse base current

6.3 Extraction result

Since we have extracted all the parameters in Mextram 504 model. It is necessary for us to use a circuit simulator to compare measurement and simulation result. Here we use ADS [31] simulator in IC-CAP. Figure 6.9 - 6.10 show the I_B and I_C versus V_{BE} in forward gummel measurement from 223-393K respectively. Figure 6.11 - 6.12 show the I_B and I_C versus V_{BE} in reverse gummel measurement from 223-393K respectively. Figure 6.13 to 6.16 give I_C-V_{CE} and V_{BE}-V_{CE} in force- I_B measurement from 223-393K. f_T-I_C at V_{CB} = -0.5, 0, 1, and 2V is shown in Figure 6.17.

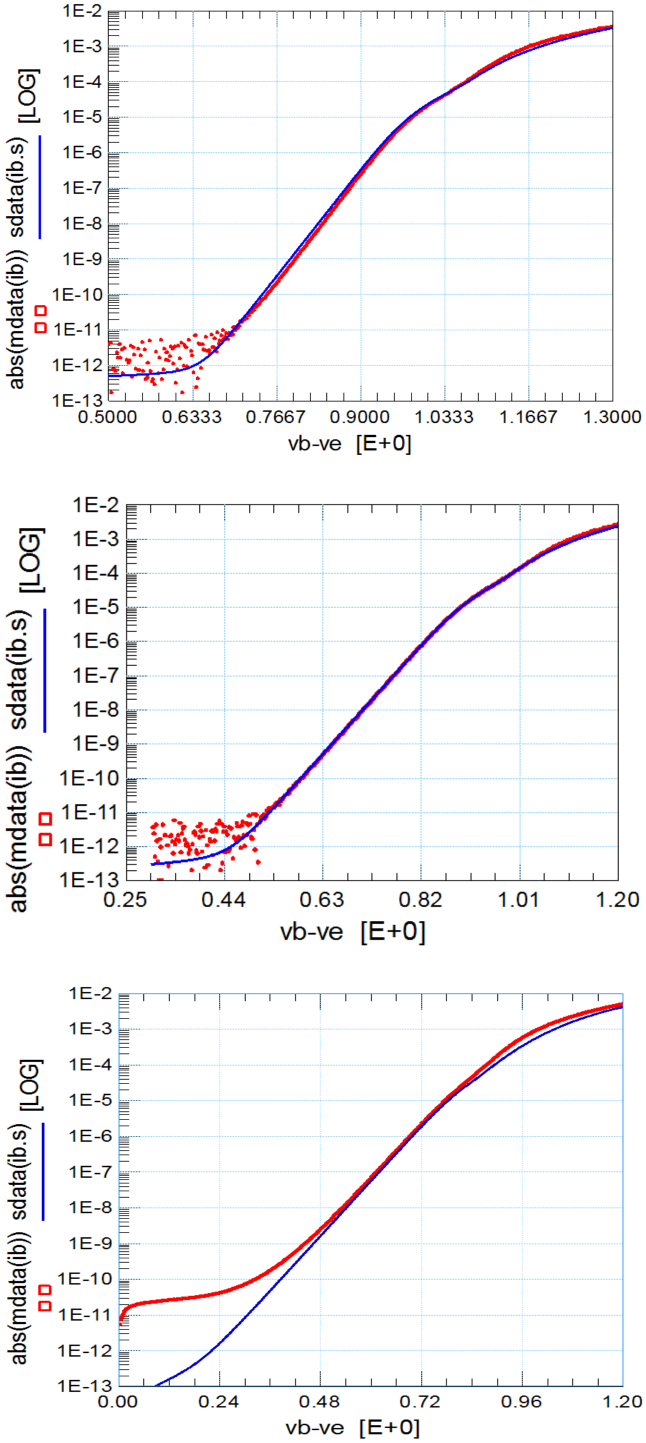

(a)

(b)

(c)

Figure 6.9: Measured (symbol) and simulated (solid line) I_B-V_{BE} from 223-393 K. (a) 223K. (b) 300K. (c) 393K.

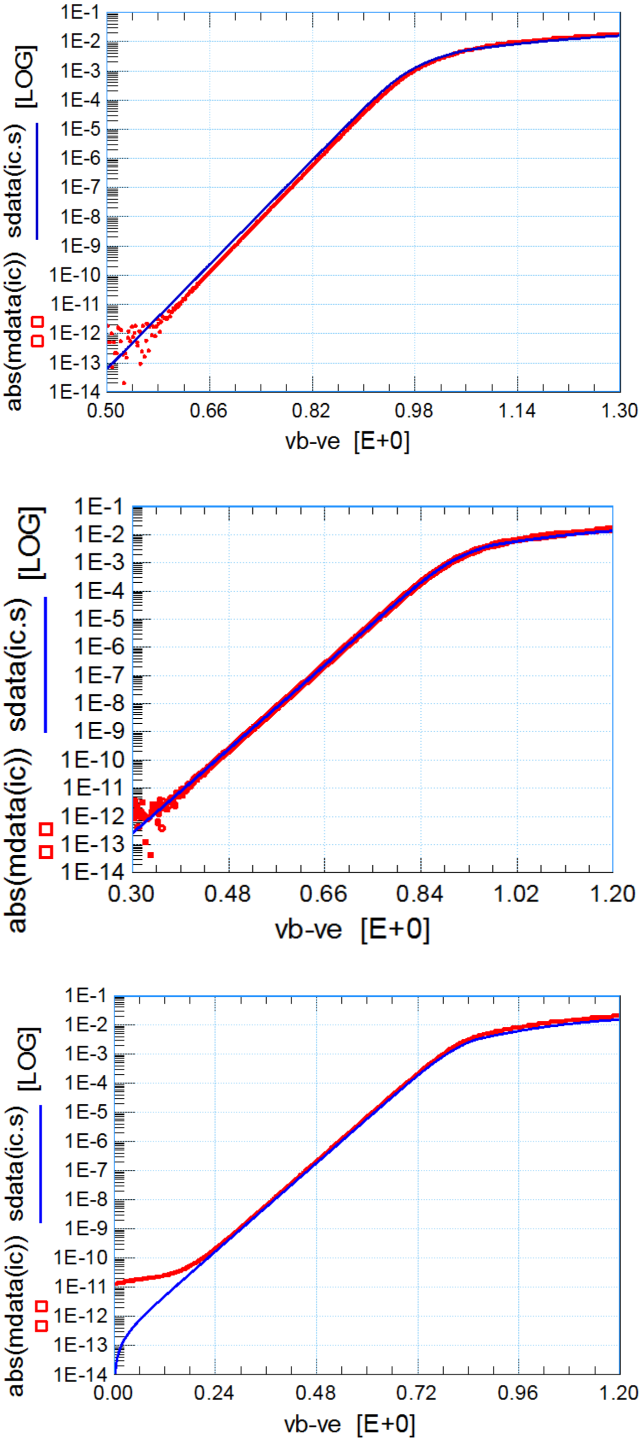

(a)

(b)

(c)

Figure 6.10: Measured (symbol) and simulated (solid line) I_C-V_{BE} from 223-393 K. (a) 223K. (b) 300K. (c) 393K.

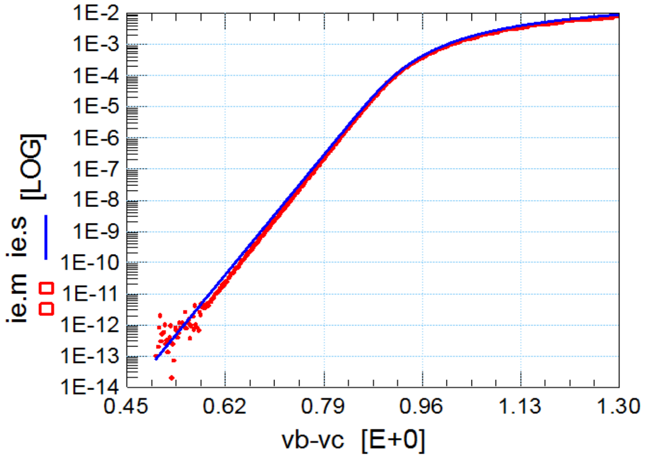

(a)

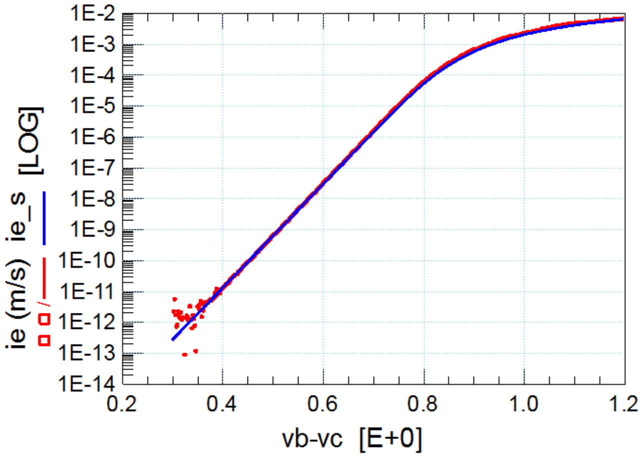

(b)

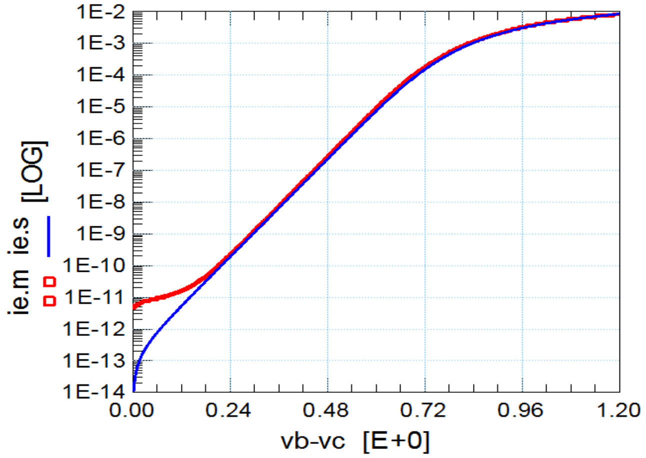

(c)

Figure 6.11: Measured (symbol) and simulated (solid line) I_E-V_{BC} from 2233-393 K. (a) 223K. (b) 300K. (c) 393K.

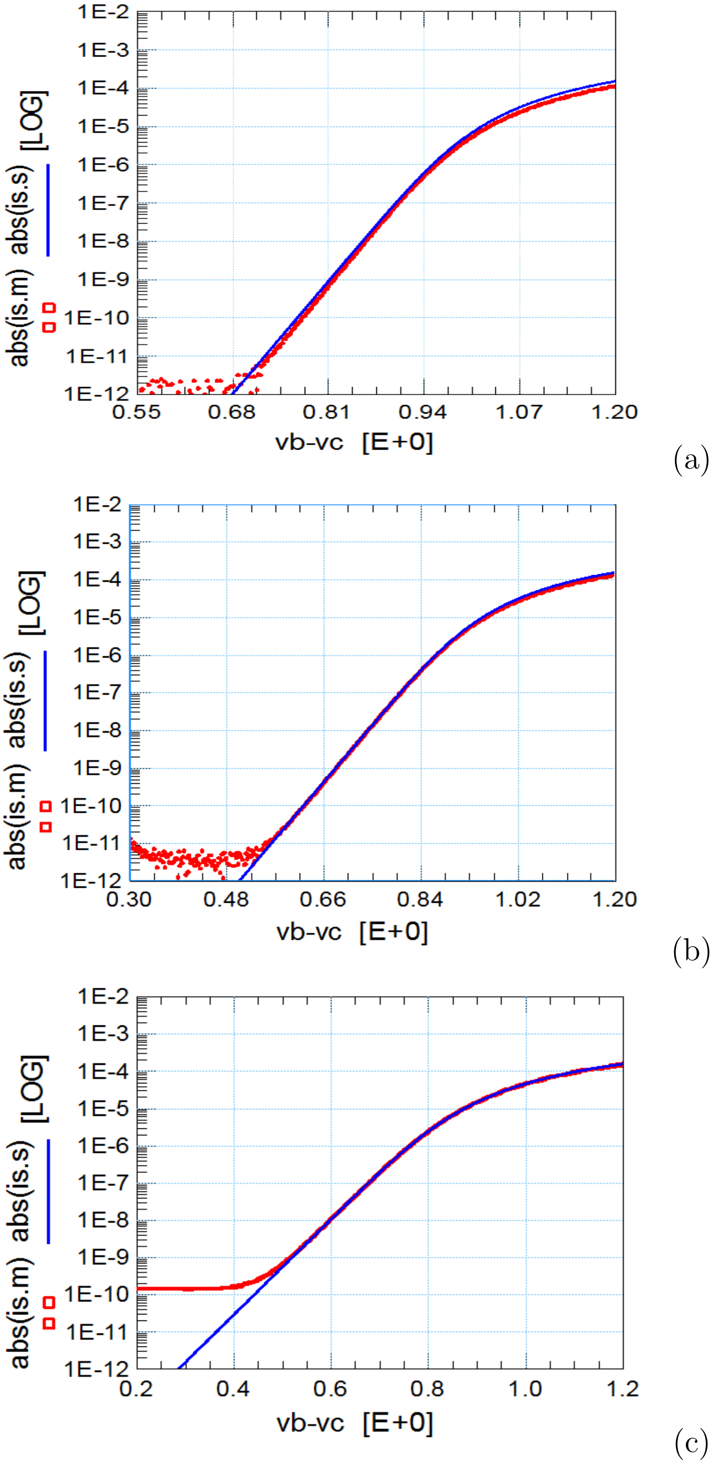

Figure 6.12: Measured (symbol) and simulated (solid line) I_{Sub}-V_{BC} from 223-393 K. (a) 223K. (b) 300K. (c) 393K.

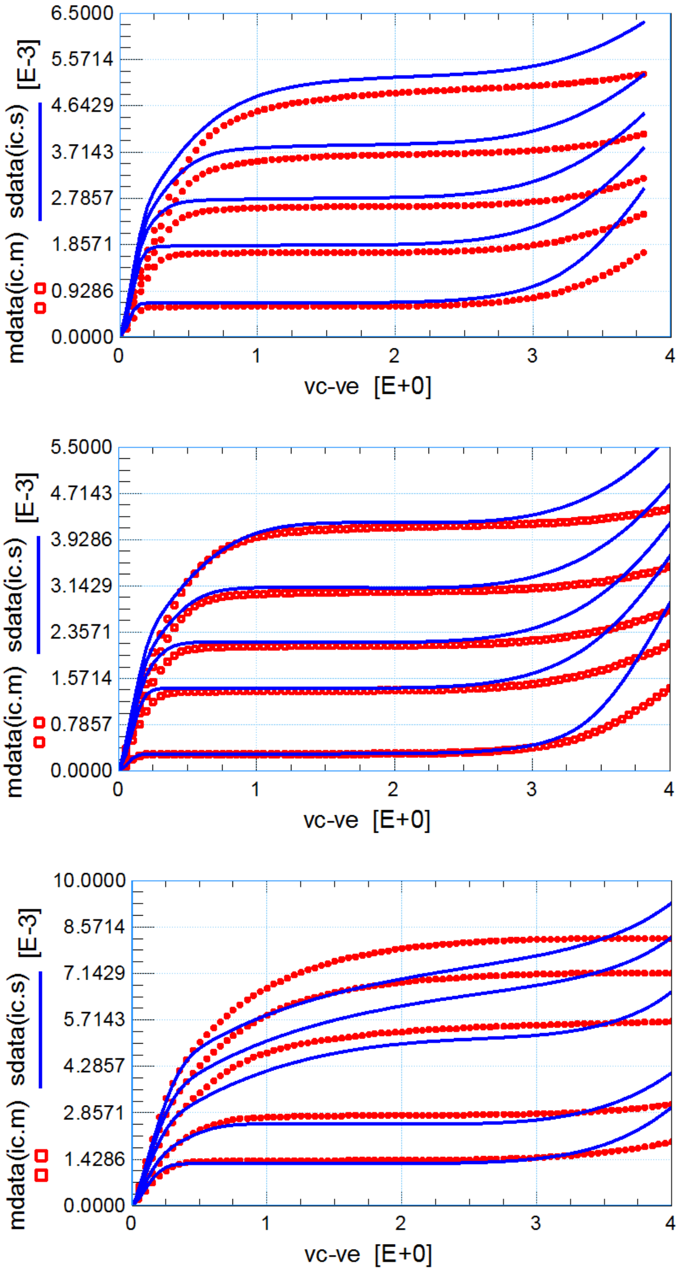

(a)

(b)

(c)

Figure 6.13: Measured (symbol) and simulated (solid line) I_C-V_{CE} from 223-393K at high IB. (a) 223K. (b) 300K. (c) 393K.

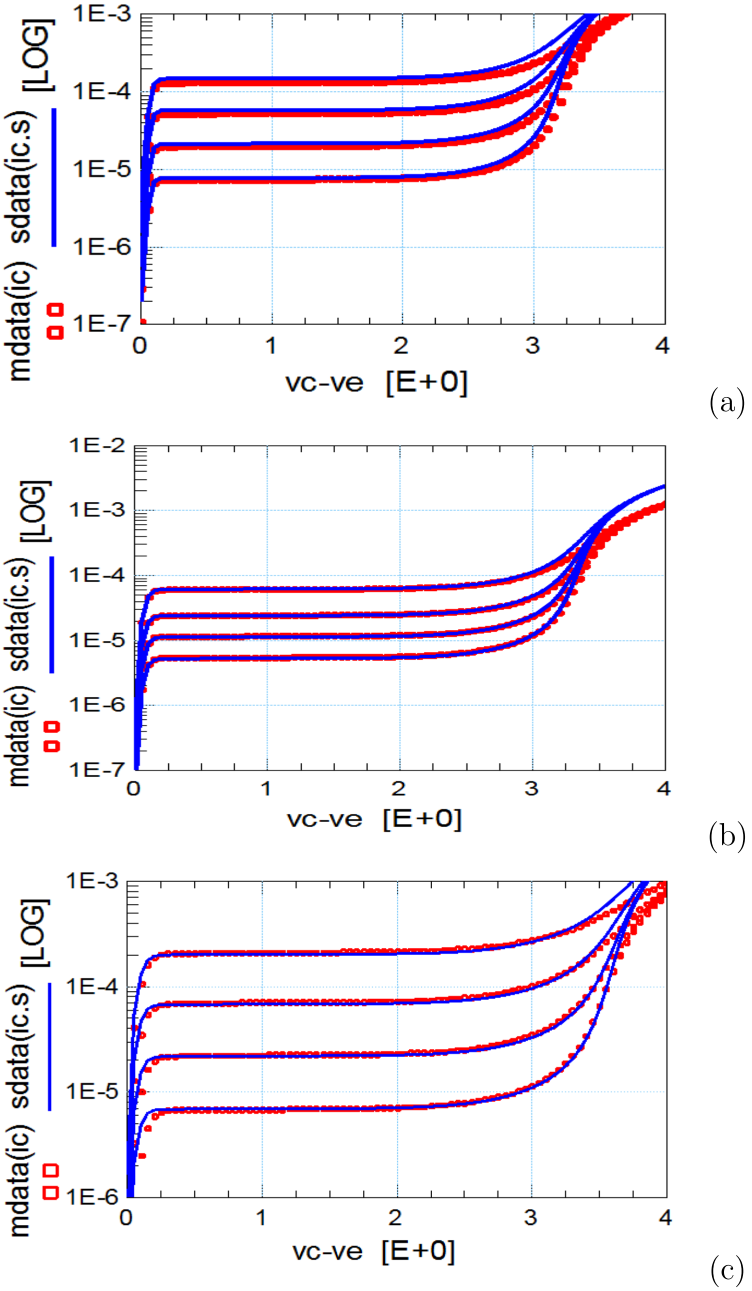

Figure 6.14: Measured (symbol) and simulated (solid line) I_C-V_{CE} from 223-393 K at low IB. (a) 223K. (b) 300K. (c) 393K.

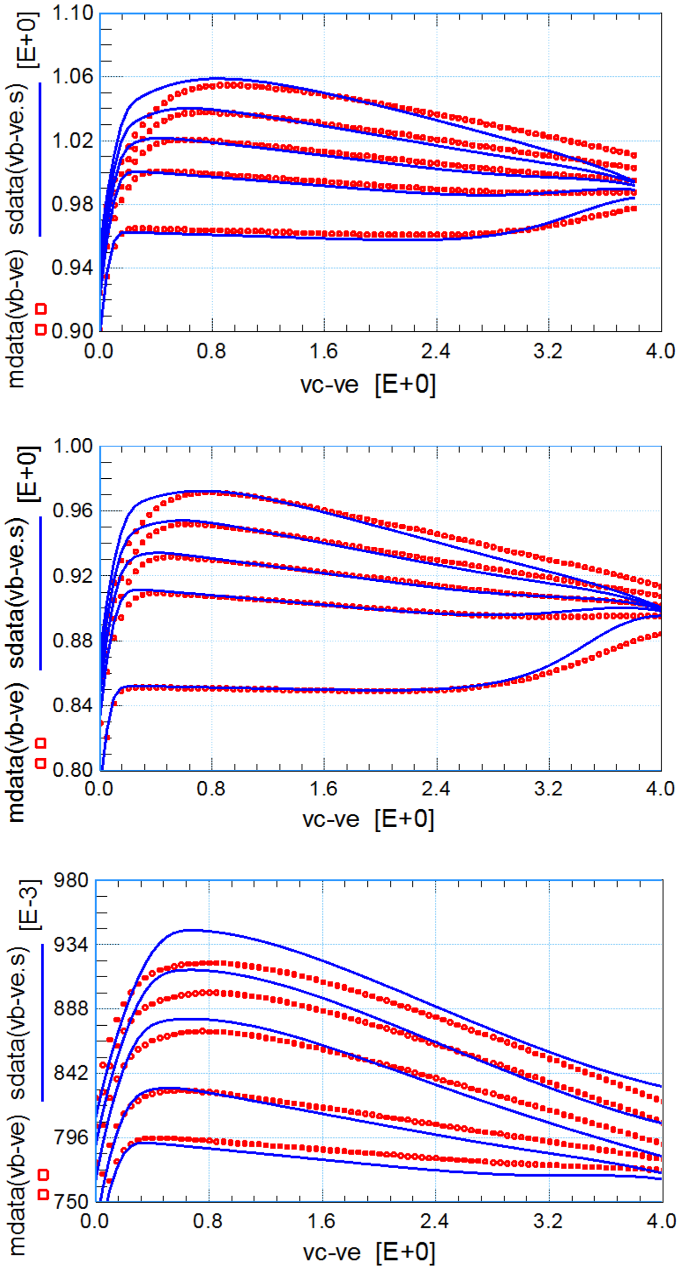

(a)

(b)

(c)

Figure 6.15: Measured (symbol) and simulated (solid line) V_{BE}-V_{CE} from 223-393 K at high IB. (a) 223K. (b) 300K. (c) 393K.

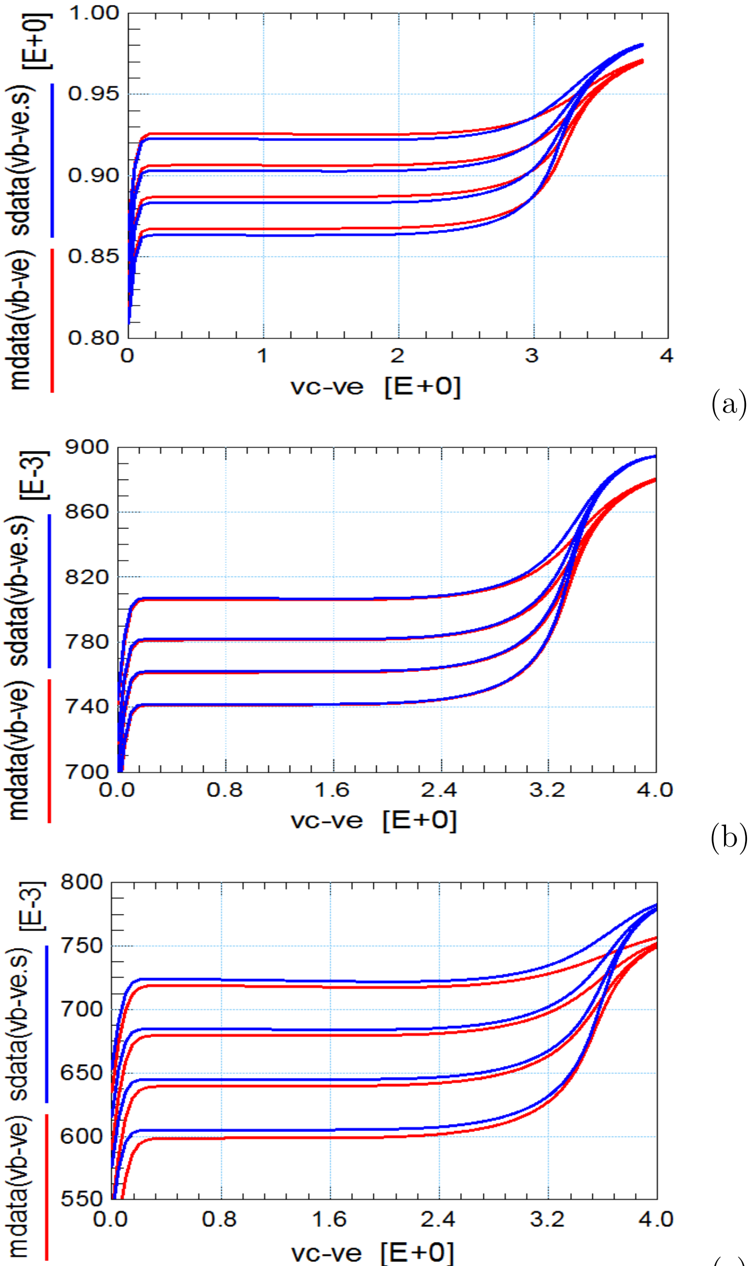

Figure 6.16: Measured (symbol) and simulated (solid line) V_{BE}-V_{CE} from 223-393 K at low IB. (a) 223K. (b) 300K. (c) 393K.

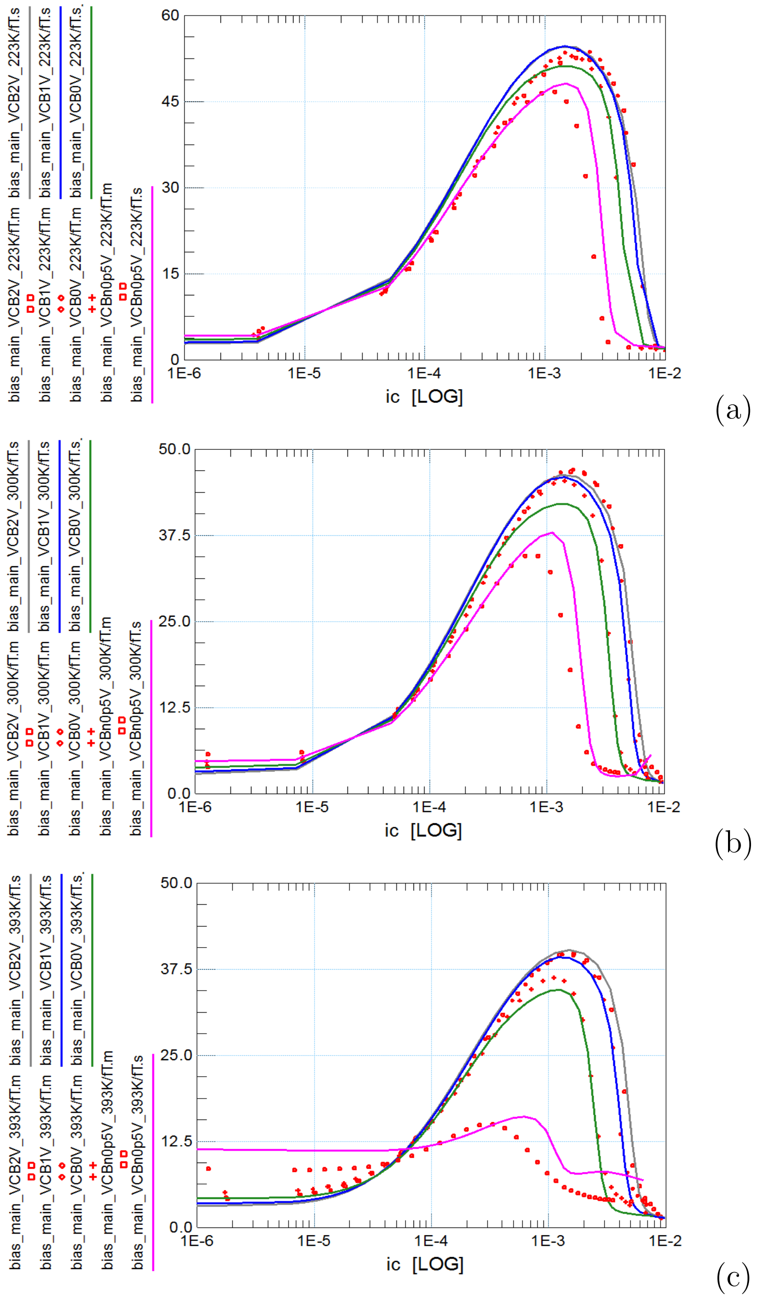

Figure 6.17: Measured (symbol) and simulated (solid line) f_T-I_C from 223-393 K. (a) 223K. (b) 300K. (c) 393K.

Bibliography

[1] G. Niu, R. V. D. Toorn, J. C. J. Paasschens, W.J. Kloosterman, , *The Mextram Bipolar Transistor Model Definition*, Auburn University, 2015.

[2] J. D. Cressler and G. F. Niu, "Silicon-Germanium Heterojunction Junction Bipolar Transistors" Artech House, 2003.

[3] J.D. Cressler, "SiGe HBT Technology: A New Contender for Si-based RF and Microwave Circuit Applications," *IEEE Transactions on Microwave Theory and Techniques*, vol.46, pp.572-589, May 1998.

[4] Z. Xu, "Physics, Modeling and Design Implications of RF Correlation Noise in SiGe HBTs," *Auburn University*, 2013.

[5] J. J. Ebers and J. L. Moll, *Large signal behaviour of junction transistors*, Proc. IRE, vol. 42, p. 1761, 1954.

[6] H. K. Gummel and H. C. Poon, *An integral charge control model of bipolar transistors*, Bell Sys. Techn. J., vol. May-June, pp. 827-852, 1970.

[7] H. C. Graaff and W. J. Kloosterman, "New formulation of the current and charge relations in bipolar transistor modeling for cacd purposes," *IEEE Transactions on Electron Devices*, vol. 32, pp. 2415–2419, Nov. 1985

[8] H. C. de Graaff, W. J. Kloosterman, and T. N. Jansen, "Compact bipolar transistor model for CACD with accurate description of collector behaviour," *in Proc. 18th Conf. Solid St. Dev. and Material*, Tokyo, Japan, 1986, p. 287.

[9] H. C. de Graaff, W. J. Kloosterman, "The Mextram bipolar transistor model," Koninklijke Philips Electronics N.V., Nat. lab. Unclassified Report NL-UR 006/94, 1994.

[10] J. C. J. Paasschens and W. J. Kloosterman, "The Mextram bipolar transistor model,level 504," Philips Nat.Lab., 2000.

[11] J. C. J. Paasschens, W.J. Kloosterman, R. V. D. Toorn, *Model Derivation of Mextram 504: The Physics behind the Model*, Koninklijke Philips Electronics, 2004.

[12] J. C. J. Paasschens,W. J. Kloosterman, and R. J. Havens, *Parameter extraction for the bipolar transistor model Mextram*, Koninklijke Philips Electronics, 2001.

[13] *Programming Language Trends - O'Reilly Radar*, Radar.oreilly.com. August 2006.

[14] *About Python* , Python Software Foundation,24 April 2012.

[15] “Verilog-A Reference Manual,” Agilent Technologies, 2003.

[16] Agilent 85190A IC-CAP 2006, “users guide.,” Agilent Technologies, 2006.

[17] Matthew Newville, Till Stensitzki, *Non-Linear Least-Squares Minimization and Curve-Fitting for Python*, The University of Chicago, 2015.

[18] L. Luo, “Physics, Compact Modeling and TCAD of SiGe HBT for Wide Temperature Range Operation,” *Auburn University*, 2011.

[19] G. M. Kull, L.W. Nagel, S. Lee, P. Lloyd, E. J. Prendergast, and H. Dirks, “Accurate measurement of emitter and collector series resistances in transistors,” *Proc. IRE*, vol. 45, p. 90, Jan. 1957.

[20] L. J. Giacoletto, “Measurement of emitter and collector series resistances,” *IEEE Transactions on Electron Devices*, vol. ED-19, pp. 692693, 1972.

[21] J.D. T. H. Ning and D. D. Tang, “Method for determining the emitter and base series resistances of bipolar transistors,” *IEEE Transactions on Electron Devices*, pp. 409412, 1984.

[22] K. Morizuka, O. Hidaka, and H. Mochizuki, “Precise extraction of emitter resistance from an improved floating collector measurement,” *IEEE Transactions on Electron Devices*, vol. ED- 42, pp. 266273, 1995.

[23] R. Gabl and M. Reisch, “Emitter series resistance from open-collector measurements influence of the collector region and the parasitic pnp transistor,” *IEEE Transactions on Electron Devices*, vol. ED-45, pp. 24572465, 1998.

[24] G. M. Kull, L.W. Nagel, S. Lee, P. Lloyd, E. J. Prendergast, and H. Dirks,“A unified circuit model for bipolar transistors including quasi-saturation effects,” *IEEE Transactions on Electron Devices*, vol. ED-32, no. 6, pp. 11031113, 1985.

[25] D. B. M. Klaassen, “A unified mobility model for device simulationII. temperature dependence of carrier mobility and lifetime,” *Solid-State Elec.,*, vol. 35, no. 7, pp. 961967, 1992.

[26] Li, G; Neugroschel, A; Sah, CT ,“Low frequency conductance voltage analysis of Si/GexSi1-x/Si heterojunction bipolar transistors,” *IEEE Transactions on Electron Devices*, vol. 47(1), pp. 187-196, 2000.

[27] S. L. Salmon, J. D. Cressler, R. C. Jaeger, and D. L. Harame,“The Impact of Ge Profile Shape on the Operation of SiGe HBT Precision Voltage References,” *IEEE Transactions on Electron Devices*, vol. 47, pp. 292-298, 2000.

[28] J.C.J. Paasschens, W.J. Kloosterman, and R.J. Havens,“Modelling two SiGe HBT specific features for circuit simulation,” *Proceedings of the Bipolar Circuits and Technology Meeting*, pp. 38-41, 2001. Paper 2.2 .

[29] J. S. Hamel,,“ASeparating the influences of neutral base recombination and avalanche breakdown on base current reduction in SiGe HBTs,” *IEEE Transactions on Electron Devices*, vol. 44, pp. 901903, 1997.

[30] I. E. Getreu,, “Modeling the bipolar transistor” Elsevier Sc. Publ. Comp., Amsterdam, 1978.

[31] Advanced Design System 1.5, “users guide.,” Agilent Technologies, 2001.

Appendices

Appendix A

Appendix A Full List of Mextram model Parameters

A.1 Compact model parameter list

Table A.1: Mextram 504.12 model parameters overview**??**

	Symbol	Description
1	LEVEL	Model level, must be set to 504
2	T_{ref}	Reference temperature. Default is 25°C
3	DTA	Difference between the local ambient and global ambient temperatures
4	EXMOD	Flag for extended modelling of the reverse current gain
5	EXPHI	* Flag for the distributed high-frequency effects in transient}
6	EXAVL	Flag for extended modelling of avalanche currents
7	EXSUB	Flag for extended modelling of substrate currents
8	I_s	Collector-emitter saturation current
9	I_k	Collector-emitter high injection knee current
10	V_{er}	Reverse Early voltage
11	V_{ef}	Forward Early voltage
12	β_f	Ideal forward current gain
13	I_{Bf}	Saturation current of the non-ideal forward base current
14	m_{Lf}	Non-ideality factor of the non-ideal forward base current
15	XI_{B_1}	Part of ideal base current that belongs to the sidewall
16	I_{zeb}	Pre-factor of emitter-base Zener tunneling current
17	N_{zeb}	Coefficient of emitter-base Zener tunneling current

Table A.1 – continued from previous page

	Symbol	Description
18	β_{ri}	Ideal reverse current gain
19	I_{Br}	Saturation current of the non-ideal reverse base current
20	V_{Lr}	Cross-over voltage of the non-ideal reverse base current
21	X_{ext}	Part of I_{ex}, Q_{tex}, Q_{ex} and I_{sub} that depends on V_{BC_3} instead of $V_{B_1C_4}$
22	W_{avl}	Epilayer thickness used in weak-avalanche model
23	V_{avl}	Voltage determining curvature of avalanche current
24	S_{fH}	Current spreading factor of avalanche model (when EXAVL = 1)
25	R_E	Emitter resistance
26	R_{Bc}	Constant part of the base resistance
27	R_{Bv}	Zero-bias value of the variable part of the base resistance
28	R_{Cc}	Collector Contact resistance
29	R_{cblx}	Resistance of the Collector Buried Layer: eXtrinsic part
30	R_{cbli}	Resistance of the Collector Buried Layer: Intrinsic part
31	R_{Cv}	Resistance of the un-modulated epilayer
32	SCR_{Cv}	Space charge resistance of the epilayer
33	I_{hc}	Critical current for velocity saturation in the epilayer
34	a_{x_i}	Smoothness parameter for the onset of quasi-saturation
35	C_{j_E}	* Zero-bias emitter-base depletion capacitance
36	V_{d_E}	Emitter-base diffusion voltage
37	p_E	Emitter-base grading coefficient
38	XC_{j_E}	* Fraction of the emitter-base depletion capacitance that belongs to the sidewall
39	C_{BEO}	* Emitter-base overlap capacitance
40	C_{j_C}	* Zero-bias collector-base depletion capacitance
41	V_{d_C}	Collector-base diffusion voltage
42	p_C	Collector-base grading coefficient

Table A.1 – continued from previous page

	Symbol	Description
43	X_p	Constant part of C_{jC}
44	m_C	Coefficient for the current modulation of the CB depletion capacitance
45	XC_{j_C}	* Fraction of the collector-base depletion capacitance under the emitter
46	C_{BCO}	* Collector-base overlap capacitance
47	m_τ	* Non-ideality factor of the emitter stored charge
48	τ_E	* Minimum transit time of stored emitter charge
49	τ_B	* Transit time of stored base charge
50	τ_{epi}	* Transit time of stored epilayer charge
51	τ_R	* Transit time of reverse extrinsic stored base charge
52	dE_g	Bandgap difference over the base
53	X_{rec}	Pre-factor of the recombination part of I_{B_1}
54	X_{Q_B}	Fraction of the total base charge supplied by the collector
55	$A_{Q_{B0}}$	Temperature coefficient of the zero-bias base charge
56	A_E	Temperature coefficient of the resistivity of the emitter
57	A_B	Temperature coefficient of the resistivity of the base
58	A_{epi}	Temperature coefficient of the resistivity of the epilayer
59	A_{ex}	Temperature coefficient of the resistivity of the extrinsic base
60	A_C	Temperature coefficient of the resistivity of the collector contact
61	A_cbl	Temperature coefficient of the resistivity of the collector buried layer
62	dA_{I_s}	Parameter for fine tuning of temperature dependence of CE saturation current
63	$dV_{g\beta f}$	Band-gap voltage difference of forward current gain
64	$dV_{g\beta r}$	Band-gap voltage difference of reverse current gain
65	V_{g_B}	Band-gap voltage of the base
66	V_{g_C}	Band-gap voltage of the collector
67	V_{g_j}	Band-gap voltage recombination emitter-base junction

Table A.1 – continued from previous page

	Symbol	Description
68	V_{gzEB}	Band-gap voltage at reference temperature relevant to the Zener effect in EB junction
69	A_{Vgz}	Temperature scaling coefficient of emitter-base Zener tunneling current
70	T_{BVgz}	Temperature scaling coefficient of emitter-base Zener tunneling current
71	$dV_{g\tau_E}$	* Band-gap voltage difference of emitter stored charge
72	A_f	* Exponent of the Flicker-noise
73	K_f	* Flicker-noise coefficient of the ideal base current
74	K_{fN}	* Flicker-noise coefficient of the non-ideal base current
75	K_{avl}	* Switch for white noise contribution due to avalanche
76	K_C	* Switch for RF correlation noise model selection
77	I_{Ss}	Base-substrate saturation current
78	$Issf$	Collector-substrate ideal saturation current
79	I_{ks}	Base-substrate high injection knee current
80	C_{j_S}	* Zero-bias collector-substrate depletion capacitance
81	V_{d_S}	* Collector-substrate diffusion voltage
82	p_S	* Collector-substrate grading coefficient
83	V_{gS}	Band-gap voltage of the substrate
84	A_S	For a closed buried layer: $\mathrm{A_S} = \mathrm{A_C}$, and for an open buried layer: $\mathrm{A_S} = \mathrm{A_{epi}}$
85	A_{sub}	Temperature coefficient for mobility of minorities in the substrate
86	R_{th}	Thermal resistance
87	C_{th}	* Thermal capacitance
88	A_{th}	Temperature coefficient of the thermal resistance
89	MULT	Multiplication factor